ORNL/TM--11716

DE91 018316

Instrumentation and Controls Division

ADVANCED AUTOMATION CONCEPTS APPLIED TO EXPERIMENTAL BREEDER REACTOR-II STARTUP

R. C. Berkan*
B. R. Upadhyaya*
R. L. Eywater*
R. A. Kisner

*Nuclear Engineering Department, The University of Tennessee, Knoxville, Tennessee 37996-2300.

ANNUAL REPORT

Program Manager: J. D. White

Date Published—August 1991

Prepared by the
OAK RIDGE NATIONAL LABORATORY
Oak Ridge, Tennessee 37831-6285
managed by
MARTIN MARIETTA ENERGY SYSTEMS, INC.
for the
U.S. DEPARTMENT OF ENERGY
under contract DE-AC05-84OR21400

MASTER

CONTENTS

Page

LIST OF FIGURES v

ABBREVIATIONS AND ACRONYMS ix

ABSTRACT xi

1. INTRODUCTION 1
   1.1 SCOPE OF ADVANCED CONTROL CONCEPT INTEGRATION IN NUCLEAR PLANTS 1
   1.2 SUMMARY OF APPROACH–GENERAL FEATURES 1
   1.3 SUMMARY OF SIGNIFICANT RESULTS 2
   1.4 ORGANIZATION OF THE REPORT 4

2. BACKGROUND 5
   2.1 DESCRIPTION OF EXPERIMENTAL BREEDER REACTOR-II 5
   2.2 EXISTING CONTROL CAPABILITIES AT EXPERIMENTAL BREEDER REACTOR-II 5
   2.3 EXPERIMENTAL BREEDER REACTOR-II STARTUP OPERATION 7

3. ADVANCED AUTOMATION CONCEPTS 24
   3.1 DEFINITION OF CONTROL ENGINE 24
      3.1.1 Signal Validation 24
      3.1.2 Command Validation 24
      3.1.3 Configuration Validator 26
      3.1.4 Strategy Validator 26
      3.1.5 Direct Control Algorithm 26
      3.1.6 Mode Selector 26
      3.1.7 Performance Analyzer 27
      3.1.8 Lifeboat System 27
      3.1.9 Decision Support 27

4. APPLICATION TO EXPERIMENTAL BREEDER REACTOR-II STARTUP 28
   4.1 STARTUP AUTOMATION STRATEGY 28
   4.2 SIGNAL VALIDATION 30
      4.2.1 On-line Signal Validation Strategy 30
   4.3 COMMAND VALIDATION 32
   4.4 CONTROL GUIDANCE 46
      4.4.1 Reconstructive Inverse Dynamics Controller 46
      4.4.2 Fuzzy Controller 51
      4.4.3 Neural Network Controller 51
   4.5 PERFORMANCE ANALYZER 54

CONTENTS (continued)

Page

4.6 MODE SELECTOR 56
4.7 FAULT TOLERANCE 58

5. SIMULATION RESULTS 63
5.1 QUALITATIVE EVALUATION 63

6. DESIGN TOOLS 72
6.1 PROCESS EMPIRICAL MODELING 72
6.2 NEURAL NETWORKS: BACKPROPAGATION PARADIGM 72
6.3 FUZZY LOGIC 75
6.4 INVERSE DYNAMICS AND CONTROL 75
6.5 NONLINEAR MODELING OF EXPERIMENTAL BREEDER REACTOR-II 80
6.6 EXPERT SYSTEMS 80

7. SUMMARY AND CONCLUDING REMARKS 86

REFERENCES 87

LIST OF FIGURES

Figure		Page
1.1.	Integrated-system components for advanced plant control	3
2.1.	Experimental Breeder Reactor-II plant schematic	6
2.2.	State transitions during startup at Experimental Breeder Reactor-II	9
2.3.	Experimental Breeder Reactor-II startup data	10
3.1.	General architecture of the integrated control system	25
4.1.	Advanced control system for Experimental Breeder Reactor-II startup	29
4.2a.	Process empirical model for power	33
4.2b.	Backpropagation network model for power	34
4.2c.	Process empirical model for intermediate heat exchanger secondary outlet temperature	35
4.2d.	Backpropagation network model for intermediate heat exchanger secondary outlet temperature	36
4.2e.	Process empirical model of secondary sodium flow; input signals are reactor exit temperature and bulk sodium tank temperature	37
4.2f.	Backpropagation network model of secondary sodium flow; input signals are reactor exit temperature and bulk sodium temperature	38
4.3a.	Process empirical model for control rod position	39
4.3b.	Backpropagation network model for control rod position	40
4.3c.	Backpropagation network model of secondary sodium flow; input signals are electromagnetic pump voltage and pump delta P	41
4.3d.	Process empirical model of secondary sodium flow; input signals are electromagnetic pump voltage and pump delta P	42
4.3e.	Process empirical model of electromagnetic pump voltage	43
4.3f.	Backpropagation network model of electromagnetic pump voltage	44
4.4.	MATRIXx reconstruction of the process empirical model	45

LIST OF FIGURES (continued)

Figure		Page
4.5a.	Three-layer, five-hidden–neuron neural network for predicting secondary sodium flow	47
4.5b.	Expanded view of the fifth hidden neuron	48
4.5c.	Expanded view of the output layer neuron	49
4.6.	Reconstructive inverse dynamics control implementation in MATRIXx/SYSTEM-BUILD environment	50
4.7a.	Fuzzy control implementation in MATRIXx/SYSTEM-BUILD environment	52
4.7b.	Interior of the super block fuzzy	53
4.8.	Backpropagation network topology for reactivity control (top) and secondary sodium flow (bottom) control	55
4.9.	Work space of the performance analyzer	57
4.10a.	Mode selector logic implementation for control signals in MATRIXx/SYSTEM-BUILD environment	59
4.10b.	Interior of super block command_logic	60
4.11.	Structural fault-tolerance nature of the integrated control system	62
5.1a.	Power change during startup at Experimental Breeder Reactor-II	64
5.1b.	Core exit temperature change during startup at Experimental Breeder Reactor-II	65
5.1c.	Sodium tank temperature change during startup at Experimental Breeder Reactor-II	66
5.1d.	Intermediate heat exchanger–secondary outlet temperature change during startup at Experimental Breeder Reactor-II	67
5.1e.	In-core sodium temperature during startup at Experimental Breeder Reactor-II	68
5.1f.	Rod motion during startup at Experimental Breeder Reactor-II	69

LIST OF FIGURES (continued)

Figure		Page
5.1g.	Secondary sodium flow control during startup at Experimental Breeder Reactor-II	70
6.1.	Topology of a three-layer backpropagation network	73
6.2.	Adaptive reconstructive inverse dynamics control system	81
6.3a.	MATRIXx super blocks representing the adaptive, nonlinear Experimental Breeder Reactor-II model	82
6.3b.	Nonlinear core model of the Experimental Breeder Reactor-II plant in MATRIXx	83
6.3c.	Nonlinear intermediate heat exchanger model of the Experimental Breeder Reactor-II plant in MATRIXx	84
6.3d.	Adaptive block to track uncertain parameters of the model	85

ABBREVIATIONS AND ACRONYMS

ACRDS	automatic control rod drive system
AI	artificial intelligence
ANL	Argonne National Laboratory
BOP	balance of plant
BPN	backpropagation network
CANDU	Canadian (heavy-water) deuterium uranium reactor
CGB	control guidance block
CVB	command validation block
EBR-II	Experimental Breeder Reactor-II
EM	electromagnetic
FP	fuzzy production
GCC	generalized consistency checking
H/A	hand/automatic
ICS	integrated control system
IHX	intermediate heat exchanger
LMR	liquid-metal reactor
LSS	large-scale system
MIMO	multi-input/multioutput
MW(t)	megawatt (thermal)
NNET	neural network
ORNL	Oak Ridge National Laboratory
PE	processing element
PEM	process empirical modeling
PWR	pressurized water reactor
RID	reconstructive inverse dynamics
SVB	signal validation block

ABSTRACT

The major objective of this work is to demonstrate through simulations that advanced liquid-metal reactor plants can be operated from low power to full power by computer control. Development of an automatic control system with this objective will help resolve specific issues and provide proof through demonstration that automatic control for plant startup is feasible. This paper presents an advanced control system design for startup of the Experimental Breeder Reactor-II (EBR-II) located at Idaho Falls, Idaho. The design incorporates recent methods in nonlinear control with advanced diagnostics techniques such as neural networks to form an integrated architecture. The preliminary evaluations are obtained in a simulated environment by a low-order, valid nonlinear model. Within the framework of phase I research, the design includes an inverse dynamics controller, a fuzzy controller, and an artificial neural network controller. These three nonlinear control modules are designed to follow the EBR-II startup trajectories in a multi-input/output regime. They are coordinated by a supervisory routine to yield a fault-tolerant, parallel operation. The control system operates in three modes: manual, semiautomatic, and fully automatic control. The simulation results of the EBR-II startup transients proved the effectiveness of the advanced concepts. The work presented in this paper is a preliminary feasibility analysis and does not constitute a final design of an automated startup control system for EBR-II.

1. INTRODUCTION

1.1 SCOPE OF ADVANCED CONTROL CONCEPT INTEGRATION IN NUCLEAR PLANTS

Computerized plant status display, consideration of human factors issues in control room design, and plant monitoring based on advanced signal processing have gained increased applications in nuclear power plants. Developers of new, advanced reactors must consider these concepts in the design phase. New and improved control strategies may be needed for efficient operation of multimodular plants, including plant startup, load following, and steady-state operation. Because of the complex nonlinear nature of multimodular nuclear reactor startup dynamics, a need exists for combining control strategies and plant monitoring schemes.

The objective of the present task under the Advanced Controls Program at Oak Ridge National Laboratory (ORNL) is to develop and integrate control algorithms and signal and command validation strategies and to demonstrate this approach with application to the startup of Experimental Breeder Reactor-II (EBR-II).

Current modular power plants do not have a fully automated startup control strategy. Automatic load following control systems for pressurized water reactor (PWR) plants are being designed by Mitsubishi Atomic Power Industries (Nakakura and Ishiguro 1988) in Japan. The primary objective is to control core axial power distribution by load-following control rods. Automation in Canadian heavy water reactors (CANDU) is the most advanced in the industry. The goal is to achieve 100% digital control and protection in new plants such as the Darlington units of Ontario Hydro (Carter and Uhrig 1990). The "operators provide information to the control system through this control panel. Input includes startup rate and the power level to be maintained. The operators adjust automatic controller parameters and/or set points." This procedure is a form of semiautomated control strategy. Husseiny et al. (1990) proposed a two-level control model for operating a typical nuclear plant. One of the conclusions of the Husseiny study is that a high-level supervisory fuzzy or rule-based controller provides a "strategy that can free the senior operator for important operational tasks other than vigilance and attendance to details of equipment or subsystems operation." The operator would be responsible for monitoring plant performance and providing global control actions. An approach based on a "forward dynamic programming technique was developed and applied to the load following control of a boiling water reactor" by Lin et al. (1989). These studies indicate a growing trend toward increased automation of power plant operations.

1.2 SUMMARY OF APPROACH–GENERAL FEATURES

The integrated control system consists of four major components:

1. control module,
2. signal validation module,
3. command validation module, and
4. system executive module.

Figure 1.1 shows this general structure. Each module has multiple approaches in its implementation. The control module incorporates inverse dynamics control, fuzzy logic control, and neural network control. The objective of the signal validation system is to monitor outputs from sensors; detect and isolate faulty sensors; and if necessary, provide an estimation of control and protection system signals. The purpose of the command validator is to verify the control signals (input to actuators) and outputs of actuators. The system executive module serves as a high-level decision support tool. It analyzes the overall performance and selects appropriate modes of control. All these systems are fully integrated and provide appropriate information to the operator.

The definitions of the various components of the above "control engine" are given in Sect. 3. The integrated system is currently implemented in a VAX 3100 computer Work Station and uses the MATRIXx Software for integration purpose.

1.3 SUMMARY OF SIGNIFICANT RESULTS

Several important milestones have been accomplished during this project. The following specific tasks have been completed.

1. The integrated control system has been developed and demonstrated with application to EBR-II startup control.

2. An archival of EBR-II startup data has been established.

3. The signal validation modules—process empirical modeling, neural networks, and consistency checking—have been implemented.

4. A new control methodology, called the reconstructive inverse dynamics control, has been developed. In addition, a fuzzy logic controller and a neural network controller are available as alternatives.

5. The command validation module developed in this project introduces a new idea—that of verifying control inputs and actuator outputs.

6. The redundancy in each of the three subsystems provides an effective method for switching from one technique to another, as demanded by the availability of process signals. This capability is also known as structural fault-tolerance because it emphasizes providing reliable control under structural anomalies.

7. The signal and command validation represented in the SYSTEM-BUILD software as superblocks provides fast interaction with the control system module.

8. The individual module, the EBR-II model, and the integrated system tests are based on startup data from EBR-II.

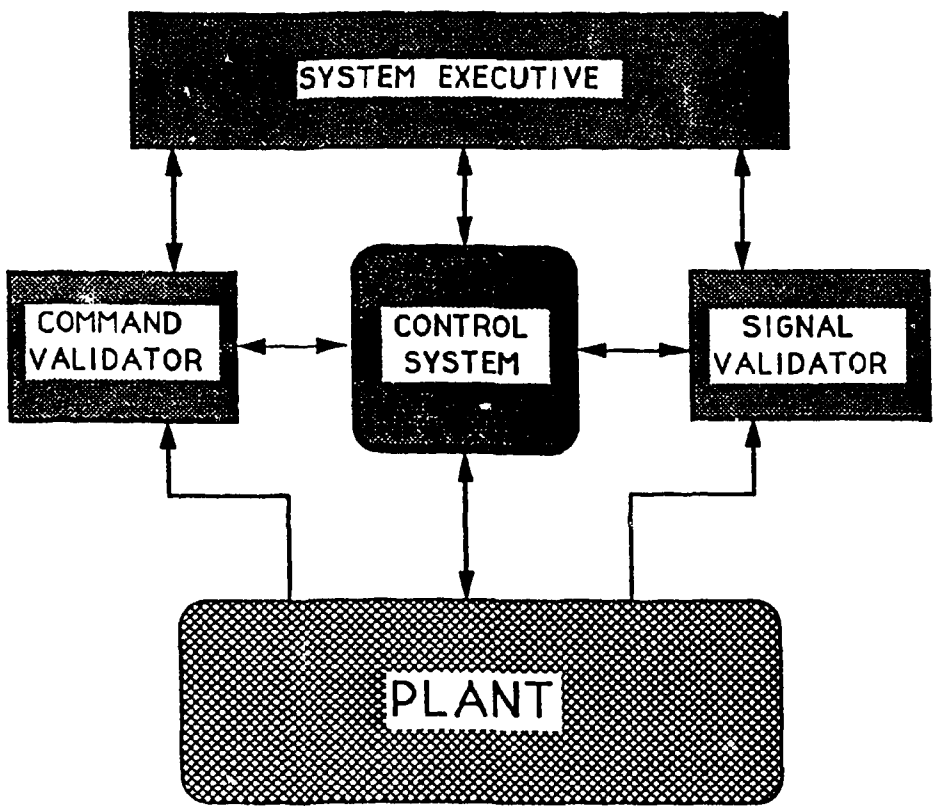

Fig. 1.1. Integrated-system components for advanced plant control.

1.4 ORGANIZATION OF THE REPORT

Section 2 provides a brief description of EBR-II, existing control systems, and steps in EBR-II startup. The concepts of advanced automation are presented in Sect. 3. The integration and implementation of control strategies, signal validation, command validation and system executive modules are described in Sect. 4. The results of demonstration using EBR-II startup data are also presented. Section 5 presents the performance verification of the new control strategy, which uses a nonlinear model of the EBR-II primary system, including the intermediate heat exchanger. The various techniques such as neural networks, fuzzy logic control, process empirical modeling, and others are described in Sect. 6. The summary and concluding remarks are presented in Sect. 7.

2. BACKGROUND

The startup of EBR-II includes a complicated procedure for calibration, status verification, and configuration validation. Automation of the EBR-II startup therefore requires a computer-based information system as an operator aid. A recent study (Corcuera et al. 1990) presents a startup procedure-prompting system developed in an expert system environment. Once the procedure is appropriately followed, control of the EBR-II startup is a straightforward task. However, the plant nonlinearities over the startup range and the multitude of control variables indicate that the advanced, nonlinear multivariate control techniques may perform more efficiently than the conventional, linear methods. Furthermore, a supervisory, intelligent system is required to cope with abnormal equipment and process conditions to maneuver around problems or provide safe routes to shutdown.

2.1 DESCRIPTION OF EXPERIMENTAL BREEDER REACTOR-II

EBR-II is a liquid-metal fast-breeder reactor located at the National Reactor Testing Station in Idaho. The original purpose of this facility was to demonstrate the feasibility of fast reactors for central station power plant applications. The purpose was later redirected to provide irradiation services for the development of fuels and structural materials. Changes were made in the operating philosophy from that of an engineering test facility to that of a high-priority neutron producer.

The plant included a heterogeneous, unmoderated, sodium-cooled reactor [62.5 MW(t)]; an intermediate sodium coolant loop; a steam plant that produces 20 MW of electrical power through a conventional turbine generator; and a fuel processing system consisting of subsystems for disassembly, decontamination, fabrication, and assembly of fuel elements and subassemblies. Both the reactor and the associated fuel recycle facilities were designed with the philosophy of providing a highly flexible installation that would permit the investigation and evaluation of various core configurations, fuel types, fuel element design, and processing techniques. The reactor, primary cooling system, and fuel-handling system components are submerged in a large primary sodium tank. This concept is sometimes referred to as the pool-type design (such as the Phoenix and Super-Phoenix liquid-metal reactors in France). A schematic of the EBR-II plant is shown in Fig. 2.1

2.2 EXISTING CONTROL CAPABILITIES AT EXPERIMENTAL BREEDER REACTOR-II

The EBR-II control systems are distributed over the subsystems and components mostly coordinated from the central control room by plant operators. These controllers are designed to function locally, and the global control decisions are made by operators. The following describes the local controllers of the EBR-II.

EBR-II reactivity control is maintained by 12 control rod and 2 safety rod subassemblies. A computer-controlled rod-drive system is capable of controlling reactor power during steady-state and power change. An error signal from the reactor power reading is the input to the digital computer. The on-line computer implements a proportional control action to minimize the error reading. The permanent automatic

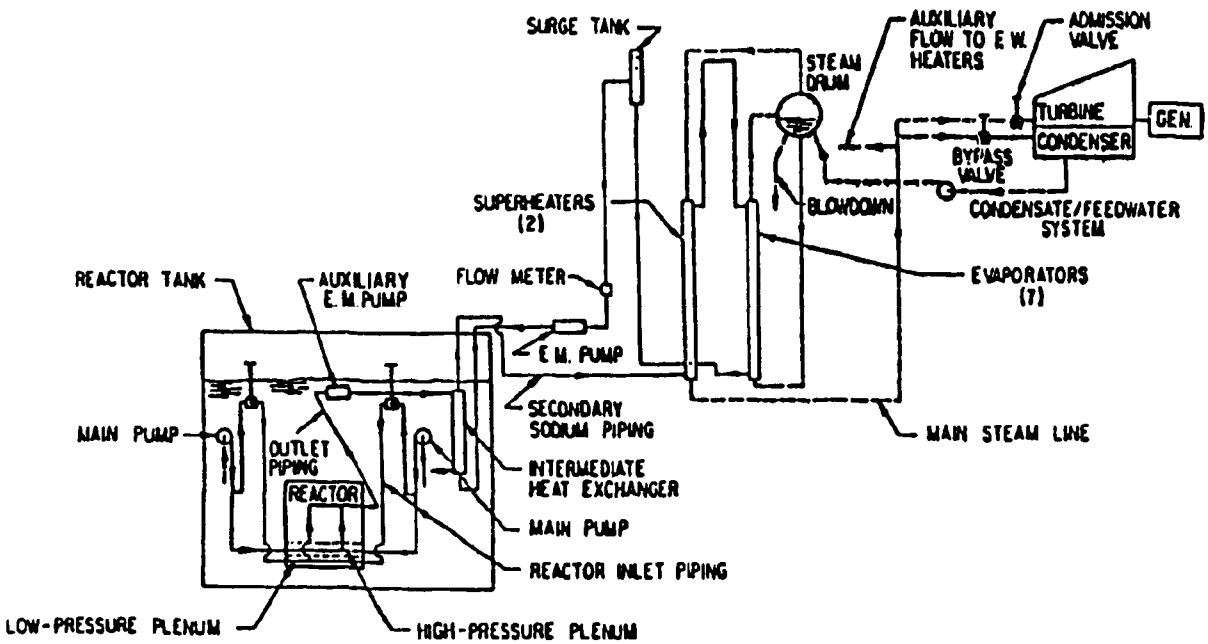

Fig. 2.1. Experimental Breeder Reactor-II plant schematic.

control rod drive system (ACRDS) provides a fast-speed automatic mode plus two slow-speed modes, manual and automatic.

The primary sodium flow [loop between core and intermediate heat exchanger (IHX)] is controlled by the primary pumps, where the pumping rate is continuously, steplessly variable from 0 to 100%. No valves or other control devices are included in the main sodium loop. The secondary sodium loop is controlled by an electromagnetic (EM) pump, where the flow is adjustable from 0 to 100% of full flow capacity by varying the voltage applied to the pump windings. The actuation signal is adjusted manually from the sodium recirculating pump panel. The control task of this actuator includes controlling reactor inlet temperature by controlling the bulk temperature in the sodium tank. Since the secondary sodium loop constitutes the coupling between the primary and secondary systems, the flow adjustment also directly affects the steam pressure and other system variables on the secondary side.

The feedwater temperature is controlled by bypassing some feedwater around the last heater, mixing a portion of 480°F feedwater with the 568°F water to maintain 550°F input. The bypass valve is manually controlled from the steam panel in the control room.

The turbine generator is controlled by two circuits. The primary circuit controls the speed and load of the turbine, and the secondary circuit controls the turbine stop valve to trip the turbine when an abnormal condition occurs.

The main control of the steam generator is performed by the steam drum level control. The control system is capable of single-element, four-element, or manual control. The controller accepts four analog signals: steam drum level, feedwater flow, steam flow, and blowdown flow. The actuator is the feedwater valve.

2.3 EXPERIMENTAL BREEDER REACTOR-II STARTUP OPERATION

The eleven identified modes of operation at the EBR-II are classified as normal or nonroutine operations. The normal operations include plant startup, plant standby, reactor restart, steady power, changing power, plant shutdown, and fuel handling. The nonroutine operations include reactor scram, anticipatory reactor shutdown, plant cooldown, and plant heatup. The startup of the EBR-II is performed in the two modes (plant startup and reactor restart) that distinguish the conditions prior to startup. The terminology "reactor restart" emphasizes that the most recent shutdown was within the past 24 hours and that no reactor loading change has been made. In the plant standby situation, all auxiliary systems meet the prestartup requirements. Unless plant standby conditions exist, no startup is allowed.

The startup procedures (ANL 1985) include raising the safety rods into the core and moving the control rods in the order specified in the Reactor Run Plan and Authorization. The control rods in the EBR-II contain fuel at the bottom and poison at the top. The core is subcritical when the fuel section of the rods is removed from the core. Therefore, criticality is achieved by withdrawing the rods, which removes the poison section from the core and replaces the fuel from the bottom. After the control rods are calibrated at about 50 kW, power is increased incrementally until the desired power level is reached. The primary pumps operate at full power throughout startup. The secondary pump flow is adjusted to maintain normal steam pressure in the drum. The steam header is pressurized when the primary sodium reaches 620°F. Increase of reactor power is regulated to maintain a 10°F/h rise in bulk sodium temperature. The secondary sodium flow adjustments also aim at maintaining the primary bulk sodium at 700°F. When the

reactor power is stable at 30 MW and adequate steam is available, the steam system is operated and the turbine-generator is started. A brief summary of the startup procedure including validity checks is shown in Fig. 2.2. Some of the important EBR-II startup transients are shown in Fig. 2.3 (personal communication, June 1987 data from E. E. Feldman, Argonne National Laboratory, Argonne, Illinois, to B. Upadhyaya, The University of Tennessee, Knoxville). Table 2.1 lists 154 measurements that are available for further analysis. These data were obtained during a startup following a standby condition. The data were sampled every 5 s.

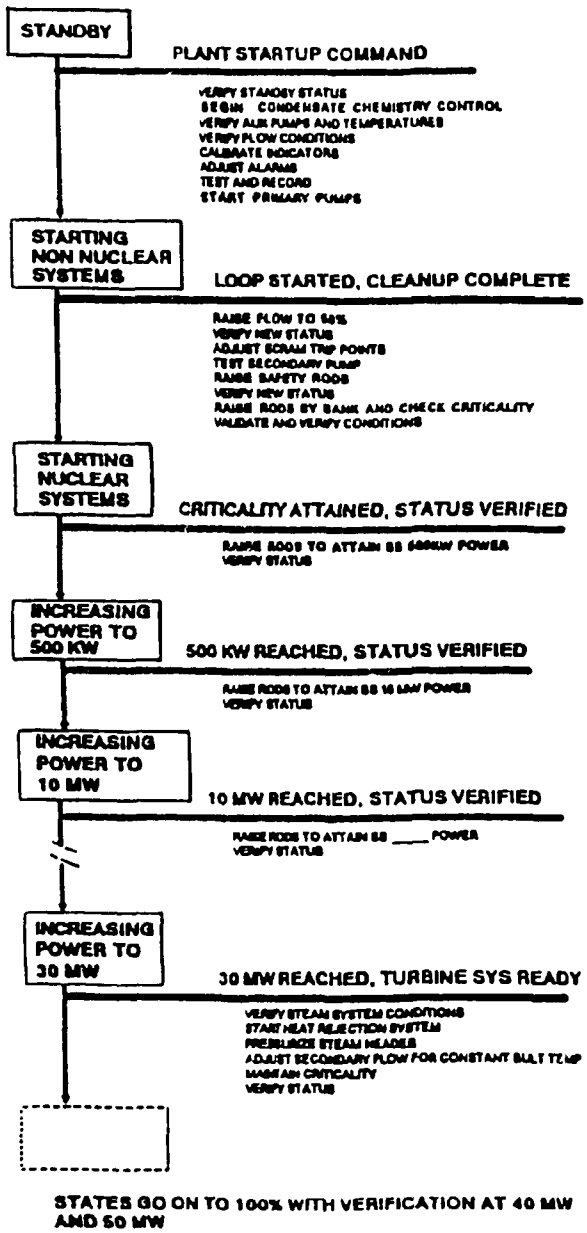

Fig. 2.2. State transitions during startup at Experimental Breeder Reactor-II.

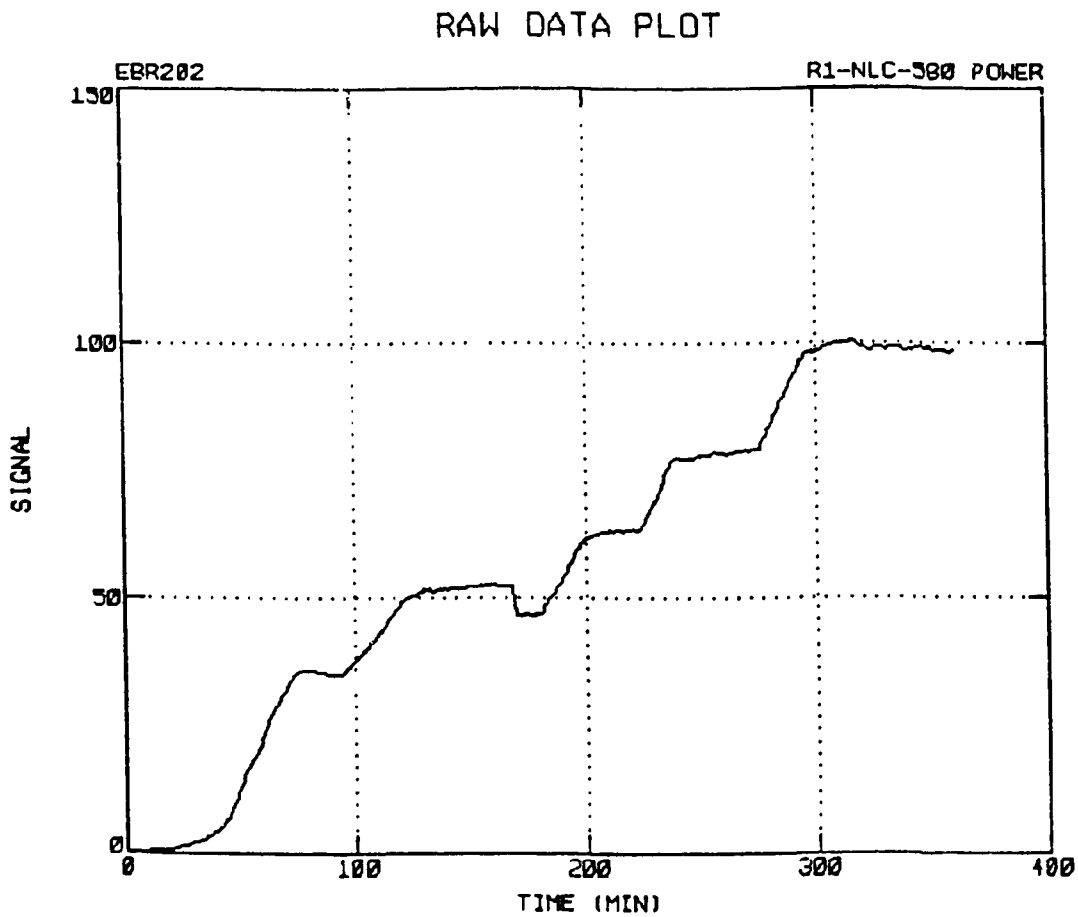

Fig. 2.3. Experimental Breeder Reactor-II startup data.

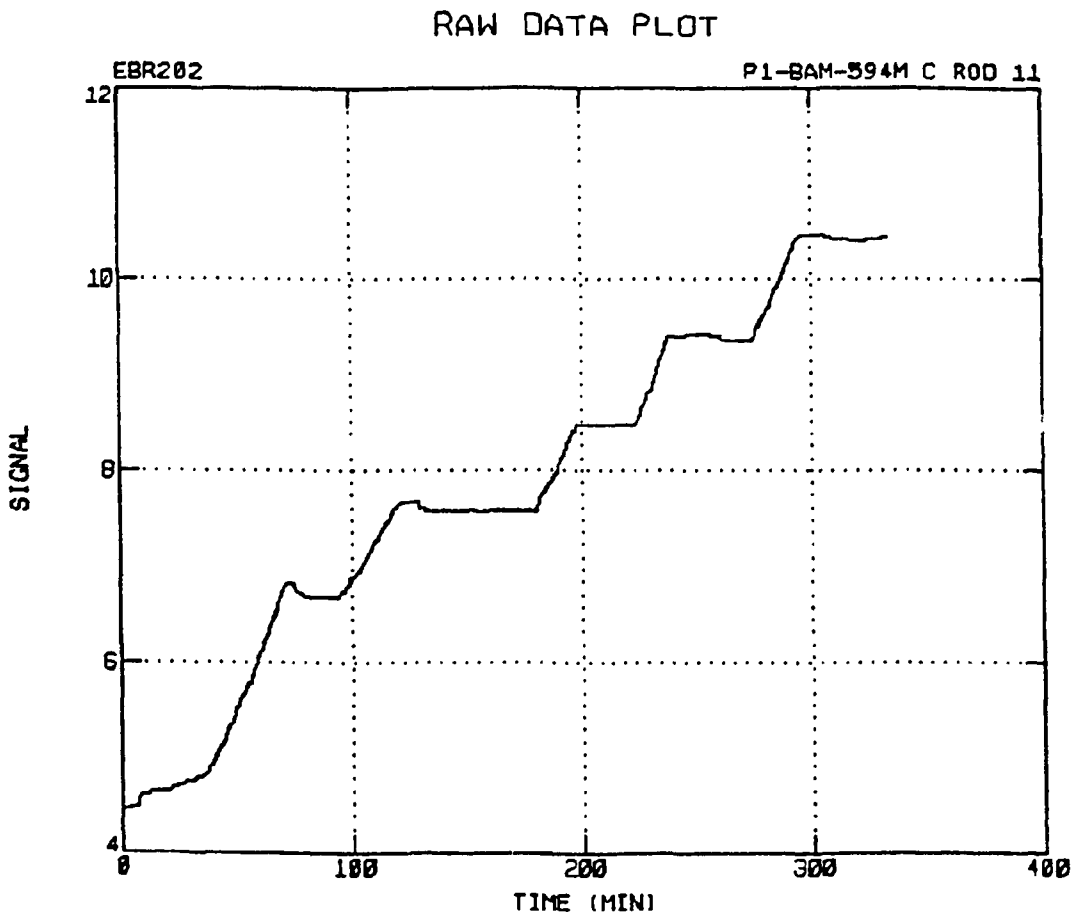

Fig. 2.3. (continued)

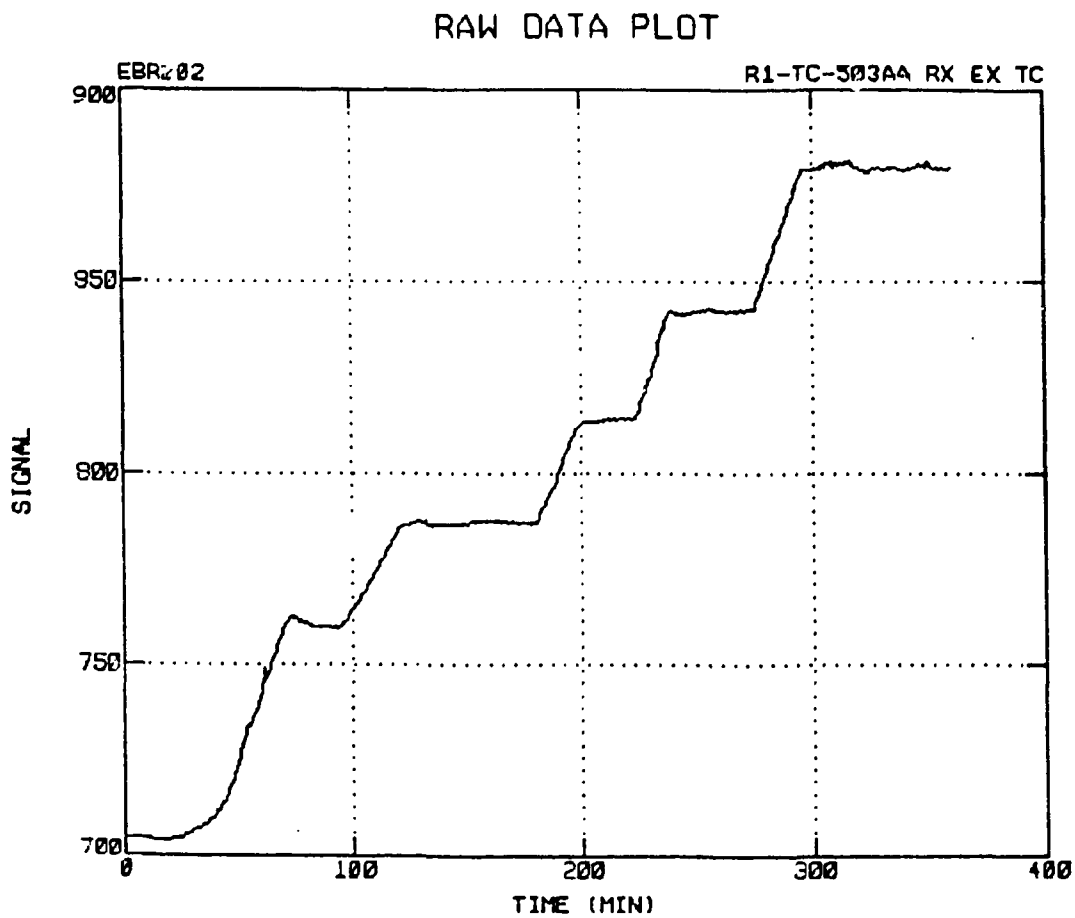

Fig. 2.3. (continued)

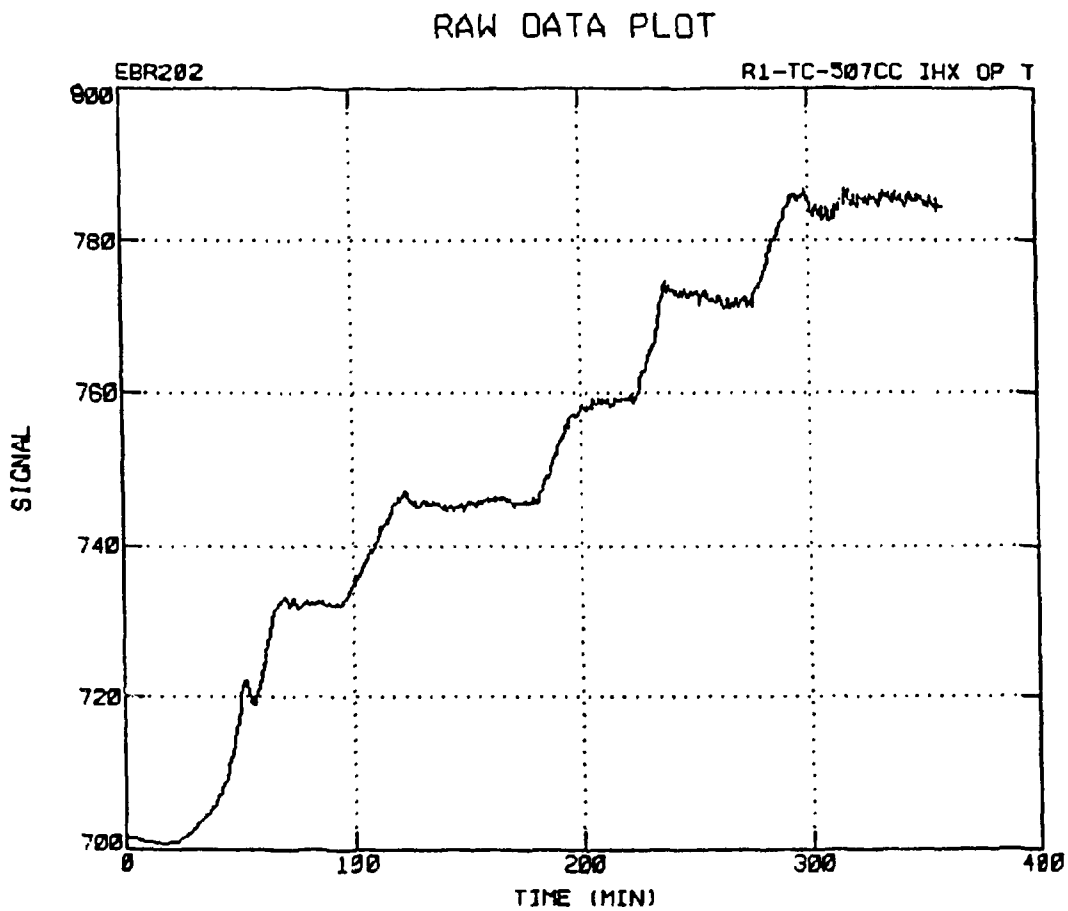

Fig. 2.3. (continued)

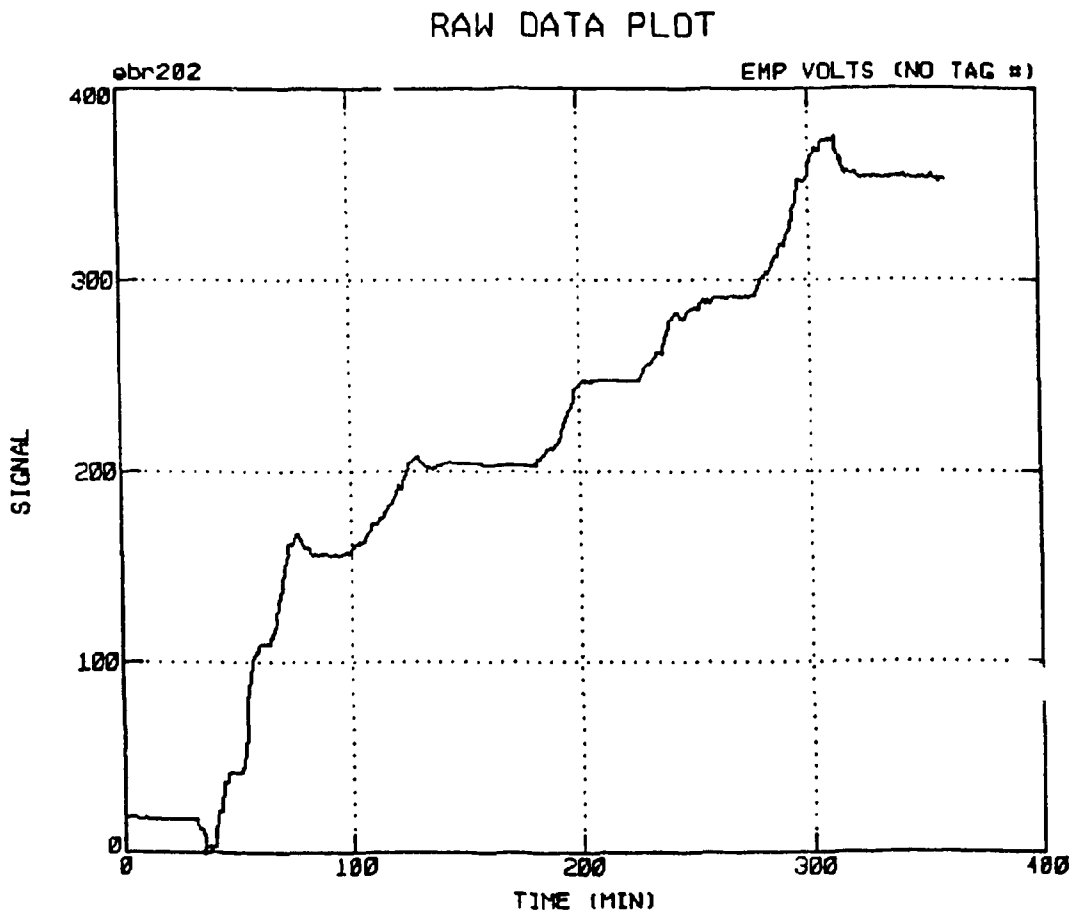

Fig. 2.3. (continued)

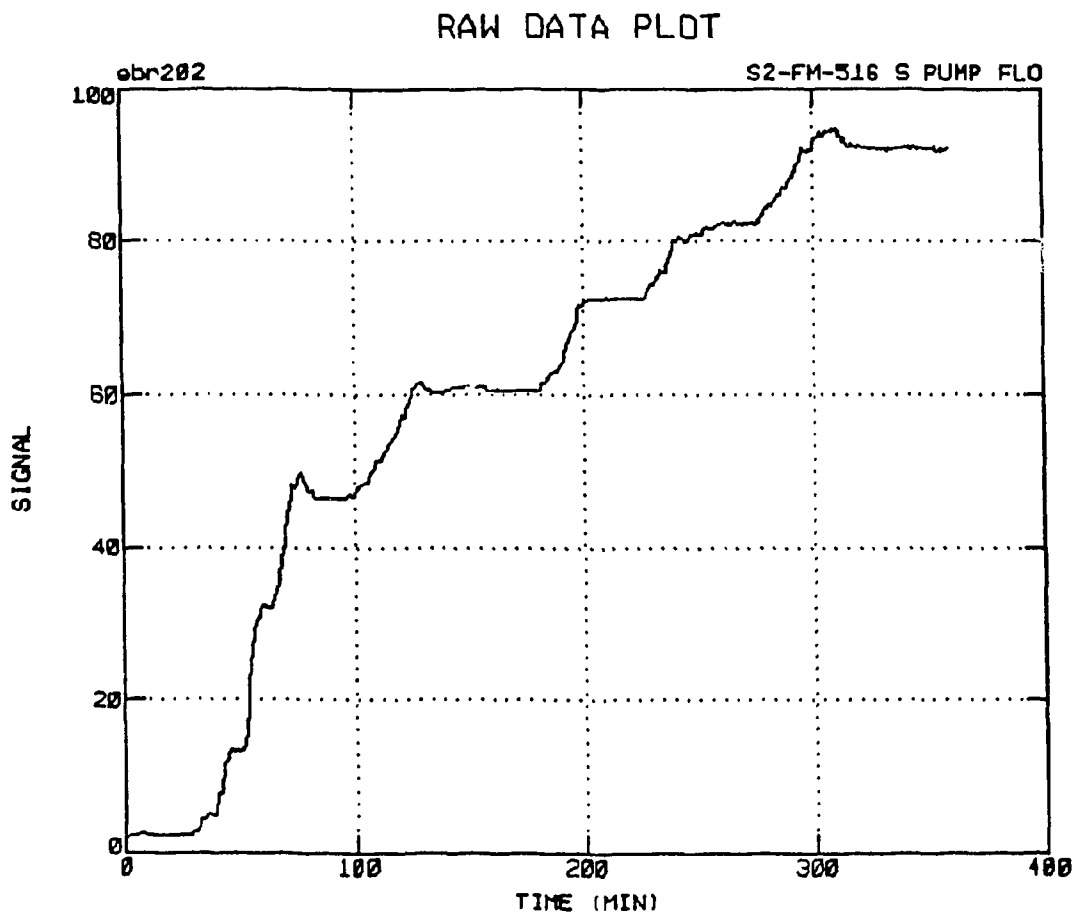

Fig. 23. (continued)

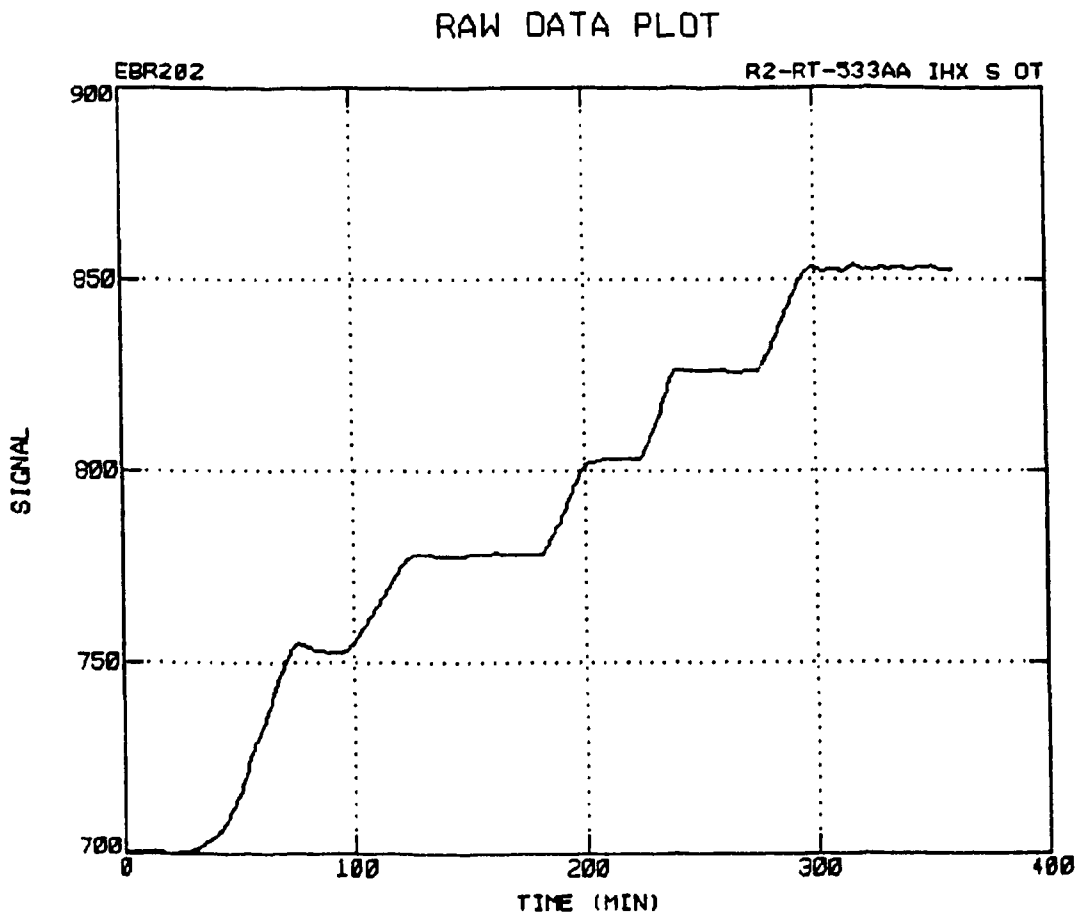

Fig. 2.3. (continued)

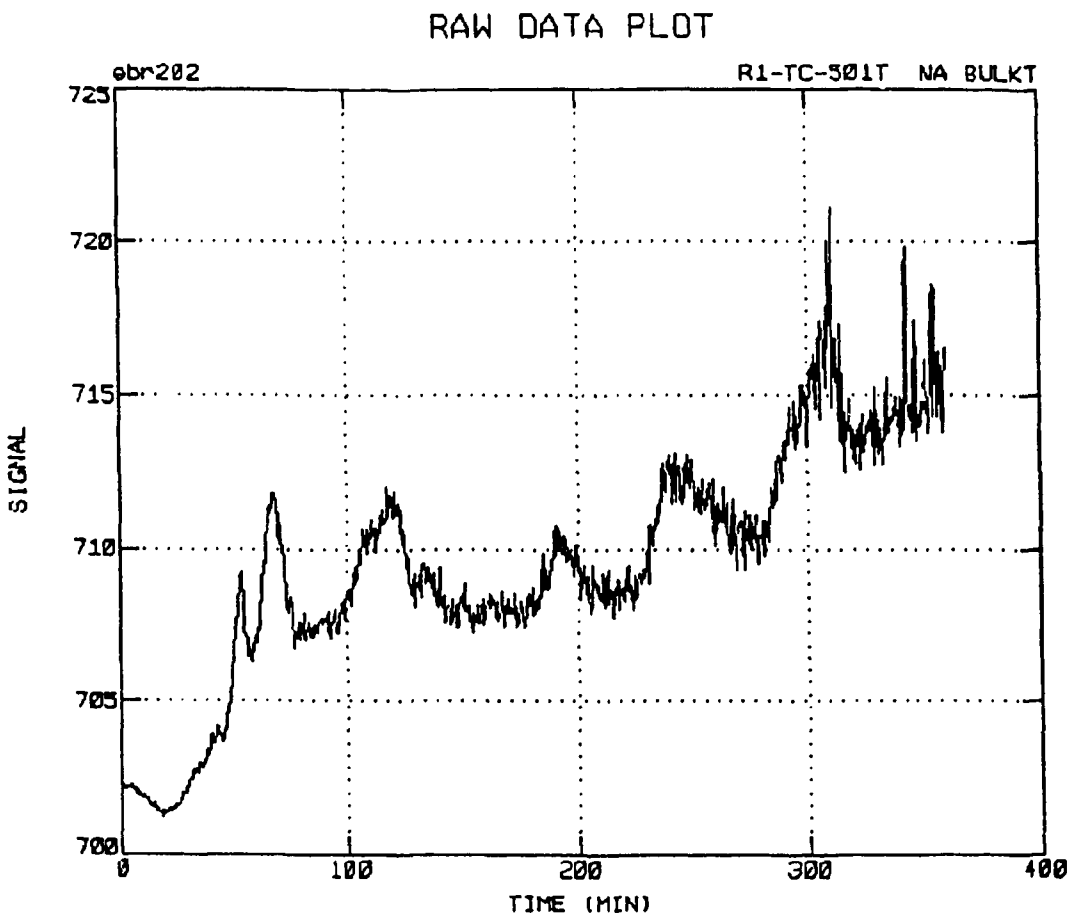

Fig. 2.3. (continued)

Table 2.1. Experimental Breeder Reactor-II process signals
(154 data channels, 4300 data samples per channel,
5.0-s sampling interval)

Signal	Sensor tag	Signal description[a]
1	R1-NLC-580	Power level (%)
2	P1-NLC-581	Power level (%)
3	P1-NLC-582	Power level (%)
4	P1-BAM-594A	Control rod 1 position (in)
5	P1-BAM-594C	Control rod 3 position (in)
6	P1-BAM-594D	Control rod 4 position (in)
7	P1-BAM-594E	Control rod 5 position (in)
8	P1-BAM-594G	Control rod 7 position (in)
9	P1-BAM-594K	Control rod 9 position (in)
10	P1-BAM-594L	Control rod 10 position (in)
11	P1-BAM-594M	Control rod 11 position (in)
12	P1-BAM-594N	Control rod 12 position (in)
13	R1-FM-512B	Primary pump 2 out flow (%)
14	R1-FM-513B	Low-pressure plenum 2 flow (%)
15	R1-FM-541E	Primary total flow (%)
16	R1-DPT-521A	Upper-plenum flow (%)
17	R1-DPT-521B	Upper-plenum flow (%)
18	R1-DPT-521A	Upper-plenum pressure (psia)
19	R1-DPT-521B	Upper-plenum pressure (psia)
20	R1-PT-522A	Primary pump 2 pressure (psi)
21	R1-TC-540AR	Low-pressure plenum sodium temperature (°F)
22	R1-TC-540AS	Low-pressure plenum sodium temperature (°F)
23	R1-TC-540AV	Low-pressure plenum sodium temperature (°F)
24	R1-TC-540AA	High-pressure plenum sodium temperature (°F)
25	R1-TC-503AA	Reactor core exit temperature (°F)
26	R1-TC-503H	Reactor core exit temperature (°F)
27	R1-TC-503E	Reactor core exit temperature (°F)
28	R1-TC-503D	Reactor core exit temperature (°F)

Table 2.1 (continued)

Signal	Sensor tag	Signal description[a]
29	R1-TC-503P	Reactor core exit temperature (°F)
30	R1-TC-503K	Reactor core exit temperature (°F)
31	R1-TC-503F	Reactor core exit temperature (°F)
32	R1-TC-503C	Reactor core exit temperature (°F)
33	R1-TC-503T	Reactor core exit temperature (°F)
34	R1-TC-503G	Reactor core exit temperature (°F)
35	R1-TC-503AC	Reactor core exit temperature (°F)
36	R1-TC-503Z	Reactor core exit temperature (°F)
37	R1-TC-503V	Reactor core exit temperature (°F)
38	R1-TC-503Q	Reactor core exit temperature (°F)
39	R1-TC-503Y	Reactor core exit temperature (°F)
40	R1-TC-503N	Reactor core exit temperature (°F)
41	R1-TC-503AB	Reactor core exit temperature (°F)
42	R1-TC-503AD	Reactor core exit temperature (°F)
43	R1-TC-503R	Reactor core exit temperature (°F)
44	R1-TC-503X	Reactor core exit temperature (°F)
45	R1-TC-503W	Reactor core exit temperature (°F)
46	R1-TC-503A	Upper-plenum temperature (°F)
47	R1-TC-521B	Upper-plenum temperature (°F)
48	R1-TC-521C	Upper-plenum temperature (°F)
49	R1-TC-521D	Upper-plenum temperature (°F)
50	R1-TC-521E	Upper-plenum temperature (°F)
51	R1-TC-521F	Upper-plenum temperature (°F)
52	R1-TC-521G	Upper-plenum temperature (°F)
53	R1-TC-521H	Upper-plenum temperature (°F)
54	R1-TC-507CC	IHX orifice plate temperature (°F)
55	R1-TC-507BX	IHX orifice plate temperature (°F)
56	R1-TC-507EF	IHX orifice plate temperature (°F)

Table 2.1 (continued)

Signal	Sensor tag	Signal description[a]
57	R1-TC-507CA	IHX orifice plate temperature (°F)
58	R1-TC-507CG	IHX orifice plate temperature (°F)
59	R1-TC-507AC	IHX primary outlet temperature (°F)
60	R1-TC-507AE	IHX primary outlet temperature (°F)
61	R1-TC-540AM	IHX primary outlet temperature (°F)
62	R1-TC-540AP	IHX primary outlet temperature (°F)
63	R1-TC-501T	Bulk sodium pool temperature (°F)
64	R1-TC-501X	Bulk sodium pool temperature (°F)
65	R1-TC-501AA	Bulk sodium pool temperature (°F)
66	R1-TC-501D	Bulk sodium pool temperature (°F)
67	R1-TC-501M	Bulk sodium pool temperature (°F)
68	R1-TC-501V	Bulk sodium pool temperature (°F)
69	R1-TC-501H	Bulk sodium pool temperature (°F)
70	R1-TC-501E	Bulk sodium pool temperature (°F)
71	R1-TC-501N	Bulk sodium pool temperature (°F)
72	R1-TC-501W	Bulk sodium pool temperature (°F)
73	R1-TC-501Z	Bulk sodium pool temperature (°F)
74	R1-TC-501F	Bulk sodium pool temperature (°F)
75	R1-TC-501P	Bulk sodium pool temperature (°F)
76	R2-RT-533AA	IHX secondary outlet temperature (°F)
77	R2-RT-546A	IHX secondary outlet temperature (°F)
78	B2-TC-508A	Superheater sodium inlet header temperature (°F)
79	B2-TC-546H	Superheater sodium inlet header temperature (°F)
80	B2-TC-546J	Superheater sodium inlet header temperature (°F)
81	B2-TC-546L	Superheater 710 sodium inlet temperature (°F)
82	B2-TC-546K	Superheater 710 sodium inlet temperature (°F)
83	B2-TC-546N	Superheater 712 sodium inlet temperature (°F)
84	B2-TC-546P	Superheater 712 sodium inlet temperature (°F)

Table 2.1 (continued)

Signal	Sensor tag	Signal description[a]
85	B2-TC-546Q	Superheater 712 sodium inlet temperature (°F)
86	B2-TC-555B	Superheater 710 sodium inlet temperature (°F)
87	B2-TC-546S	Superheater 710 sodium inlet temperature (°F)
88	B2-TC-546BB	Superheater 710 sodium inlet temperature (°F)
89	B2-TC-546U	Superheater 712 sodium inlet temperature (°F)
90	B2-TC-546BC	Superheater 712 sodium inlet temperature (°F)
91	B2-TC-546D	Superheater 712 sodium inlet temperature (°F)
92	B2-TC-546AA	Evaporator 701 sodium inlet temperature (°F)
93	B2-TC-546AB	Evaporator 702 sodium inlet temperature (°F)
94	B2-TC-546AC	Evaporator 703 sodium inlet temperature (°F)
95	B2-TC-546BA	Evaporator 704 sodium inlet temperature (°F)
96	B2-TC-546AE	Evaporator 705 sodium inlet temperature (°F)
07	B2-TC-546AK	Evaporator 705 sodium inlet temperature (°F)
98	B2-TC-546AF	Evaporator 707 sodium inlet temperature (°F)
99	B2-TC-546AG	Evaporator 708 sodium inlet temperature (°F)
100	B2-TC-555E	Evaporator 701 sodium outlet temperature (°F)
101	B2-TC-555F	Evaporator 702 sodium outlet temperature (°F)
102	B2-TC-545AH	Evaporator 702 sodium outlet temperature (°F)
103	B2-TC-555G	Evaporator 703 sodium outlet temperature (°F)
104	B2-TC-555H	Evaporator 704 sodium outlet temperature (°F)
105	B2-TC-546AD	Evaporator 704 sodium outlet temperature (°F)
106	R1-TC-555K	Evaporator 705 sodium outlet temperature (°F)
107	R1-TC-546AJ	Evaporator 705 sodium outlet temperature (°F)
108	R1-TC-555E	Evaporator 707 sodium outlet temperature (°F)
109	B2-TC-555P	Evaporator 708 sodium outlet temperature (°F)
110	R2-TC-546AR	IHX secondary inlet temperature (°F)
111	R2-RT-533BB	IHX secondary inlet temperature (°F)
112	B2-FM-539	Superheater 710 sodium outlet flow (V)

Table 2.1 (continued)

Signal	Sensor tag	Signal description[a]
113	B2-FM-539	Superheater 712 sodium outlet flow (V)
114	B2-FM-538	Evaporator 704 sodium inlet flow (V)
115	B2-FM-538	Evaporator 705 sodium inlet flow (V)
116	S2-FM-516	Secondary pump inlet flow (%)
117	B2-PT-527	Superheater sodium inlet pressure (psi)
118	P3-PT-501A	Turbine inlet pressure (psi)
119	P3-FT-587	Blowdown flow (lb_m/h)
120	S5-LT-596	Steam drum level (in.)
121	B3-PT-505	Steam drum pressure (psig)
122	P3-FT-590	Steam drum feedwater flow (lb_m/h)
123	B5-PT-594	Steam drum feedwater flow (lb_m/h)
124	B5-PR-503	Steam drum feedwater pressure (psi)
125	P5-TC-552	Steam drum feedwater temperature (°F)
126	B5-RTT-1600	Steam drum feedwater temperature (°F)
127	B5-TC-555S	Evaporator 701 feedwater temperature (°F)
128	B5-TC-555T	Evaporator 702 feedwater temperature (°F)
129	R1-TC-555V	Evaporator 703 feedwater temperature (°F)
130	B5-TC-555W	Evaporator 704 feedwater temperature (°F)
131	B3-TC-546AZ	Evaporator 704 feedwater temperature (°F)
132	R1-TC-555X	Evaporator 705 feedwater temperature (°F)
133	R1-TC-546AS	Evaporator 705 feedwater temperature (°F)
134	B3-TC-546AT	Evaporator 705 feedwater temperature (°F)
135	R1-TC-555Z	Evaporator 707 feedwater temperature (°F)
136	B5-TC-555AA	Evaporator 708 feedwater temperature (°F)
137	B3-TC-555AB	Evaporator 701 steam outlet temperature (°F)
138	B3-TC-555AC	Evaporator 702 steam outlet temperature (°F)
139	B3-TC-555AD	Evaporator 703 steam outlet temperature (°F)
140	B3-TC-555AE	Evaporator 704 steam outlet temperature (°F)

Table 2.1 (continued)

Signal	Sensor tag	Signal description[a]
141	B3-TC-555AF	Evaporator 705 steam outlet temperature (°F)
142	B3-TC-555AH	Evaporator 707 steam outlet temperature (°F)
143	B3-TC-555AK	Evaporator 708 steam outlet temperature (°F)
144	B3-TC-546AU	Superheater 710 steam inlet temperature (°F)
145	B3-TC-546AV	Superheater 712 steam inlet temperature (°F)
146	B3-TC-546AW	Superheater 710 steam outlet temperature (°F)
147	B3-TC-555AN	Superheater 710 steam outlet temperature (°F)
148	B3-TC-546AX	Superheater 712 steam outlet temperature (°F)
149	B3-TC-555AQ	Superheater 712 steam outlet temperature (°F)
150	B3-PT-520	Superheater outlet pressure (psig)
151	P5-FT-580	Superheater outlet flow (lb_m/h)
152	P3-PT-588	Turbine inlet steam flow (lb_m/h)
153	P3-PT-501B	Turbine inlet steam pressure (psig)
154	P3-TC-545	Turbine inlet steam temperature (°F)

[a]IHX = intermediate heat exchanger.

3. ADVANCED AUTOMATION CONCEPTS

Automatic control systems can improve overall performance as well as increase the reliability and availability in system operations. Recently, interest has increrased in automating nuclear power stations to reduce human involvement and operating errors during routine reactor operations. The existing commercial power plants make use of automatic control with applications continuously extending toward new goals. However, it has not yet been possible to implement an automatic control that can incorporate all of the routine modes of operation of a nuclear reactor. This limitation is due to the large variations in conditions and configurations among the different modes of operation and the complexity involved in the corresponding procedures. The available technology requires operator intervention for discrete-event control between the different modes of continuous processes.

The design presented in this paper has a general architecture applicable to any mode of plant operation. The primary goal has been to develop an intelligent environment to integrate control, diagnostics and monitoring aspects. The proposed system, however, includes modules that require a set of specific knowledge of the operation (mode). Thus, it is a general design that can be tailored for a specified task. A high-level decision-making system can be incorporated to supervise goal switching (i.e., from startup to steady state) to enlarge the scope of operations. Section 3.1 describes the details of the integrated control system, its general architecture, and its application to a particular task, namely the automation of EBR-II startup.

3.1 DEFINITION OF CONTROL ENGINE

The conceptual environment including the necessary functional blocks is shown in Fig. 3.1. This architecture is called the Integrated Control System (ICS) which incorporates innovative concepts in monitoring, diagnostics, and control. The ICS is equipped with artificial-intelligence (AI) methods for decision making, verification, and validation. Advanced control methods are used for a multivariate, nonlinear plant control.

3.1.1 Signal Validation

This function block contains multiple methods for processing raw sensor data and generating validated data prepared for specific use. It is envisioned that multiple validation techniques will be used concurrently to observe the data. An intelligent supervisor then evaluates the outcomes of the various techniques to arrive at a validity parameter. Data sample and validated parameter are broadcast to a specified destination.

3.1.2 Command Validation

The objective of the command validation block is to determine the accuracy of the command generated by the control system or by the operator and to validate the resulting output of the actuator system. A command validator as a distinct function is a relatively new concept to process control. It parallels, to some extent, sensor signal validation. The overall command validation involves verification of control signal input (to actuator) and

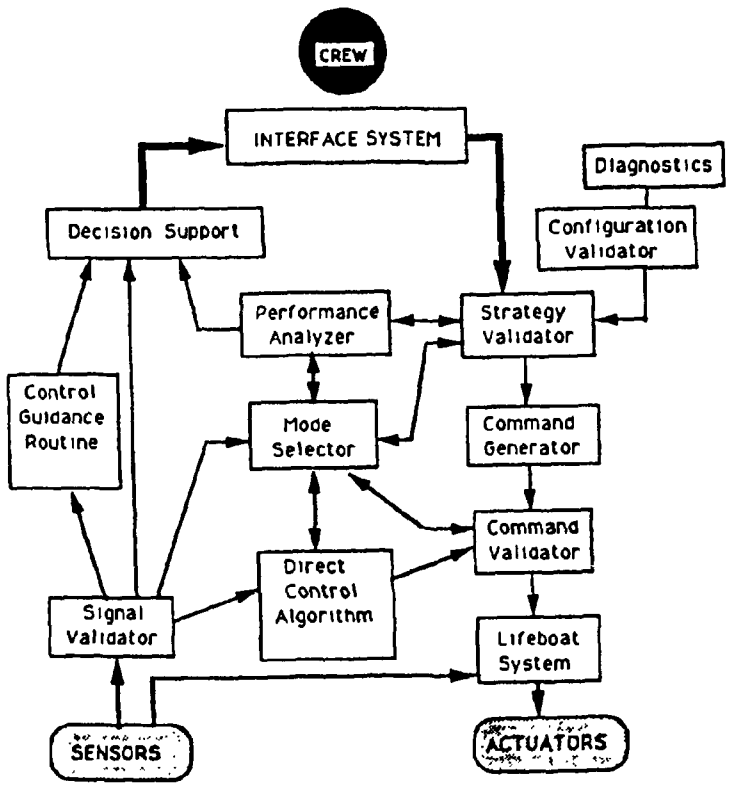

Fig. 3.1. General architecture of the integrated control system.

actuator system output (plant response). For illustration, the classic example of a command validator is the conflict resolver circuit of a traffic-light controller. Should the timers and phase sequencers produce simultaneous *green* lights at an intersection, the conflict resolver overrides the situation to produce flashing *red* or *yellow* lights.

A definition of the requirement for valid control strategy is that the controller's output to the actuator and the actuator's output must remain within certain bounds of a desired strategy or trajectory. The procedure for command validation consists of (1) identifying faulty control signals, (2) isolating plant component malfunction, and (3) quantifying the control signal's variation from the nominal value.

3.1.3 Configuration Validator

This function block identifies the current plant mode and subsystem operability status. The data generated consists of current mode of each subsystem, current status of each piece of equipment (e.g., in-operation, available/unavailable, undermaintenance, and faulted), and look-ahead status (i.e., planned outage).

3.1.4 Strategy Validator

This function block determines whether the current strategy in use by the control system (or operator) is valid for the conditions of the plant and the desired objective. This form of validation answers questions such as (1) Does the current strategy suit the current configuration of the system? (2) Are there any expected critical points in the chosen strategy? (3) Are there any alternative strategies in case of anomalies? and (4) Are the future control actions appropriate for the current operation?

3.1.5 Direct Control Algorithm

This function block houses the continuous control algorithms for all systems employed during the operation. The control algorithms must be robust to handle the wide range of conditions and parameter variations encountered during operation. This block contains algorithms that operate in parallel and use different sets of plant measurement to provide an alternative control solution in case of corrupted signals feeding into the on-line algorithm. Provided the outputs of all other control algorithms are valid and jump conditions exist, the on-line algorithm can be shifted to one that is not affected by the measurement corruption. This block also includes different algorithms for different modes of operation (such as steady-state control and startup control). The direct control block and the guidance block differs only between the manual and automatic modes of control.

3.1.6 Mode Selector

The mode selector controls the discrete changes required by the specifics of an operation(s). It can change the mode of the direct control algorithm block or the plant directly by actuating pumps, motors, aligning block, and isolation valves to distinct configurations. The mode selector's task includes on-line manipulation of parallel-control algorithms in case of anomalies in the measurement or command set.

3.1.7 Performance Analyzer

This function block identifies failures and deteriorating performance in the major components and subsystems of the plant. Performance of various systems is tracked and compared with tolerance limits. Various tests can be performed to detect long-term problems such as bearing wear, tube leak, and heat-exchanger fouling.

3.1.8 Lifeboat System

The *lifeboat* concept is that of a simple controller employing a simple algorithm designed to bring the specific system under its scope of control to a preestablished safe and stable state. The lifeboat system is implemented on separate hardware from the remainder of the startup control system. Thus, hardware (or software) failures in the principal controller are captured by the lifeboat and not allowed to propagate through the process. Because the lifeboat is functionally upstream from the actuators, it is reasonable that the lifeboat module also functions as a local hand-automatic (H/A) station.

3.1.9 Decision Support

This block contains the information system to support the operator's decision-making process. Included in the block are the procedure prompting system and an intelligent planning system. The decision support system provides also an advanced operator interface for monitoring the key variables of the plant and the status of each block of the ICS.

4. APPLICATION TO EXPERIMENTAL BREEDER REACTOR-II STARTUP

This section describes a preliminary ICS design for the EBR-II startup operation. The ICS, as shown in Fig. 4.1, includes some of the major function blocks explained earlier. Detailed structures of these blocks are explained in the following text. The control design and simulation studies use the software systems MATRIXx and SYSTEM-BUILD (ISI 1989). The ICS blocks are developed with the use of SYSTEM-BUILD model building blocks. These details are also provided in the following sections.

Recent accomplishments at EBR-II include automatic power increase capability between 20 and 62.5 MW(t) using Bailey digital controllers. However, no supervisory approach exists to coordinate multi-input/output (MIMO) control, diagnostics, and validation for the startup operation. Some areas are reported to be potentially open for advanced methods (personal communication, 1988 letter from G. Lentz, Argonne National Laboratory, Argonne, Illinois, and May 1988 meeting with R. Kisner, Oak Ridge National Laboratory, Oak Ridge, Tennessee). These areas are

1. startup reactivity monitoring capability to determine control rod worth and movement and core configuration (such systems must compare these measurements and calculations against limits);

2. technical specification (tech spec) monitoring system that determines from measurements whether a tech spec has been violated and to a limited extent whether the plant is approaching a tech spec limit; and

3. any other system that leads improved performance, reduced cost, and improved safety.

The objectives in designing an advanced control system may

1. increase availability by reducing operator error and plant trips;
2. reduce startup time [currently requires 1 week to bring balance-of-plant (BOP) from ambient to hot standby, 4 h to bring the reactor to zero power conditions, 4 h to bring reactor and BOP to power operation, and 9 h to bring the turbine-generator on line (may be parallel with other BOP startup activities)];
3. decrease crew size [current crew size is ~12, of which 8 are actually active: 4 operators are required for reactor startup (2 console, 1 plant watch, 1 helper), >4 operators are needed for BOP startup];
4. minimize highly repetitive operations;
5. avoid penalties to help operators eliminate tech spec violations; and
6. lower operator stress by implementing effective plant diagnostics and alarm priority systems.

4.1 STARTUP AUTOMATION STRATEGY

EBR-II startup is primarily controlled by two actuators, the control rod bank and EM pump (sodium loop between the secondary side of IHX and sodium side of the steam generator). Several discrete-event control actions are on the steam side of the reactor,

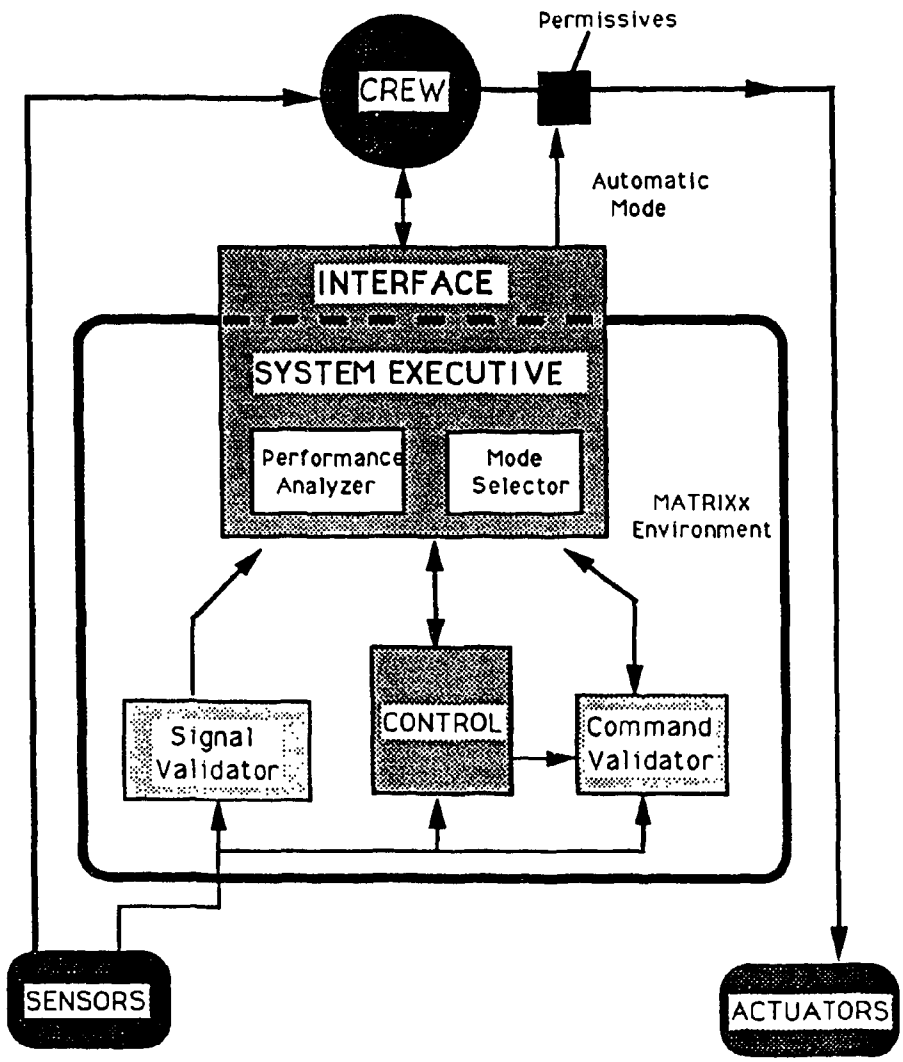

Fig. 4.1. Advanced control system for Experimental Breeder Reactor-II startup. Phase I systems in MATRIXx environment.

most of which consist of one-time actions. These actuators are not remotely controlled, and the control action is taken manually by a plant technician who, in some cases, walks to the physical location of the actuator. Therefore, the steam side of the EBR-II reactor is by no means suitably equipped for automation. System upgrading for remote control on the steam side is considered unnecessarily costly since EBR-II is a small-scale test reactor and the existing operations are verified to be efficient. Thus, the automation control task is reduced to a somewhat limited scale consisting of controlling only the two actuators as stated above.

When the automation task is constrained to one part of the system, the control task may become quite complicated or sometimes impossible, depending on the nature of subsystem couplings. Fortunately, the couplings between EBR-II subsystems do not impose difficulty for the startup task, in particular. The automation strategy for the ICS implementation consists of imitating a previous startup that is considered as the reference. The imitation simply means that the state variables of the EBR-II primary side should follow the trajectories of the reference startup (desired behavior). In addition, the output from the primary side to the steam side should agree with the demand (the reference trajectory) in the existence of a boundary condition(s) that represent the downstream effects on the primary system.

The corresponding coupling in the EBR-II reactor takes place in the piping between the IHX and steam generator. The IHX secondary outlet piping carries liquid sodium to the steam generator. Accordingly, the requirement includes following the demand that represents the energy output of the primary system. Energy is characterized by temperature and mass flow rate. Thus, demand is stated in terms of the secondary sodium temperature and flow rate. Other important state variables include the reactor power, core exit temperature, bulk sodium temperature, IHX primary outlet temperature, and primary flow. According to the control technique, some of these variables are selected for trajectory following. However, the controllers are expected to perform such that all state variables are within the desired boundaries.

4.2 SIGNAL VALIDATION

Operational records of the EBR-II indicate several measurement problems encountered in the past. Especially nonredundant measurements such as the secondary sodium flow may sometimes provide misleading information because of sensor degradation or additive noise. Thus, an on-line signal validation capability is necessary for a fault-tolerant control strategy. Table 4.1 lists 16 different measurements that are important to design and implement the ICS. Table 4.1 indicates the redundant and nonredundant measurements. This distinction plays a major role in the signal-validation strategy.

4.2.1 On-line Signal Validation Strategy

The strategy consists of creating a set of *base* signals. Signals obtained from a redundant-measurement set are called base signals. A generalized consistency-checking (GCC) routine verifies the validity of the base signals. In case of an abnormal reading in the set, the corresponding signal is disqualified. The output of the GCC is a reading averaged over the redundant readings that are normal.

Validation strategy includes empirical models to estimate the measurements from the nonredundant sensors. The empirical models are developed off-line from a data set

Table 4.1. Selected signals from Experimental Breeder Reactor-II data acquisition system (to implement integrated control system for automatic startup)

Tag	Base signal[a]	Redundancy	Used by[b]
P1-NLC	Reactor power	3	RID,Fuzzy,PA,SV,CV
R1-TC	Core exit temperature	20	RID,Fuzzy,NNET, SV,CV,PA
R1-TC	IHX primary inlet temperature	5	SV,CV,PA
R1-TC	IHX primary outlet temperature	4	RID,SV,CV
R1-TC	Bulk sodium temperature	13	RID,SV,CV,PA
B2-TC	SU sodium inlet temperature	5	PA
B2-TC	EV sodium outlet temperature	7	PA

Tag	Signal[a]	Redundancy	Used by[b]
P1-BAM594M	Rod position	1	CV
R1-FM-512B	Primary sodium flow	1	RID,PA
R1-TC-540AT	HP plenum temperature	1	NNET
R2-RT-533AA	IHX secondary outlet temperature	1	RID,Fuzzy,NNET
R2-TC-546AR	IXH secondary inlet temperature	1	RID,PA
S2-FM-516	Secondary flow	1	RID,CV,PA
(no tag)	EM pump voltage	1	CV
B3-PT-505	Steam drum pressure	1	PA
P3-FT-588	Turbine inlet flow	1	PA

[a]Definitions (column 2):
- EM = electromagnetic.
- EV = evaporator.
- HP = high-pressure.
- IHX = intermediate heat exchanger.
- SU = superheater.

[b]Definitions (column 4):
- RID = reconstructive inverse dynamics controller.
- Fuzzy = fuzzy controller.
- NNET = neural network controller.
- CV = command validation block.
- SV = signal validation block.
- PA = performance analyzer block.

obtained during a previous startup at EBR-II. This data set includes the base signals. Thus, the empirical models are developed by using only the base signals because the redundant measurements are more reliable than the nonredundant ones. The base signals of this application are indicated in Table 4.1.

The signal validation block (SVB) shown in Fig. 4.1 includes two different routines that check the validity of the signals independently. The first routine uses a nonlinear, process empirical modeling (PEM) technique previously developed (Upadhyaya et al. 1987). The second routine uses a well-known artificial neural network paradigm called the backpropagation network (BPN). This routine was also previously developed for diagnostic purposes (Upadhyaya, Eryurek, and Mathai 1989). Thus, the SVB includes two models (PEM and BPN) for each nonredundant measurement.

Development of the empirical models stated above includes off-line computations. The PEM routine uses a nonlinear curve-fitting method and is known to provide efficient results. PEM is suitable for rapid updating since the development process takes relatively short CPU time. BPN is a learning algorithm that requires off-line training. The training period can be long, thus it is not easily updated. However, BPN is robust against abnormal situations and is also known to be a powerful generalization tool. The different characteristics of the two methods cover a variety of anomalies so that the fault-tolerance can be handled by at least one of the two routines. More detailed information on empirical modeling techniques are given in Sect. 6.

During the on-line implementation, the SVB receives the 16 selected signals. It uses the base signals as the inputs to the models to estimate the rest of the measurements. A comparison takes place between the estimated value and the actual reading. If the deviation exceeds a predefined band, the SVB disqualifies the corresponding signal. The estimation results obtained from the empirical models compared with the actual data are shown in Figs. 4.2a–4.2f. As can be seen from these figures, the SVB functions favorably.

4.3 COMMAND VALIDATION

As described in Sect. 4.2, the purpose of command validation is to provide an intermediate confirmation stage before the commands are sent to the plant actuators. From the practical point of view, the command validation is the same as the signal validation, except the signals to be validated are obtained from the operator, controller, and/or actuator. The concept of command validation covers the failure possibilities of the command-generating components such as the hardware, software and operator.

In application to the EBR-II startup, the command validation task includes two signals, (1) control rod position and (2) voltage applied to the EM pump (determines secondary sodium flow). The command validation block (CVB) shown in Fig. 4.1 uses two empirical models for each command. The routines used for the CVB are the same as those used in the SVB. Similarly, the empirical models in CVB are developed off-line from the available EBR-II startup data. The strategy consists of using the base signals to estimate the commands, which are compared with the actual commands. When a large deviation occurs between the estimated and actual command, CVB disqualifies the corresponding command. Figures 4.3a–4.3f show the CVB estimates of the commands used in the EBR-II startup.

Figure 4.4 shows the MATRIXx/SYSTEM-BUILD implementation of the PEM routine for the estimation of reactor power signal. An example to the BPN

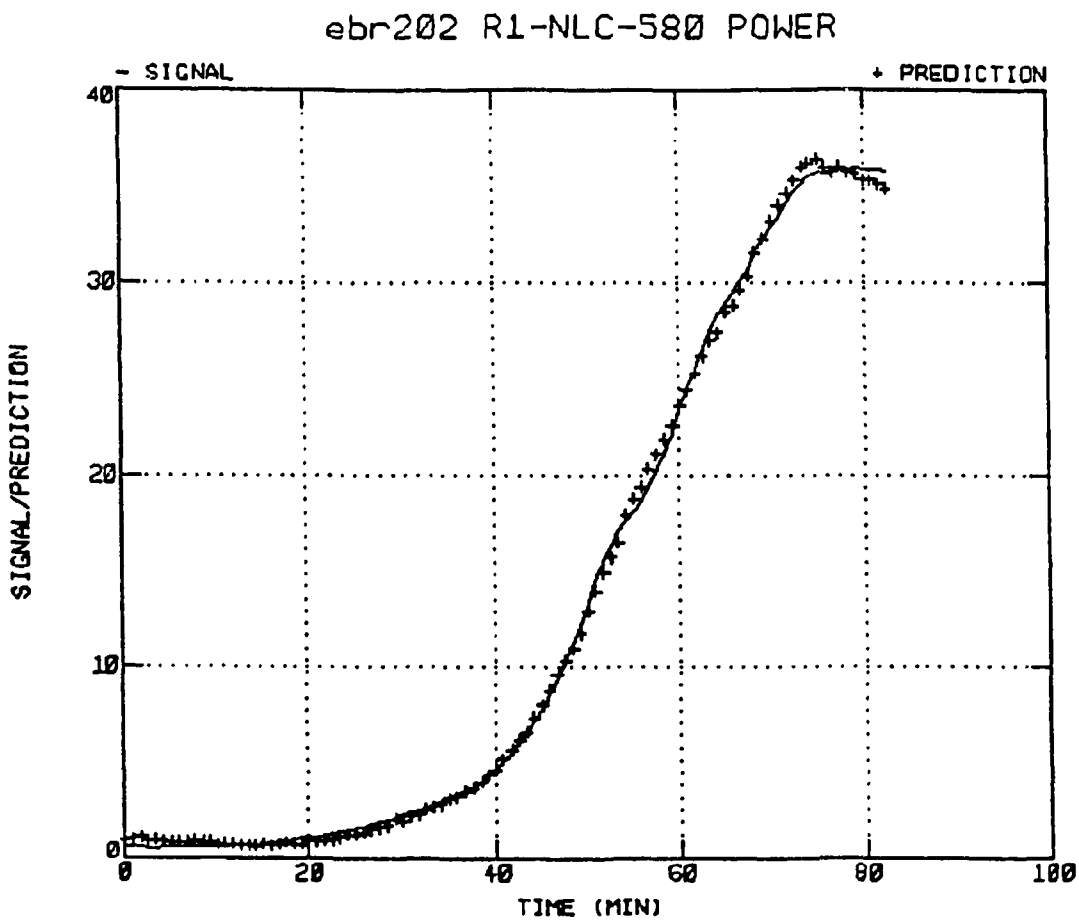

Fig. 4.2a. Process empirical model for power; input signals are reactor exit temperature and intermediate heat exchanger primary outlet temperature; modeling error is 2.11%.

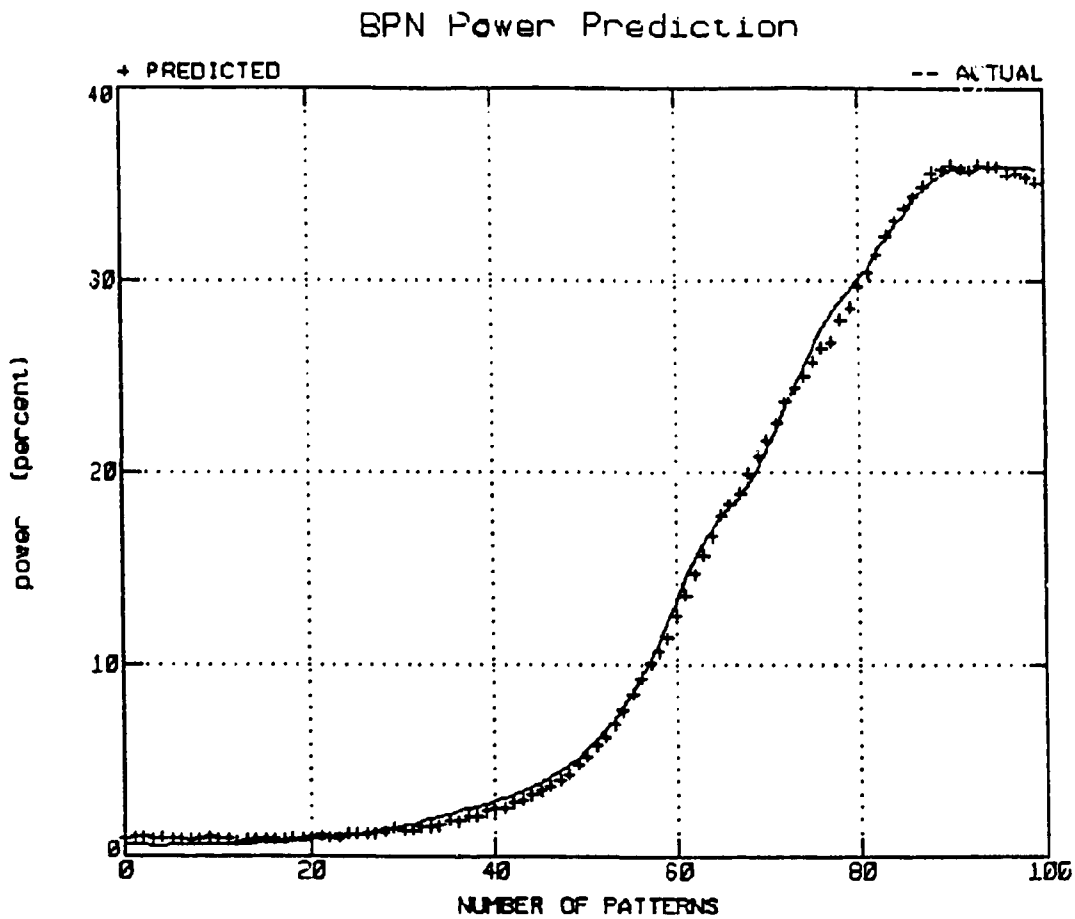

Fig. 4.2b. Backpropagation network model for power; input signals are reactor exit temperature and intermediate heat exchanger primary outlet temperature; modeling error is 2.14%.

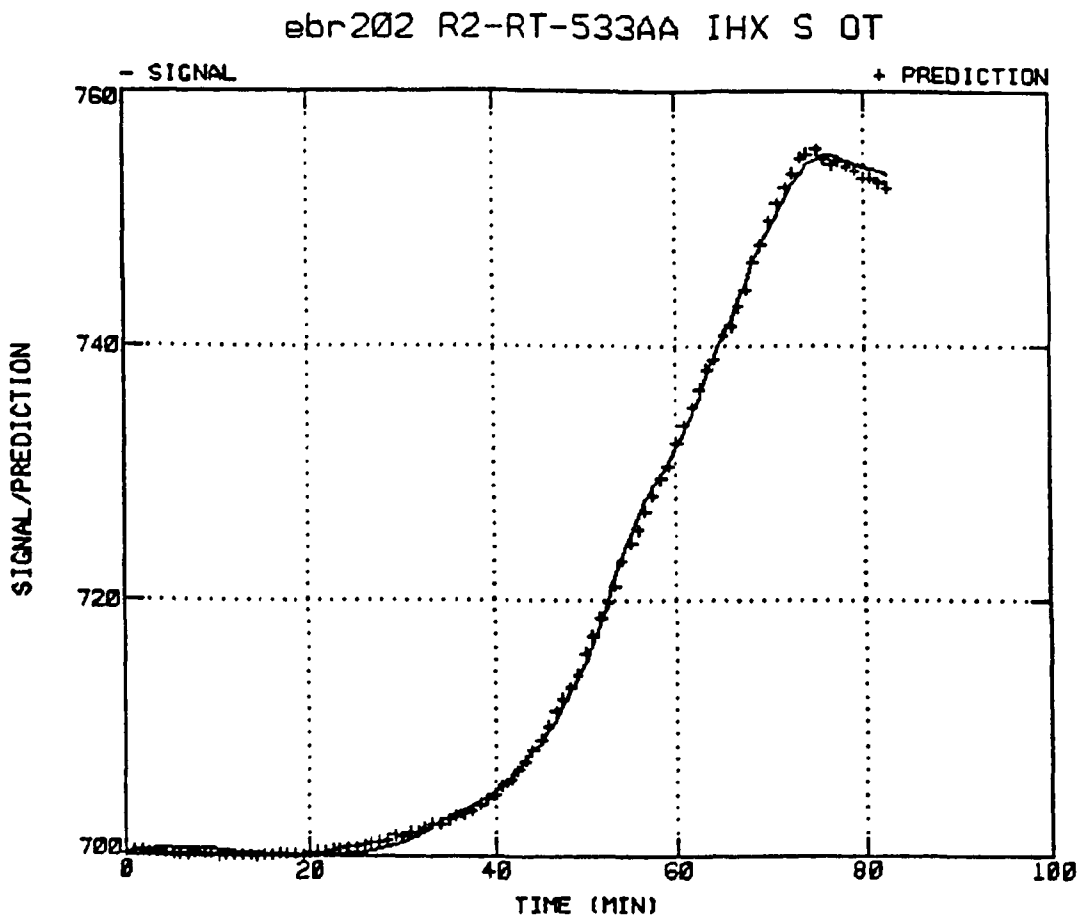

Fig. 4.2c. Process empirical model for intermediate heat exchanger (IHX) secondary outlet temperature; input signals are reactor exit temperature and IHX primary outlet temperature; modeling error is 0.067%.

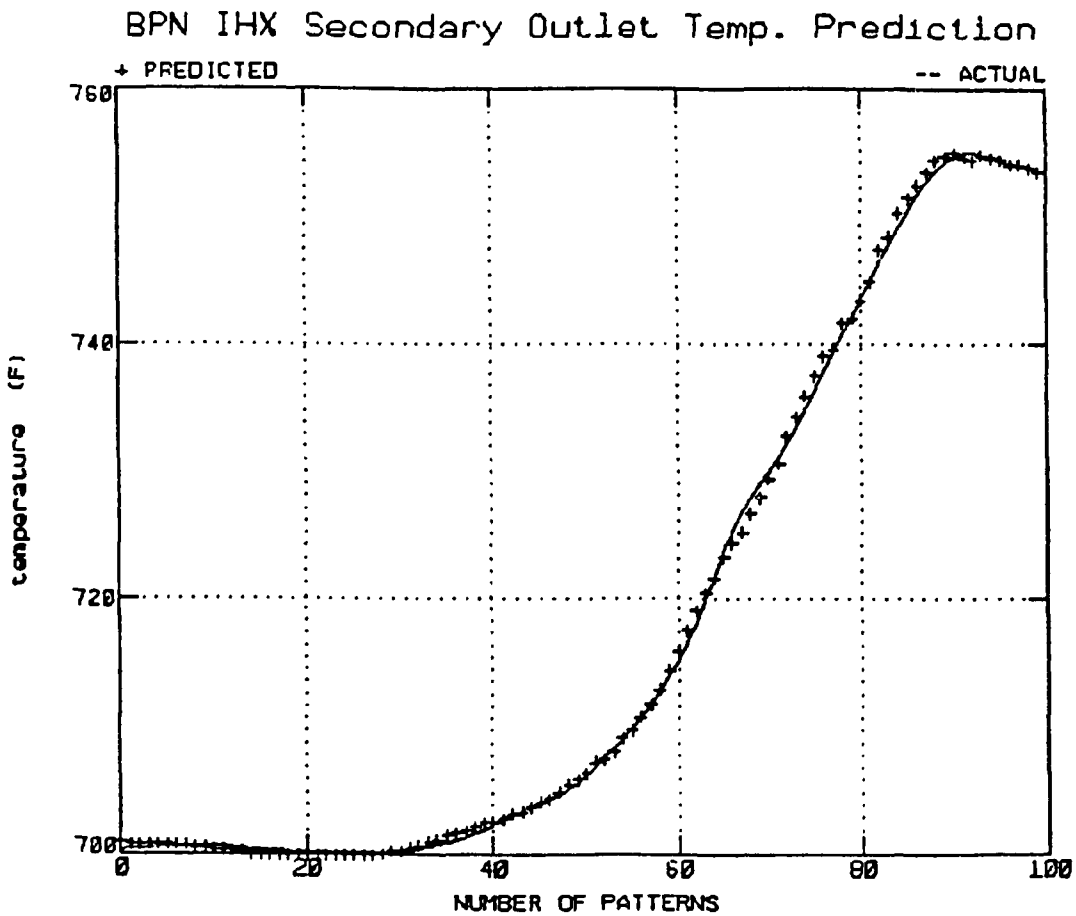

Fig. 4.2d. Backpropagation network model for intermediate heat exchanger (IHX) secondary outlet temperature; input signals are reactor exit temperature and IHX primary outlet temperature; modeling error is 0.071%.

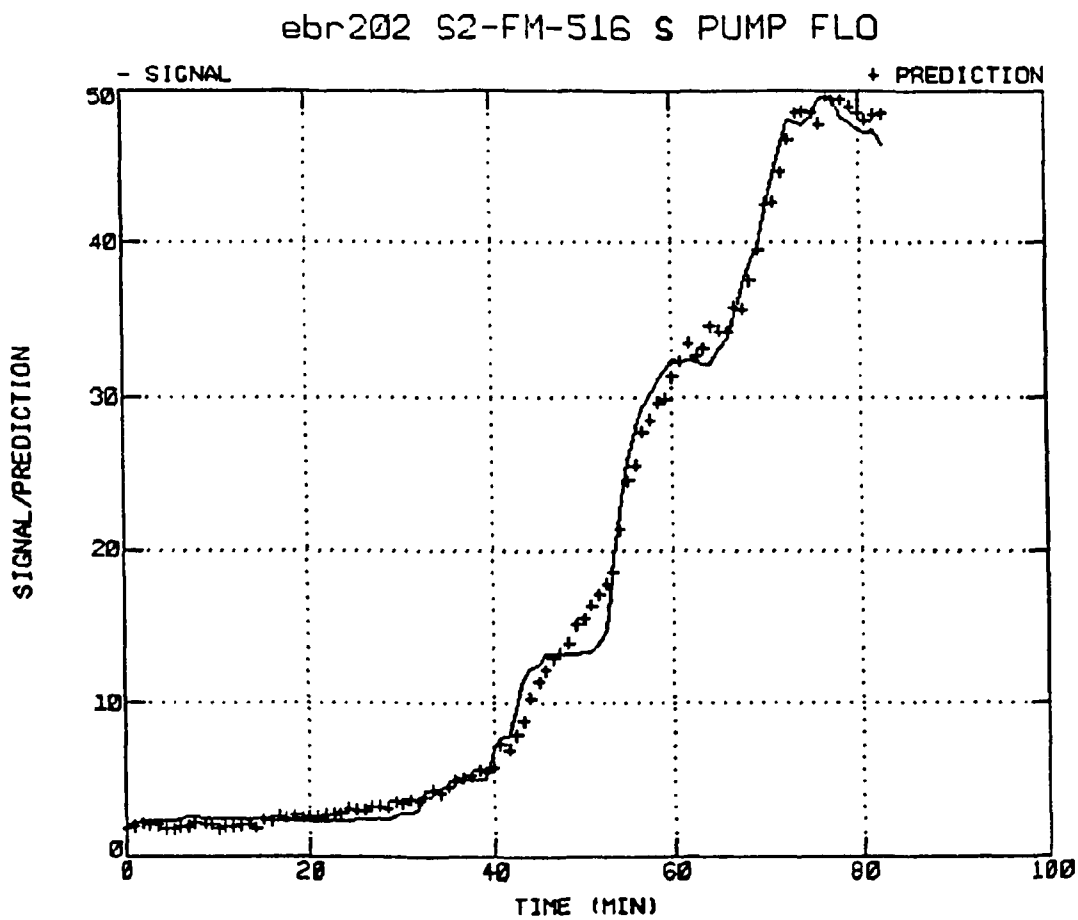

Fig. 4.2e. Process empirical model of secondary sodium flow; input signals are reactor exit temperature and bulk sodium tank temperature; modeling error is 4.54%.

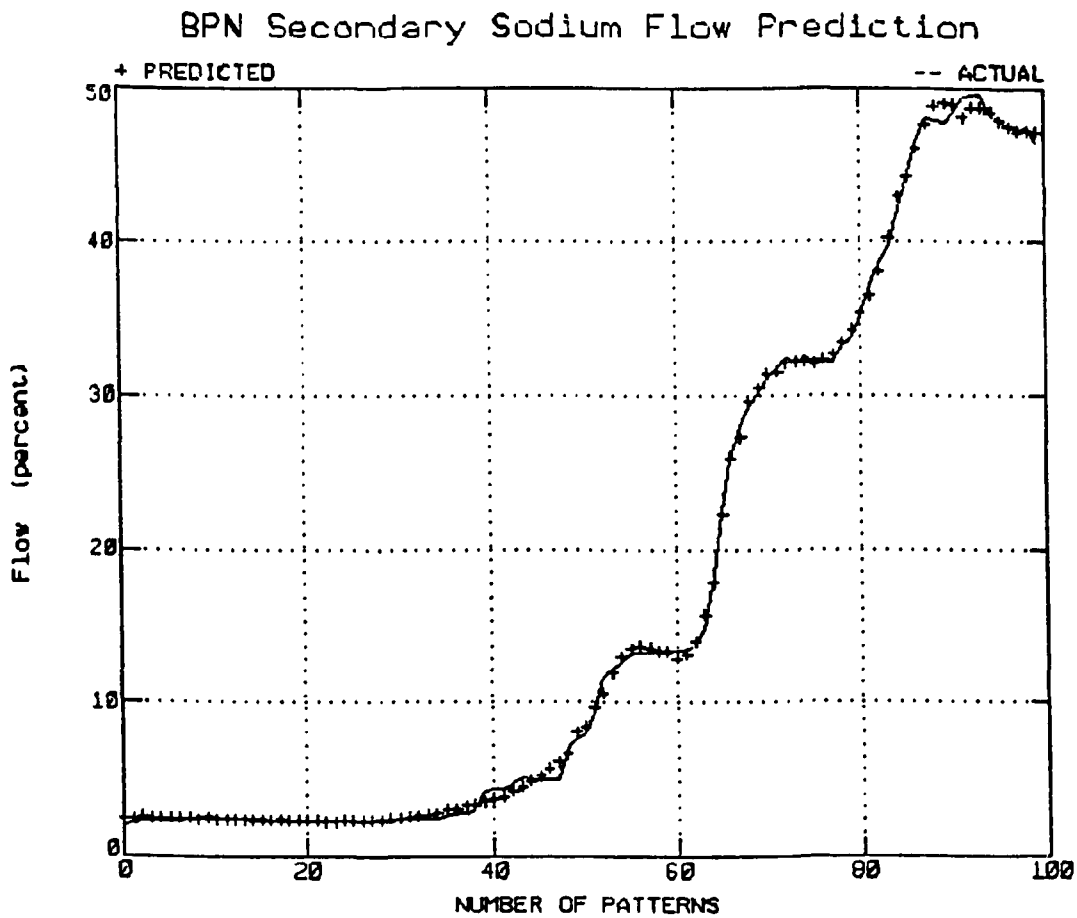

Fig. 4.2f. Backpropagation network model of secondary sodium flow; input signals are reactor exit temperature and bulk sodium temperature; modeling error is 2.23%.

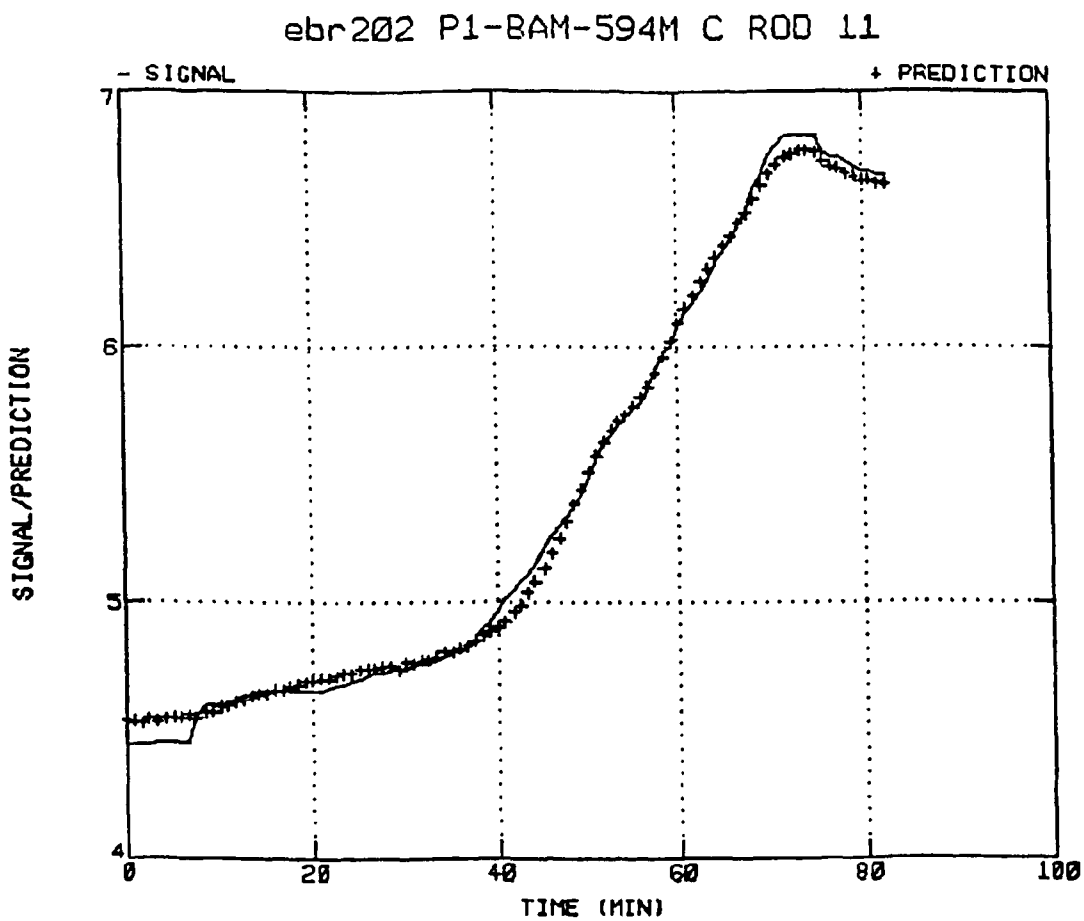

Fig. 4.3a. Process empirical model for control rod position; input signals are power and reactor outlet temperature.

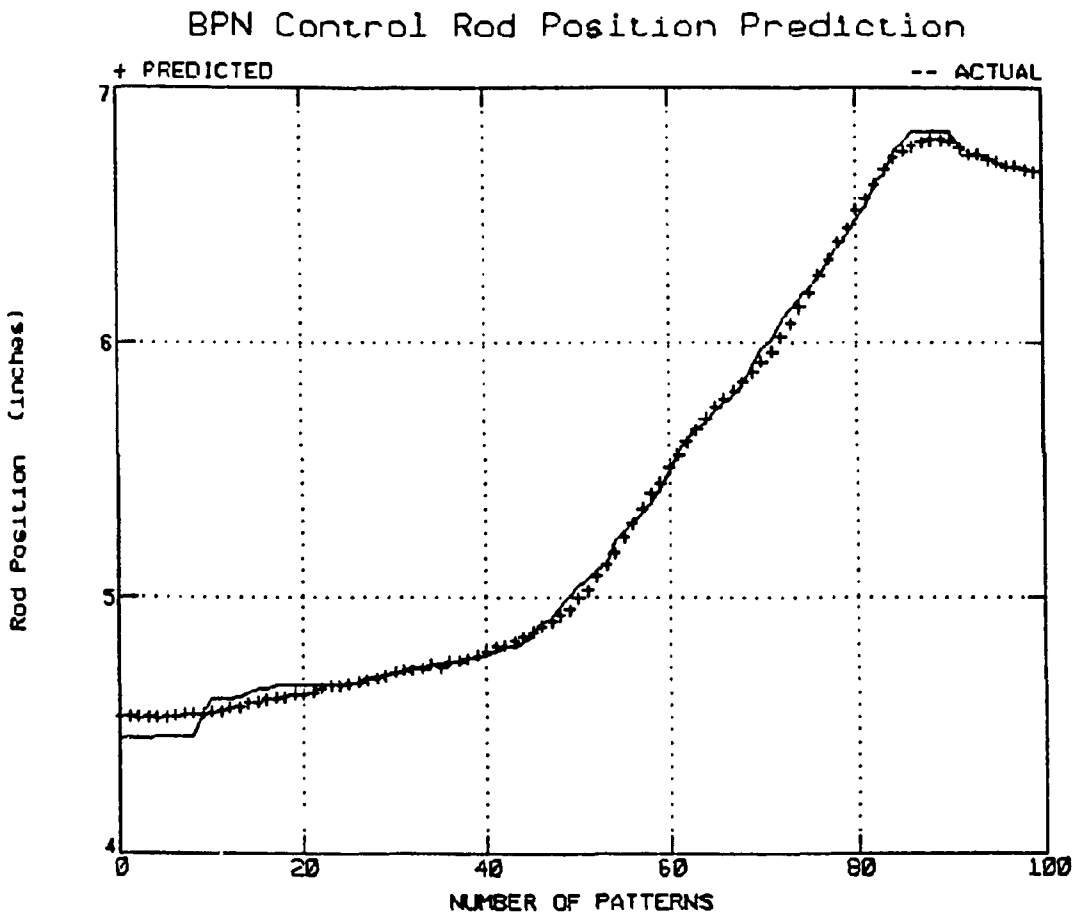

Fig. 4.3b. Backpropagation network model for control rod position; input signals are power and reactor outlet temperature.

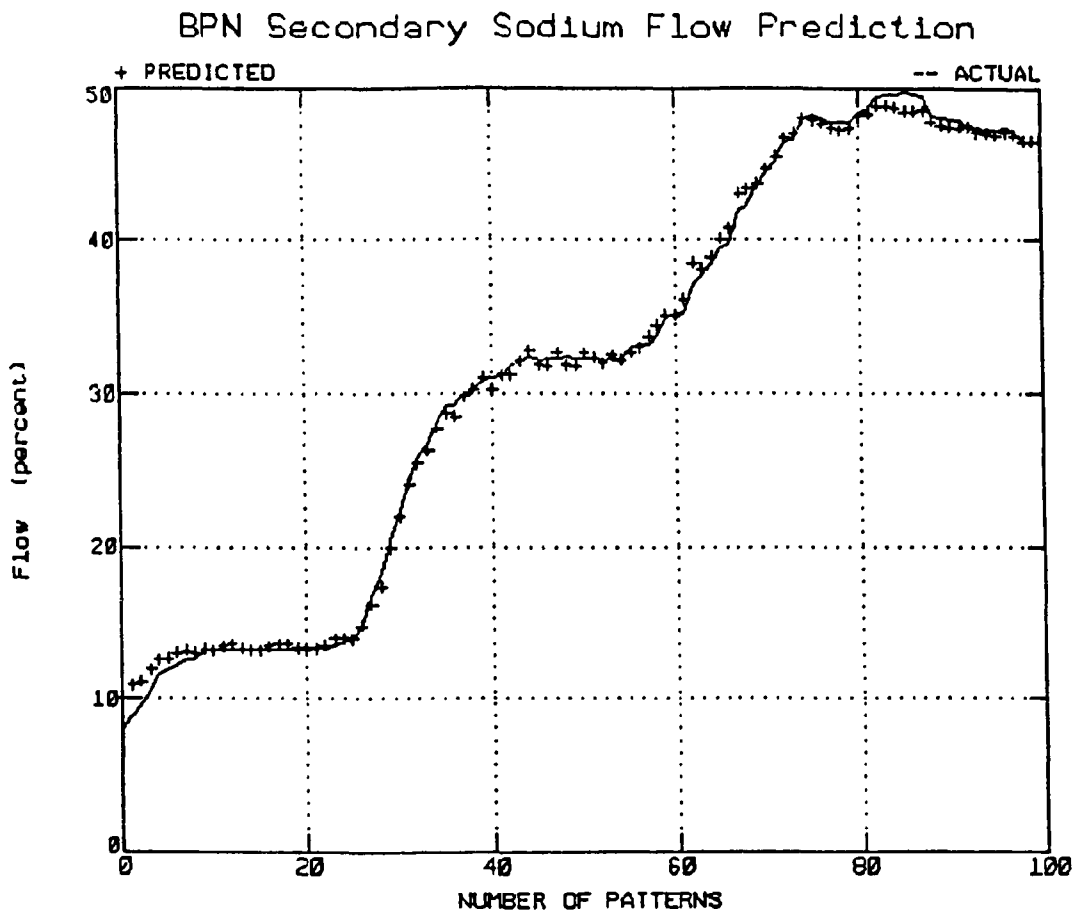

Fig. 4.3c. Backpropagation network model of secondary sodium flow; input signals are electromagnetic (EM) pump voltage and EM pump delta P. This model is used for actuator output validation. The detectable anomaly is the EM pump failure.

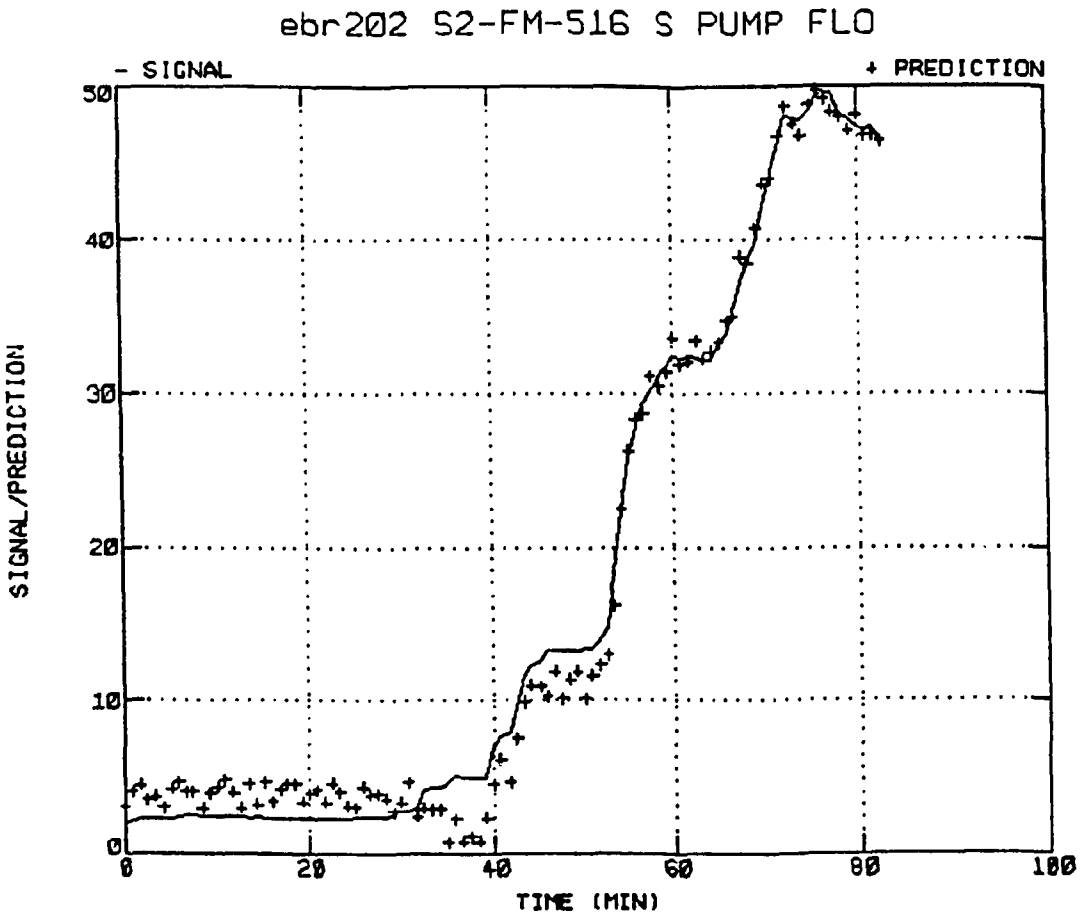

Fig. 4.3d. Process empirical model of secondary sodium flow; input signals are electromagnetic (EM) pump voltage and EM pump delta P.

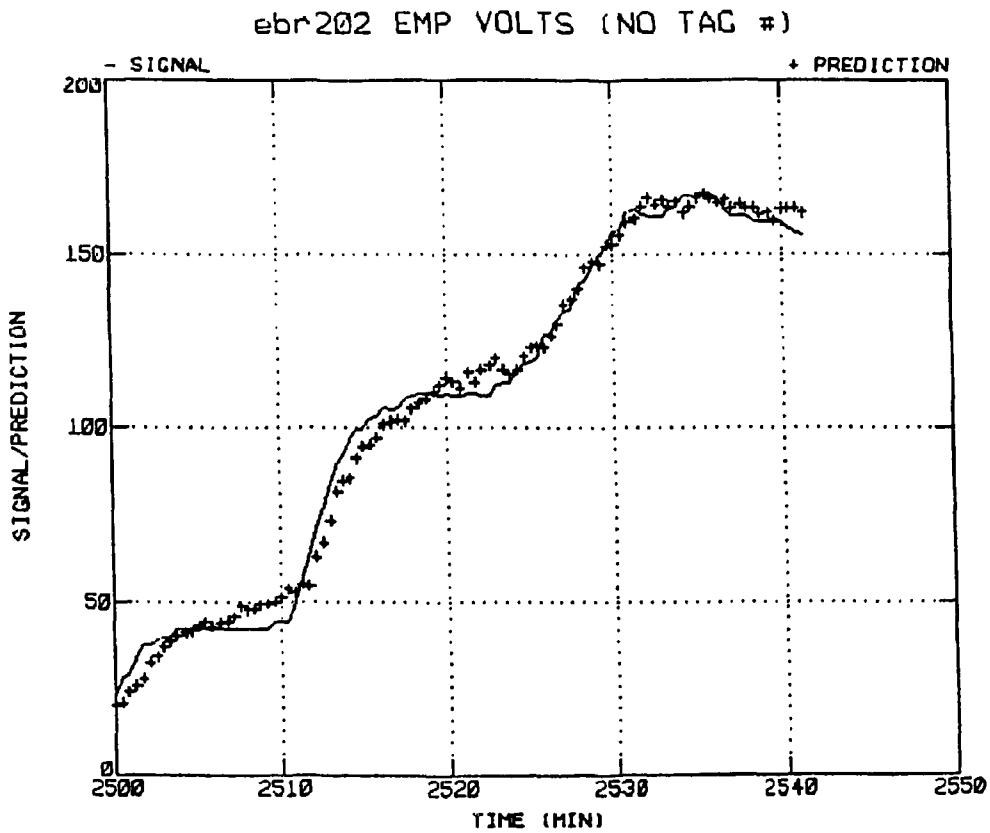

Fig. 4.3e. Process empirical model of electromagnetic pump voltage; input signals are reactor exit temperature and bulk sodium temperature.

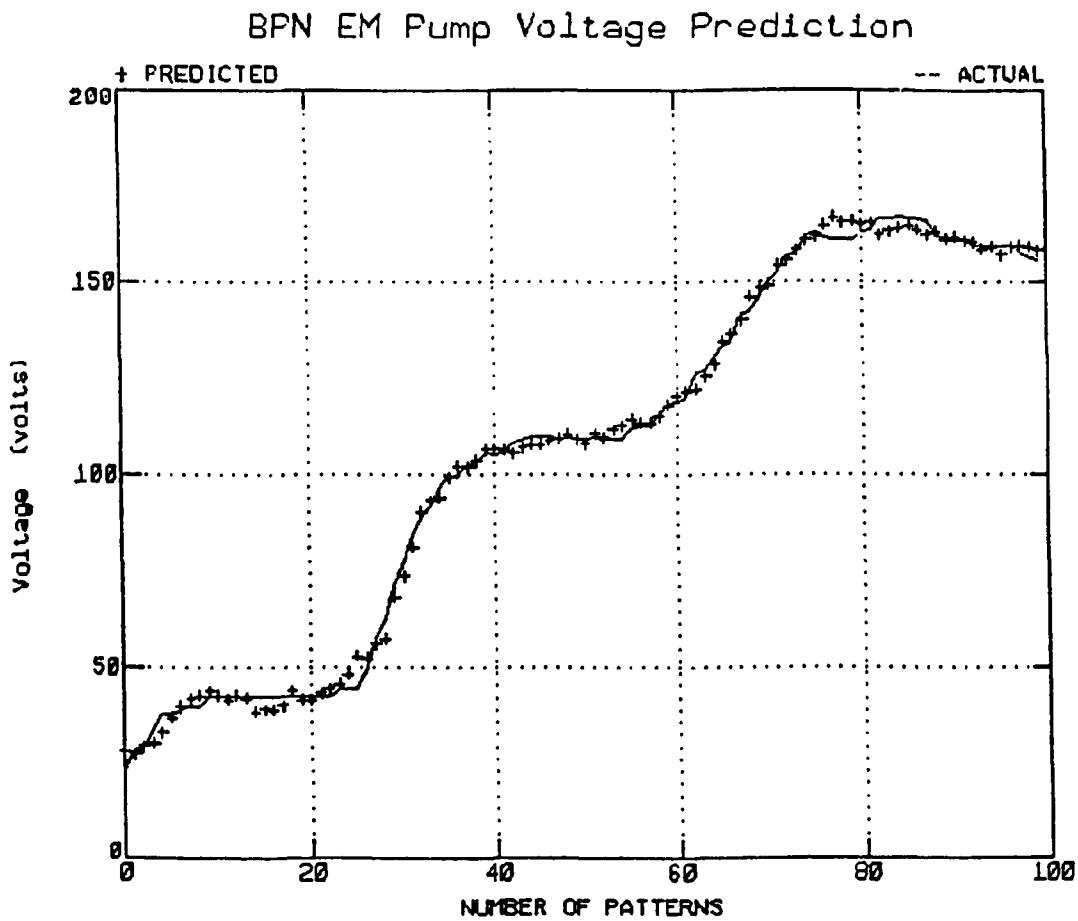

Fig. 4.3f. Backpropagation network model of electromagnetic pump voltage; input signals are reactor exit temperature and bulk sodium tank temperature.

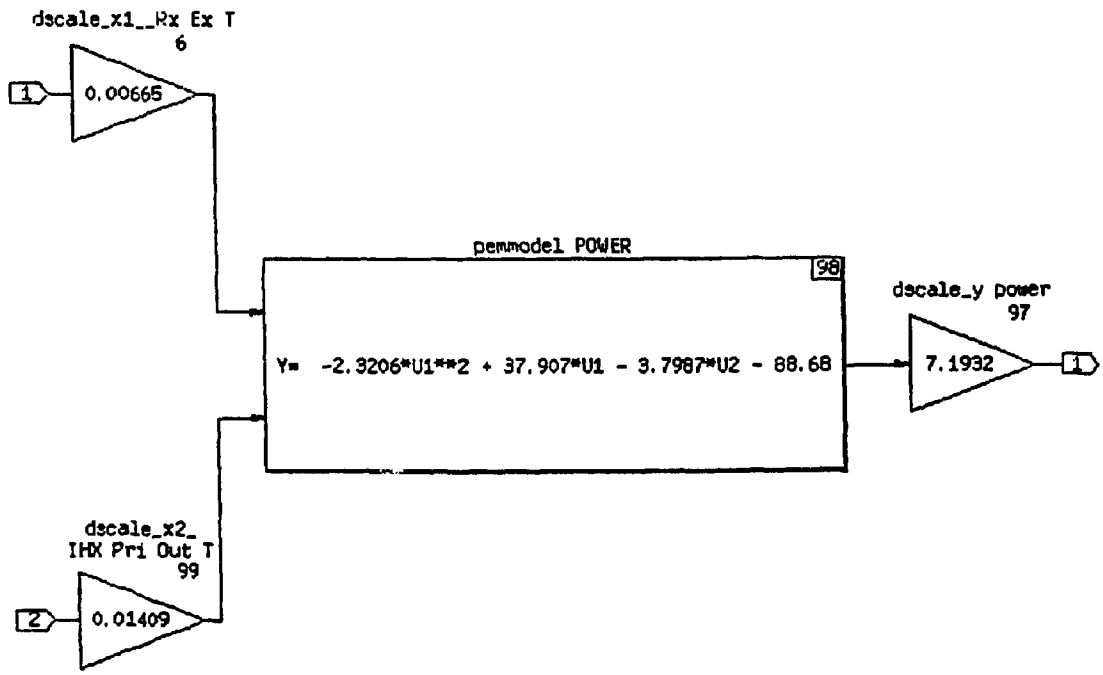

Fig. 4.4. MATRIXx reconstruction of the process empirical model.

implementation is also shown in Figs. 4.5a–4.5c. In this example, the BPN estimates the secondary sodium flow for command validation.

4.4 CONTROL GUIDANCE

The control guidance block (CGB) houses three different nonlinear controllers operating in the MIMO regime. The two actuating signals are the control rod position and the EM pump voltage that drives the secondary sodium flow between the IHX and the steam generator. As described earlier, the three controllers operating in parallel provides a fault-tolerant operation. The design differences among the controllers are made carefully to distribute the capabilities over the alternative control systems. This logic helps confine the anomaly propagation through only one controller, thus isolating others from the external disturbances. The design also aims at building robustness within each control system against abnormal situations.

The ICS interface with the EBR-II actuators (including the operator) has three modes: (1) manual control, (2) semiautomatic control, and (3) full-automated control. In the manual mode, the control block directly interacts with the operator. It provides a set of suggestions for the adjustment of the control variables. In the semiautomatic and full-automatic modes, the control block is manipulated by the operator to send the control signals directly to the plant actuators. The distinction between the semiautomatic and full-automatic modes is determined by the frequency of operator intervention. The scope of this work does not include the specifics of the full-automatic and semiautomatic modes.

Parallel operation of the three controllers includes the use of three adaptive models (on line) of the plant. In the parallel mode, all of the controllers are active including the two that are fed back from the adaptive models and the one that interacts with the plant. Note that the adaptive models are capable of accurately representing the plant dynamics. Detailed information on adaptive modeling is given in Sect. 6.

4.4.1 Reconstructive Inverse Dynamics Controller

The background of the reconstructive inverse dynamics (RID) control design is given in Sect. 6. The underlying principle includes creating the inverse dynamics of the process from a model-based, adaptive paradigm (Berkan et al. 1989). RID is a nonlinear technique and yields accurate trajectory-following control. It is inherently robust against modeling errors and unknown dynamics. Thus, the instability problem often experienced in model-reference control techniques can be avoided provided such discrepancies are within the acceptable limits. The RID method can be enhanced with an adaptive routine that further reduces the effects of uncertainties.

The EBR-II startup control task consists of a MIMO design with control rod position and secondary sodium flow as the actuating signals. The RID controller design uses two trajectories to be followed: (1) reactor power and (2) IHX secondary sodium outlet temperature. These trajectories are obtained from the available startup data. Figure 4.6 shows the RID design of rod reactivity to follow the reactor power and secondary sodium flow to follow the IHX secondary outlet temperature, and it illustrates the implementation in the MATRIXx/SYSTEM-BUILD environment.

In the RID technique, all available measurements (that are adequate to represent the inverse dynamics) are used in the feedback loop. An on-line model is incorporated with the control system to provide estimates of the unmeasured state variables such as

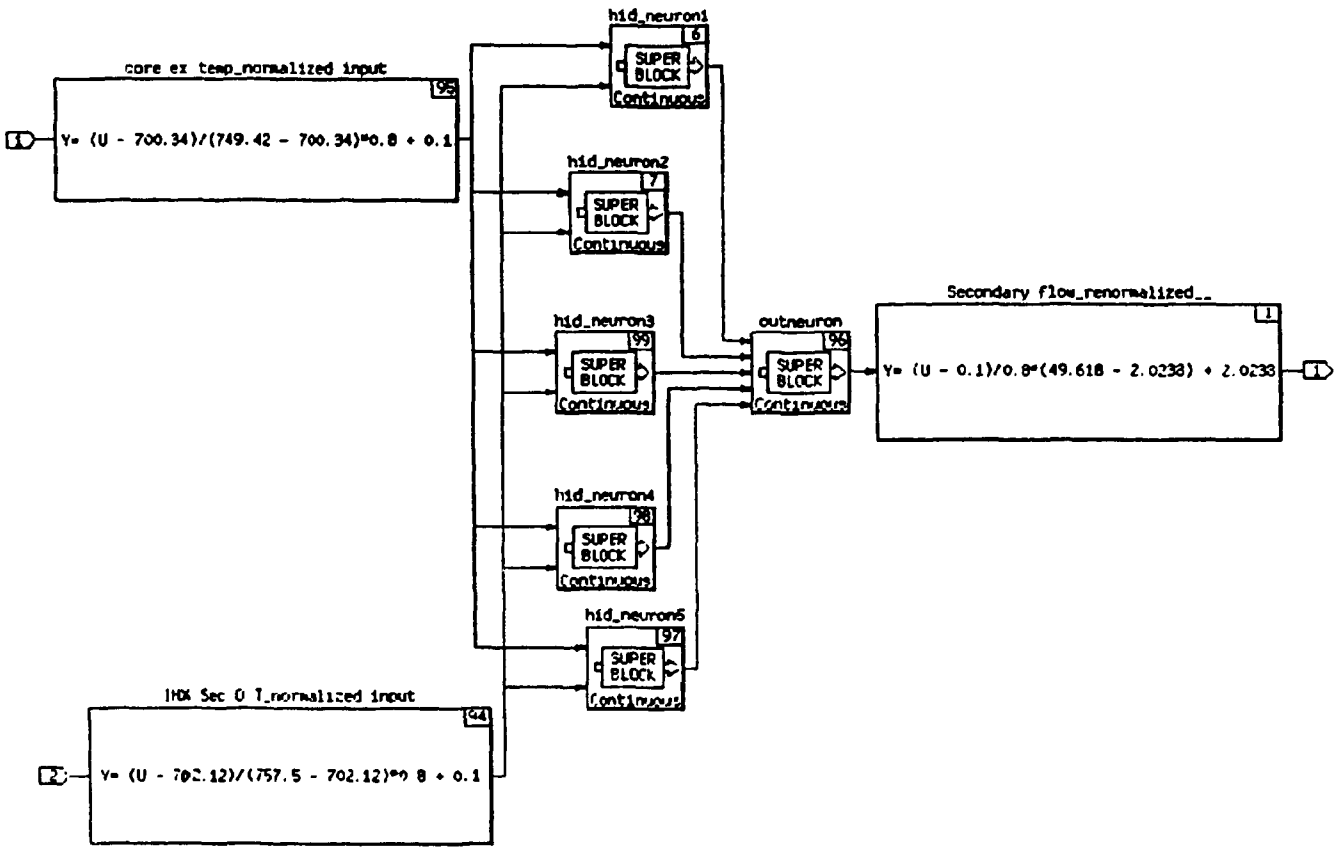

Fig. 4.5a. Three-layer, five-hidden–neuron neural network for predicting secondary sodium flow; input signals are core exit temperature.

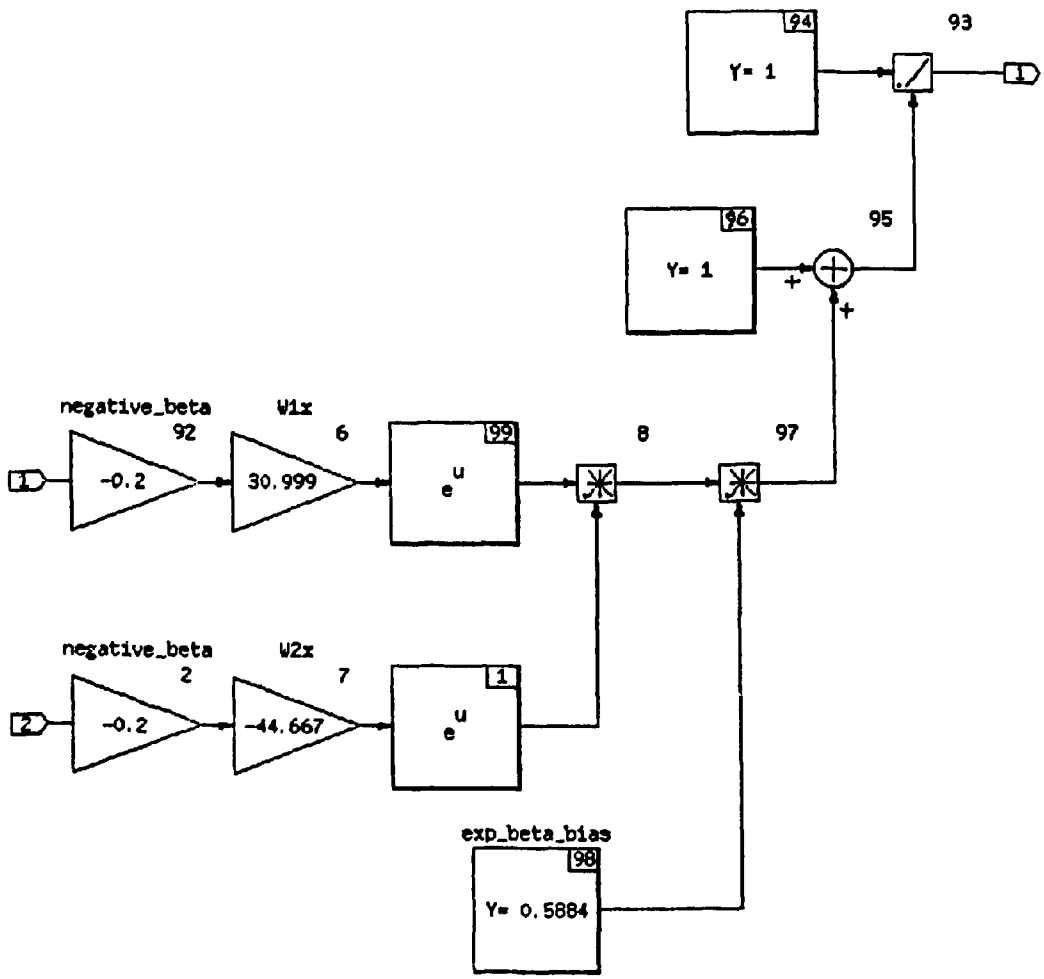

Fig. 4.5b. Expanded view of the fifth hidden neuron.

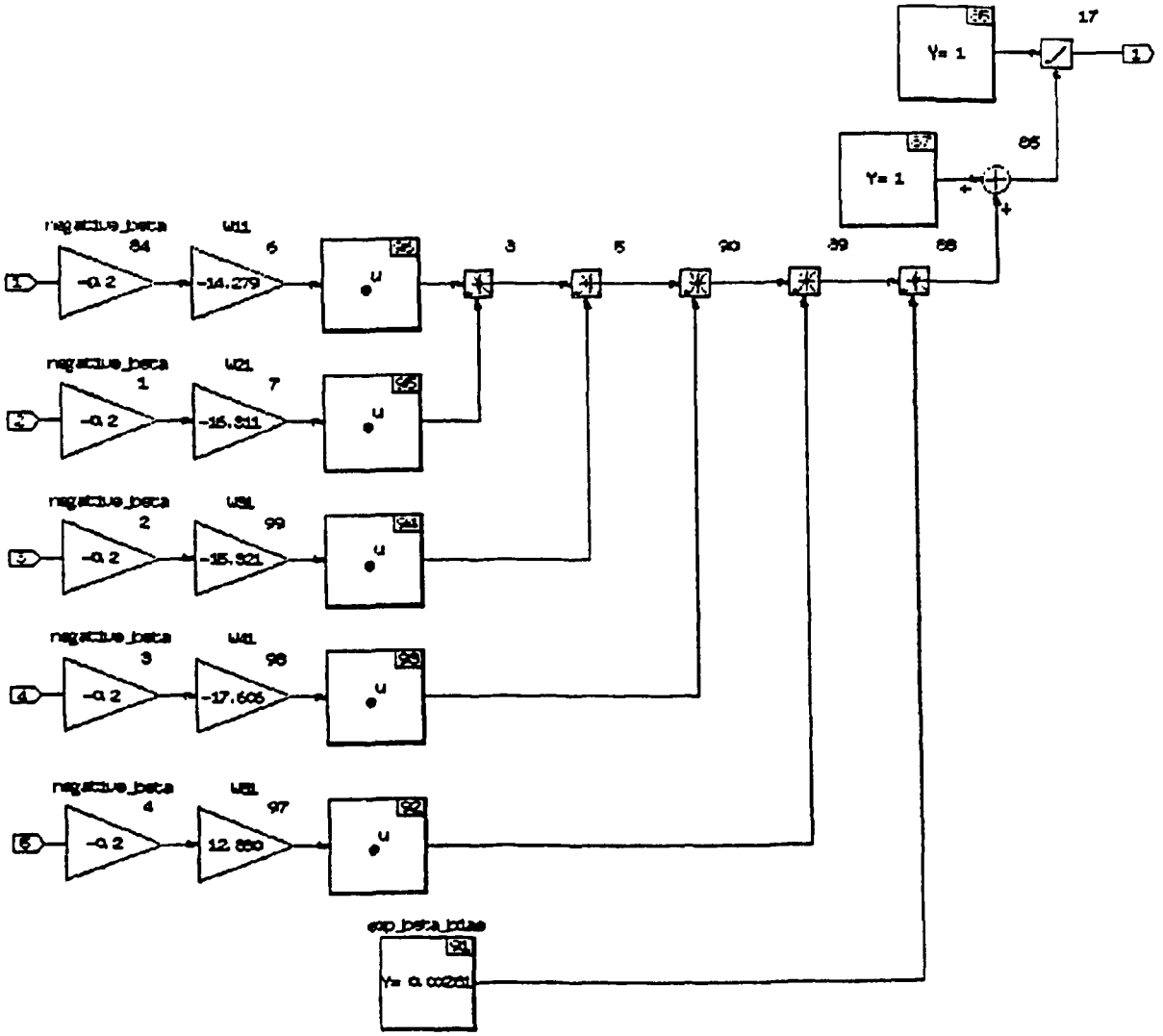

Fig. 4.5c. Expanded view of the output layer neuron.

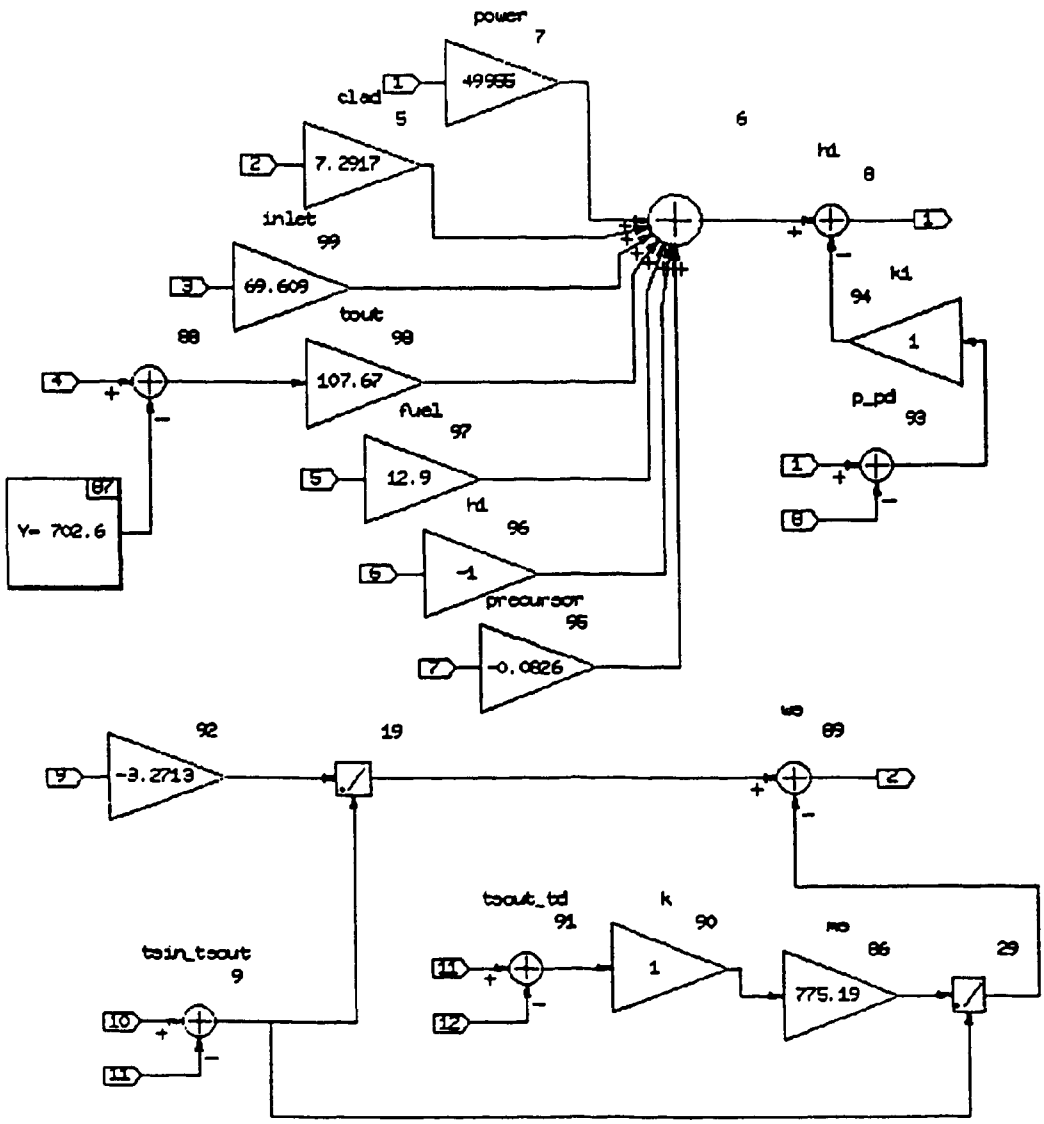

Fig. 4.6. Reconstructive inverse dynamics control implementation in MATRIXx/SYSTEM-BUILD environment. Output 1 corresponds to rod positioning, and output 2 corresponds to secondary sodium flow.

precursor concentration, fuel temperature, cladding temperature, and IHX wall temperature. The on-line model also provides corrections for the uncertainty in reactivity and heat transfer coefficients. The final design used in simulations does not include adaptive features, because the performance is satisfactory without complicating the control system (see Sect. 5).

4.4.2 Fuzzy Controller

Use of fuzzy logic in control is briefly presented in Sect. 6. Fuzzy control has become increasingly popular in industrial applications, mainly because of the simplicity in implementing a nonlinear control law that can handle imprecise information. In application to the EBR-II startup, the fuzzy paradigm is considered to provide a reliable control solution that does not rely on an on-line model. Also, it uses only three measurements from the plant: the reactor power, core exit temperature, and IHX secondary sodium outlet temperature. Because only the latter measurement is nonredundant, this control module is quite isolated from measurement anomalies.

Automation of the EBR-II startup procedure with a fuzzy controller requires a trajectory-following strategy for both rod reactivity and secondary sodium flow. Unlike the steady-state control of dynamic systems, the trajectory-following control presents some difficulties when employed within the fuzzy control paradigm. A new approach that employs fuzzy control in the feedback loop is used. The fuzzy control block includes a truth table identifying the state and control variables in a common phase plane. The table is constructed from a data set previously recorded during a successful startup of EBR-II. In the feedback loop, the fuzzy block shown in Fig. 4.7a provides correction to the startup commands (fixed trajectories) to ensure that the plant states remain within the phase plane of the table. Figure 4.7a shows the MATRIXx/SYSTEM-BUILD blocks representing the EBR-II model, fuzzy controller, and correction block "wire." The interior of the fuzzy block is shown in Fig. 4.7b, where input channels 1, 2 and 3 correspond to the on-line readings of the three measurements stated above. The outputs of fuzzy blocks are equally weighted to yield the final form of the control signal.

4.4.3 Neural Network Controller

A brief description of the artificial neural networks, particularly the backpropagation network (BPN), is given is Sect. 6. Recent advances in neural networks have made it possible to design control systems for dynamic systems. The BPN paradigm, when designed as a controller, does not use an on-line model. Thus, it provides another reliable control solution after fuzzy controller. Development of the BPN module requires off-line training that can be complicated, in general. It also requires data preparation and careful data operations.

In application to the EBR-II automated startup task, the BPN module is considered to provide a short-cut solution with a high degree of robustness. It is designed to use only three measurements, similar to the fuzzy controller. However, the measurement set is chosen differently to yield a maneuvering capability around the problems in power measurement that affect both fuzzy and RID controllers. The three measurements that the BPN module uses are the core exit temperature, IHX secondary sodium temperature, and high-pressure plenum inlet temperature. Note that it is impossible to avoid using nonredundant measurements from the IHX to implement startup control successfully.

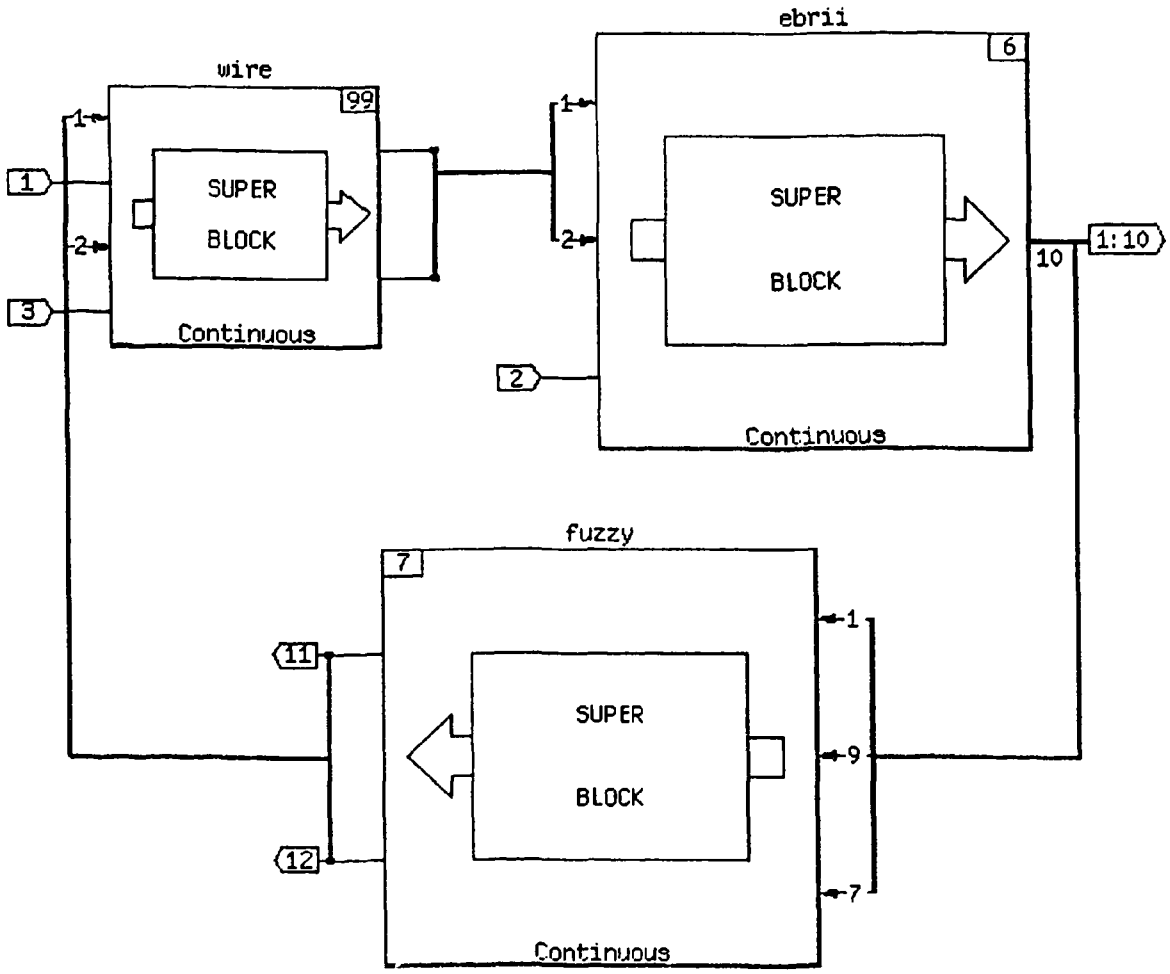

Fig. 4.7a. Fuzzy control implementation in MATRIXx/SYSTEM-BUILD environment. Super block "wire" generates regulation to the external commands by the fuzzy controller in the feedback loop.

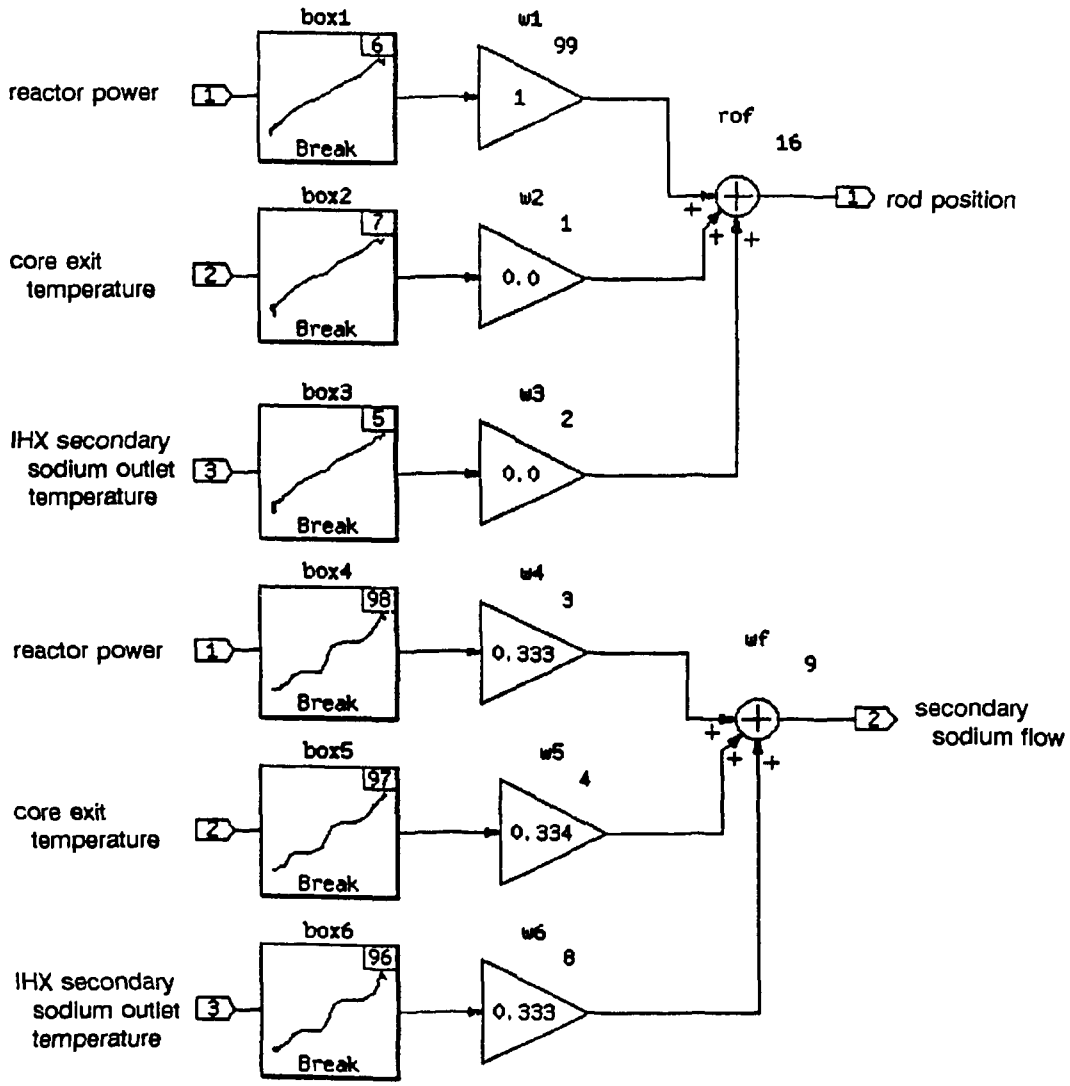

Fig. 4.7b. Interior of the super block fuzzy (IHX = intermediate heat exchanger, rof = rate of flow, wf = flow rate).

The use of neural networks for the trajectory-following control imposes a difficulty just like that in the fuzzy control paradigm. The problem is that the BPN controller can produce control output for only the current state of the plant but not the future state. Therefore, the desired future states of the plant must be introduced to the control system to drive the plant toward higher power levels by simply imitating the operator's actions in a previous startup. The trajectories of the two control variables are introduced to the plant every fifth time point. During the remaining time period, the plant states are fed back to the BPN controller to provide regulative (corrective) control action around the new future state.

The BPN controller is trained by using the startup data shown in Fig. 2.3. Training requires normalization of the data. Each of two BPN algorithms is trained to predict one control variable. The training data set includes normalized signals from the core exit temperature, IHX secondary sodium outlet temperature, and high-pressure plenum inlet temperature.

The choice of a proper network architecture constitutes a major problem in neural network applications. The number of hidden-layer neurons determines the prediction capability of the network. The optimal number of hidden-layer neurons is an unknown that can be determined through only intuition. A large number of neurons slow down the training, and sometimes solutions may never converge. Thus, the BPN architectures are designed to contain a minimum number of hidden-layer neurons, provided the performance is acceptable. Another difficulty in handling large networks appears in the implementation stage. The MATRIXx/SYSTEM-BUILD environment is not designed particularly to contain networks with a large number of connections. Thus, the design philosophy in this application is to obtain a neural network controller with reasonable size and performance. The BPN algorithms include three hidden-layer neurons for the reactivity control and five hidden-layer neurons for the secondary sodium flow control (as shown in Fig. 4.8). Off-line training results indicate that the BPN controller efficiently produces the expected control actions given the plant states. The simulation results are given in Sect. 5.

4.5 PERFORMANCE ANALYZER

The performance analyzer shown in the general architecture of Fig. 3.1 includes several vitally important diagnostics tasks. In this application, its function is concentrated on the recognition of plant behavior. Because the work presented in this report is based on computer simulations only, additional functions of the performance analyzer are omitted. The omitted functions include determining the component status and wearing effects.

Recognition of the plant behavior is an important diagnostics task when the plant is subject to unanticipated transients. During scheduled normal operations, the behavior-recognition task determines the degree of consistency in following the planned operation. The ICS design includes a performance-analyzing routine to determine whether the startup trajectories are followed properly by the ICS control actions. The routine uses a data set previously recorded during a successful startup operation. A multidimensional phase plane is developed to correlate all state variables of the plant for a given power level. Figure 4.9 illustrates the phase plane for only three state variables. The minimum distance between the current plant state R' and the desired state R determines the quality of performance. Recognition of the current operation is calculated percentagewise from

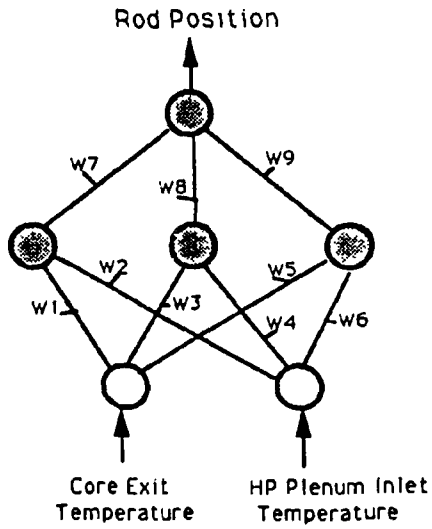

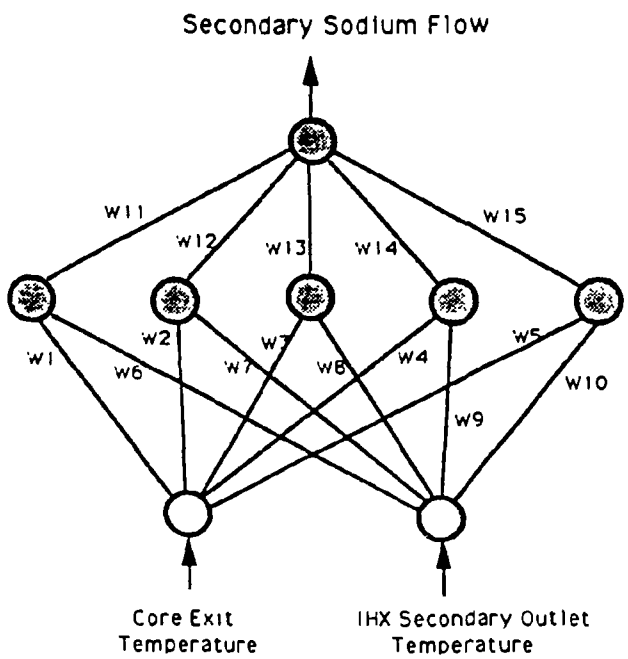

Fig. 4.8. Backpropagation network topology for reactivity control (top) and secondary sodium flow (bottom) control.

the normalized distance. When the minimum distance is zero, recognition is 100%. The lower bound of this measure is 1 to correspond to a 0% recognition. This calculation is repeated every time point the measurements become available. The ring shown in Fig. 4.9 is a linguistic evaluator and can be adjusted through experience. In this application, the recognition level below 90% is considered to be medium performance. When performance is in the medium range, the mode selector intervenes the control system and evaluates the candidate controllers for continuation of the ICS implementation. Note that this function provides an anticipatory trip-avoidance capability, mainly because of the recognition of a deteriorating range that may drag the plant into abnormal regimes during later stages of the operation.

4.6 MODE SELECTOR

As stated previously, the integrated control system shown in Fig. 4.1 is a simplified version of the general design shown in Fig. 3.1, which is appropriate for determining the feasibility of the conceptual design at a preliminary level. The mode-selector block of the ICS system shown in Fig. 4.1 also includes the performance-analyzer block.

In this application, the mode-selecting logic is designed to initially activate the RID controller since this technique yields accurate trajectory-following control (see Sect. 5). The mode-selecting logic is constructed on top of this initial status. The causes for a mode change from the initial status, described by Nakakura and Ishiguro (1988), are

1A. input measurement(s) is/are corrupted,
1B. command(s) is/are unacceptable,
1C. performance is low,
1D. operator intervenes (not applicable in manual control),
1E. emergency system intervenes (not applicable in manual control).

Note that 1A, 1B, and 1C are obtained from the signal validator, command validator, and performance analyzer respectively. These causes are connected by an OR gate. Intervention by the emergency system or operator is not applicable in manual control where the ICS output is observed by only the operator as guidance. Thus, such intervention capability already exists and the ICS does not need to process this information.

The transition to any secondary mode due to an anomaly requires a broadening in the logic tree. The two remaining control systems are to be checked for their availability. The availability check includes the following verifications: Is the candidate controller

2A. affected by the detected signal anomaly?
2B. generating acceptable commands?
2C. able to take over (jump condition)?

If the measurement anomaly is unavoidable by both remaining controllers, the ICS enters into the invalid range: a halt condition is declared. An identical reasoning applies to the commands being generated by the two candidate controllers at the time of anomaly detection. The verification 2C determines the magnitude of the disturbance that will affect the system when the controllers are switched. Although the candidate controllers generate acceptable commands at the time of anomaly, the transition is not allowed in

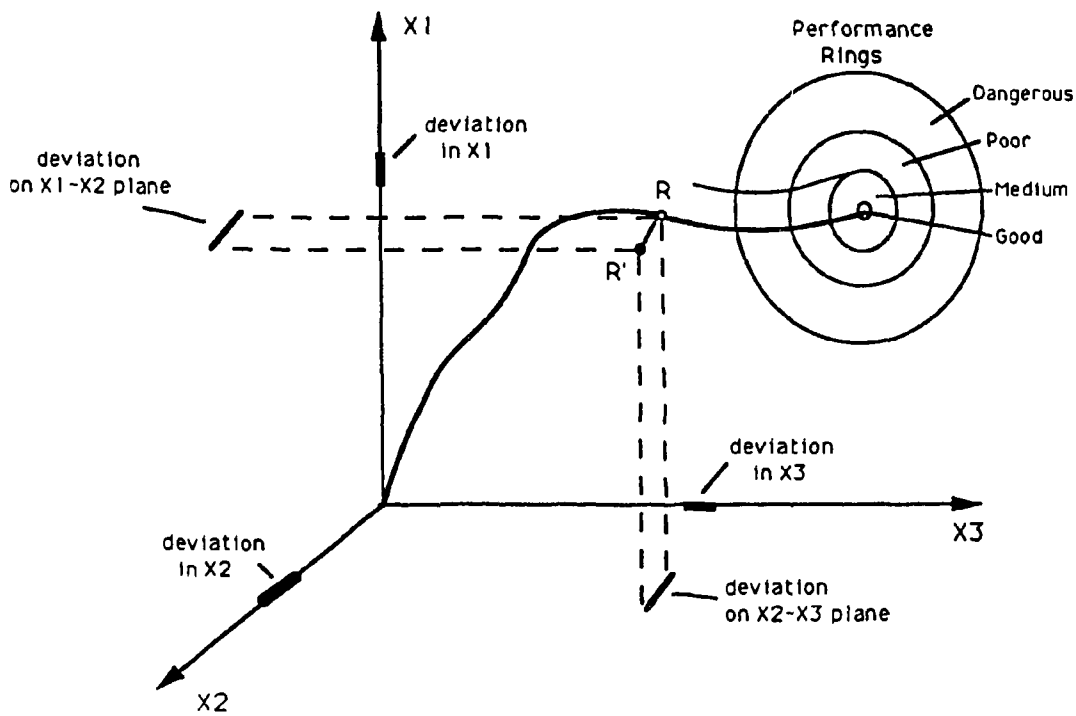

Fig. 4.9. Work space of the performance analyzer.

case of anticipated unacceptable jumps. When the secondary verifications are satisfied by the two candidates, the closeness becomes the criterion. The closeness is calculated from the jump condition, which is a measure of distance between the control variables and their expected values.

In case of continuing anomalies, the third and other transitions are possible. However, the third and other transitions are confined within the fuzzy and neural network controllers. When the abnormality is detected through the command validator and performance analyzer, but not by the signal validator, the third and higher transitions can include the RID controller since the on-line model will not be affected.

It is important to note that the error margins (acceptable band of signals) can be kept small to enhance the anticipatory failure detection. However, the band thickness, if not properly chosen, may cause several unnecessary transitions between the controllers. Thus, adjustment of the band thickness plays an important role in building fault tolerance.

Figures 4.10a and 4.10b show the implementation of mode-selecting logic in the MATRIXx/SYSTEM-BUILD environment. Figure 4.10a shows the details of the super block "command logic" shown in Fig. 4.10b. The rod reactivity and sodium flow control signals are evaluated in the upper and lower parts of Fig. 4.10a respectively. For every controller, a corresponding "command-logic" superblock exists. The output of the command-logic superblock is 1, indicating abnormality and zero for normal operation. In Fig. 4.10b, the outputs from these blocks are connected to an OR gate. The OR gate's second input comes from the performance analyzer. Thus, the performance analyzer itself has the capability of disqualifying the on-line control implementation. The superblock "mode" provides a signal transmission path for the control signals to reach actuators. Other inputs to superblock "mode" include similar signals from the signal validator block. The signal validator has an equal weight in disqualifying the on-line controller. The superblock "final control" receives control signals from the controllers and functions as a bridge to the actuation channel. The superblock "on-line model" chose the coupling of the on-line model with the two standby controllers, and the third one is coupled to the plant.

4.7 FAULT TOLERANCE

The ICS architecture shown in Fig. 3.1 represents a fault-tolerant strategy to maneuver around those problems that may cause reactor trips in conventional systems. Trip avoidance is an important issue because the availability of the power output must be maximized for economy. The fault-tolerant capability in ICS is designed such that the problems are solved in an anticipatory fashion before their effects reach to the point of reactor trips. It is important to note that the definition of fault tolerance does not include avoidance maneuvers in the vicinity of the prescribed safety limits.

In application to EBR-II autostartup control, the fault-tolerance strategy deserves special attention, mainly because the startup operation is quite complicated compared with other modes of operation. An average startup at EBR-II requires 8 h. An automated control system at EBR-II subject to the full load of control and diagnostics tasks is required to maintain high performance throughout the startup and transition to steady state at full power. The duration of the normal startup transient is long enough for the plant abnormalities to build up. Furthermore, the startup mode represents the case where the actuators are used extensively. In the most dynamic mode such as startup, component

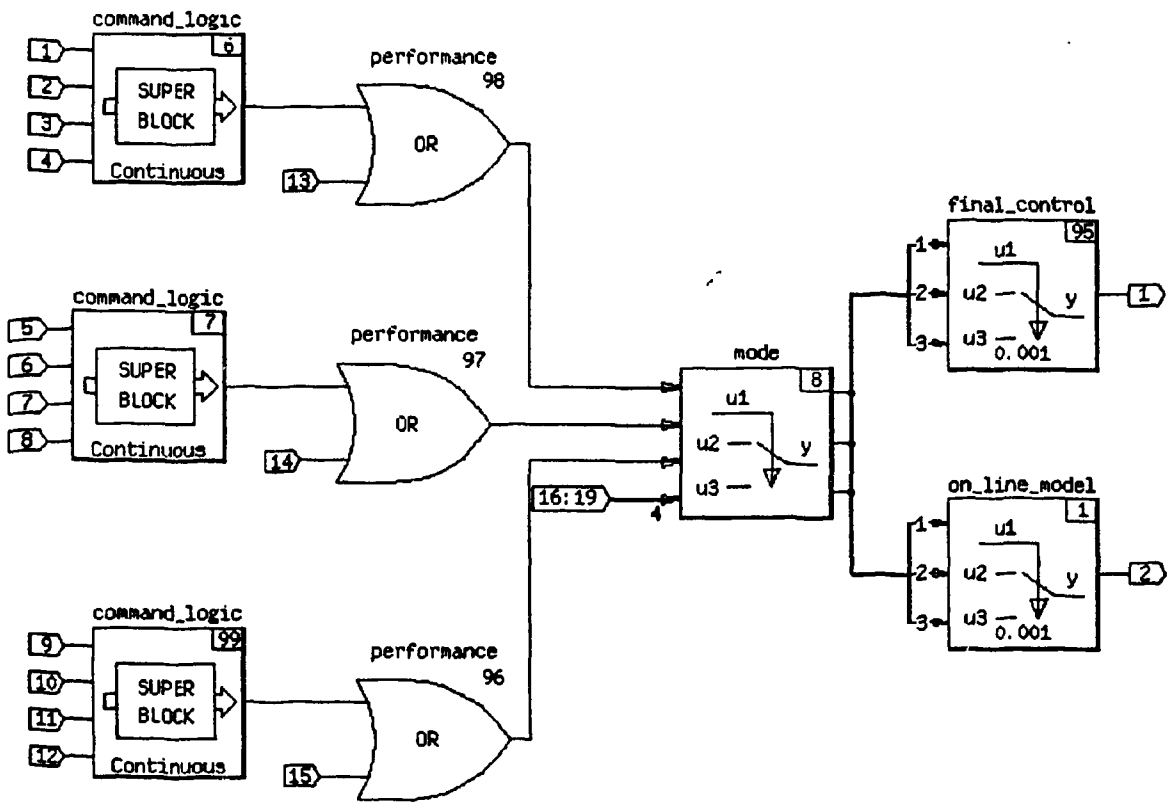

Fig. 4.10a. Mode selector logic implementation for control signals in MATRIXx/SYSTEM-BUILD environment.

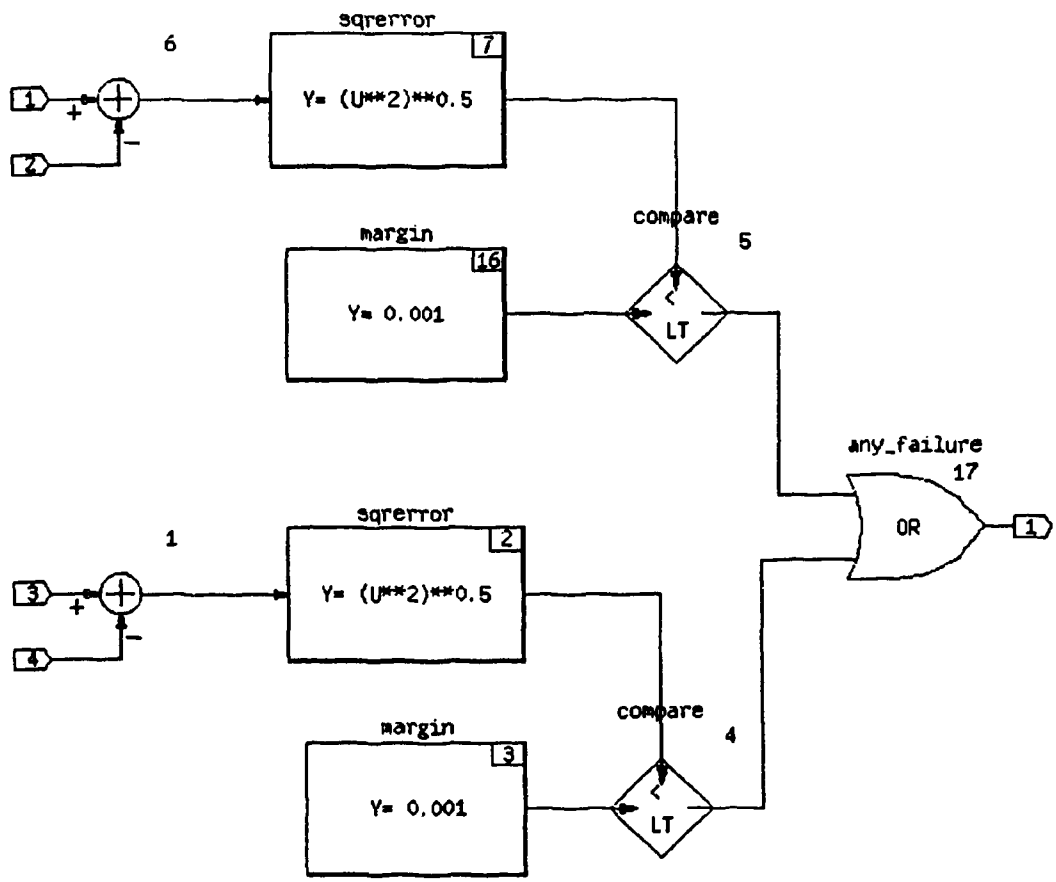

Fig. 4.10b. Interior of super block command_logic.

failure possibilities are higher than in steady-state or standby conditions. Thus, the ICS design concept includes a fault-tolerant logic to resolve some of the likely problems.

The ICS includes signal and command validation blocks, whose major contribution to the fault-tolerant strategy is the fault-detection capability. In addition, such a capability can be performed fast enough that the anomalies are not allowed to propagate. For example, the signals used in control systems are analyzed on-line to check their validity. Anomalies are detected promptly, and the relevant systems are warned. The lack of such a capability often causes plants to operate under abnormal regimes without detection up to the point where the severity of the anomaly requires emergency systems to intervene. A similar logic holds for the command validation task. Bad commands are not allowed to affect the system. Thus, the validation blocks function like an early-failure–detection system. However, early detection does not complete the fault-tolerant logic since the question of "what to do next" must be answered.

The decision of what to do after anomaly detection constitutes one of the most significant issues. This problem is solved in the ICS design by creating a redundancy in control systems that operate in parallel. The redundancy built into the ICS not only introduces a software-fault tolerance but offers a number of solutions in case of anomalies. The control block houses three different controllers that (1) use different sets of plant measurements, (2) use different control laws, and (3) have different robustness characteristics. A signal anomaly can be bypassed by activating one of the controllers that does not use the corrupted signal. This solution holds if the anomaly is caused by the measurement system. Similarly, if the on-line controller starts generating unacceptable commands, the alternative control systems takes over. A safety measure is also built into this type of implementation. This measure indicates whether the jump condition from one controller to the other is acceptable. The ICS fault-tolerant logic cannot resolve equipment malfunctioning, because it is not generally an expected capability from any control system. In addition, the multiple anomalies occurring simultaneously may not be avoidable. The ICS is designed to declare a halt situation when the severeness of the anomaly exceeds the designed tolerance capacity of the ICS. In such cases, the operator and the emergency systems are warned. Note that the emergency systems and the ICS operate independently with an overriding protocol that disqualifies ICS under any conflicting situation.

Figure 4.11 shows the fault-tolerant feature of the parallel control system interacting with the validation blocks. The three controllers use different sets of measurements. The mode selector continuously receives status information from the signal and command validators. In case of anomalies, the destination of the corresponding signals are inactivated. The Y/N flags in the figure correspond to permissions to activate/inactivate the controllers. The performance analyzer is also linked to the network. Its output determines the overall recognition of the operation. When no signal or command anomaly is present, the ICS is expected to drive the plant around the predetermined trajectories. These trajectories are obtained from the previous startup data. If the plant response shows unrecognized behavior, the performance analyzer can declare a halt situation.

The fault tolerance built into the ICS system can also include the software/hardware failures which, in a simulated environment, requires isolating redundant control algorithms from each other by using different computers. This feature is not included in the scope of this work.

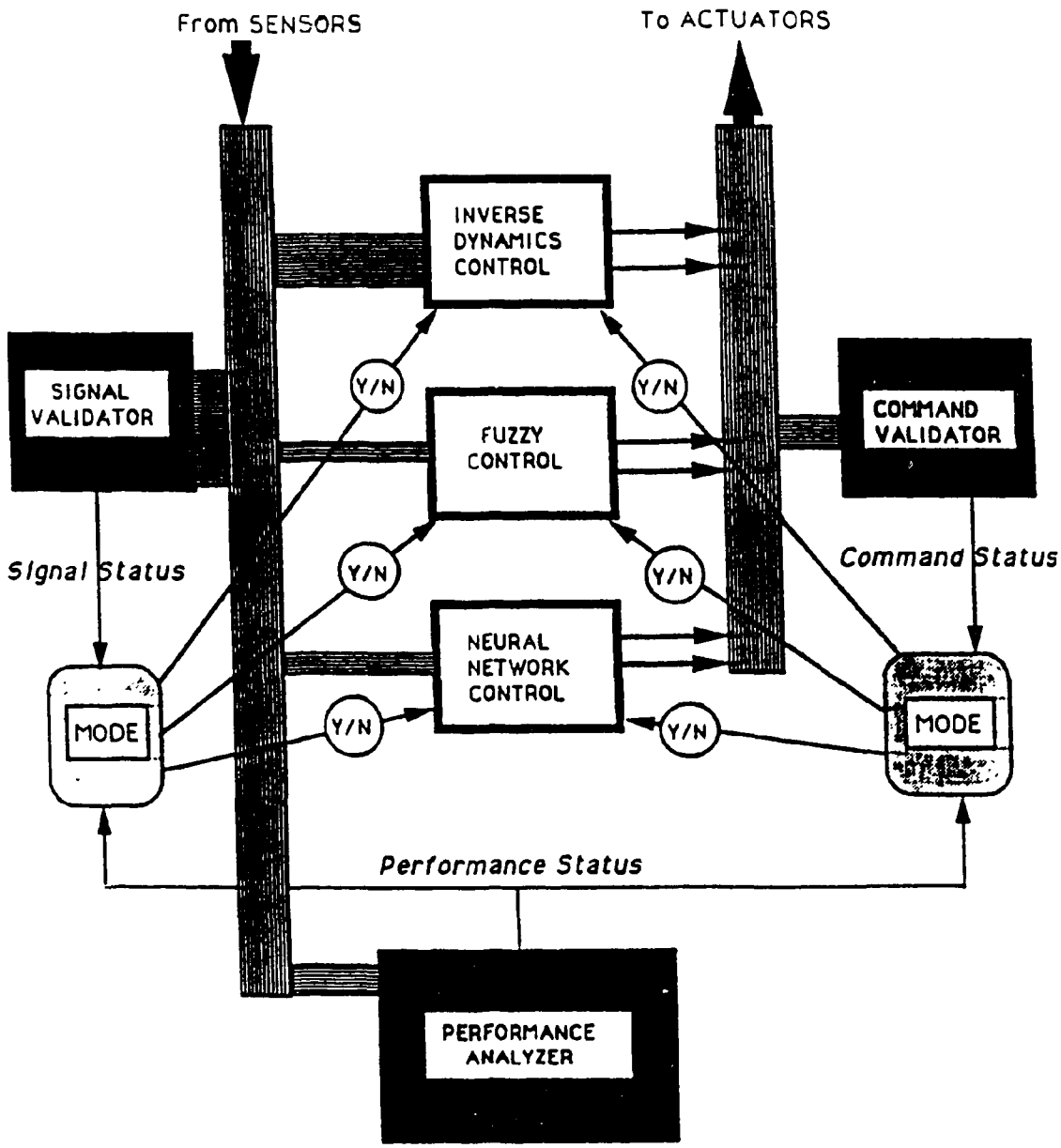

Fig. 4.11. Structural fault-tolerance nature of the integrated control system.

5. SIMULATION RESULTS

The ICS design is performed entirely in the MATRIXx/SYSTEM-BUILD environment with a VAX 3100 machine. The simulation environment includes a nonlinear, valid model representing the EBR-II plant. The EBR-II model is coupled to the ICS to test the startup capability. First simulation includes the RID controller to start up the reactor. The diagnostic systems continuously evaluate the performance and the validity of commands. The simulation results show that the RID performance is outstanding, with an average recognition of ~97%. During the simulation, all the commands are validated, and the mode selector remained silent. The candidate controllers (fuzzy and neural network controller) are tested for the same task. The startup responses show that the fuzzy controller (with 96% recognition) and the neural network controller (with 93% recognition) also yield satisfactory trajectory-following, while the mode selector remains silent during each separate simulation. The simulation results in the range of 0–35% power level, compared with the operator-driven EBR-II data (dotted lines), are shown in Figs. 5.1a–5.1g.

Figure 5.1a shows the power response controlled by three different controllers and by the operator during startup. The figures include the core exit temperature (Fig. 5.1b), bulk tank temperature (Fig. 5.1c), IHX secondary sodium outlet temperature (Fig. 5.1d), in-core sodium temperature (Fig. 5.1e), control rod motion (Fig. 5.1f) and secondary sodium flow (Fig. 5.1g).

5.1 QUALITATIVE EVALUATION

The responses shown in Figs. 5.1a–5.1g indicate that the three controllers accomplish the startup task quite efficiently. However, the differences in their performances as well as their advantages should be mentioned.

The RID controller is designed to follow two trajectories (core exit and IHX secondary outlet temperatures). These trajectories are taken from the operator-driven startup data shown in the figures by dotted lines. Figure 5.1b and 5.1d indicate that the trajectories are followed so closely that they cannot be distinguished in these figures. The other state variables also strongly agree with the actual data. Note that the control rod motion taken by this controller in Fig 5.1f is almost identical to the operator's actions. However, the secondary sodium flow in Fig. 5.1g is controlled more abruptly. The difference in flow control between the operator and RID controller exhibits itself in the power response as a small delay because of the deviation in reactor inlet temperature (and tank temperature of Fig. 5.1c). It is important to note that the RID controller is tuned extra tightly to accomplish efficient trajectory following.

The fuzzy control results show a strong agreement with the RID and operator actions. The system responses are also consistent with the startup data. The trajectory of the IHX secondary outlet temperature is followed with more error when compared with the RID performance. However, this error is negligible for all practical purposes. The fuzzy controller is not dependent on a model, and it is very simple to implement. Thus, the trade-off between the RID and fuzzy controllers represents a bargain between the performance and complexity.

The neural network controller yield[illegible] the least preferable strategy because of deviations in system responses wit[illegible] the desired behavior. However, the neural

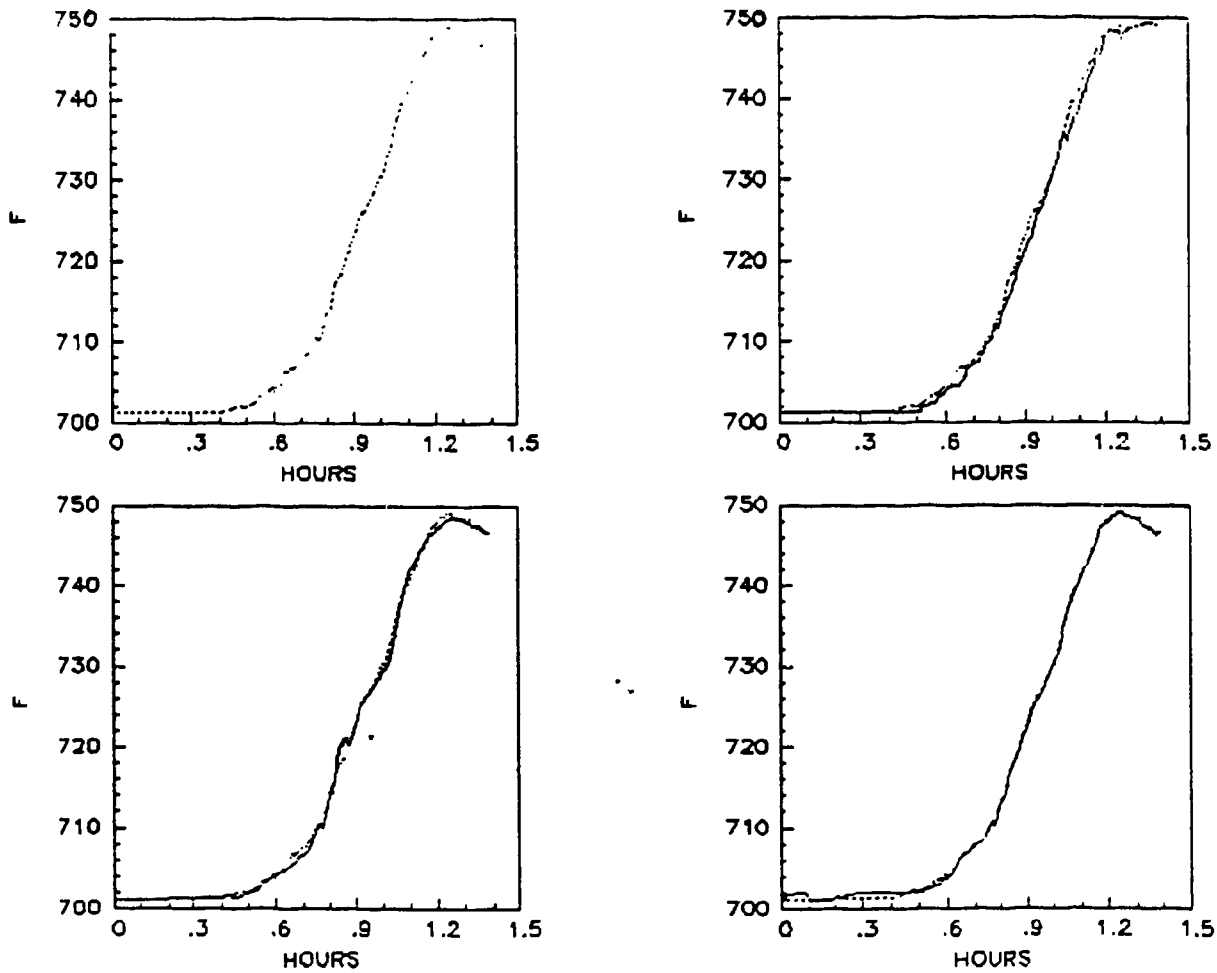

Fig. 5.1a. Power change during startup at Experimental Breeder Reactor-II. (1) Operator-driven actual data. Comparison of actual data with the simulation results of (2) fuzzy controller, (3) neural network controller, and (4) reconstructive inverse dynamics controller.

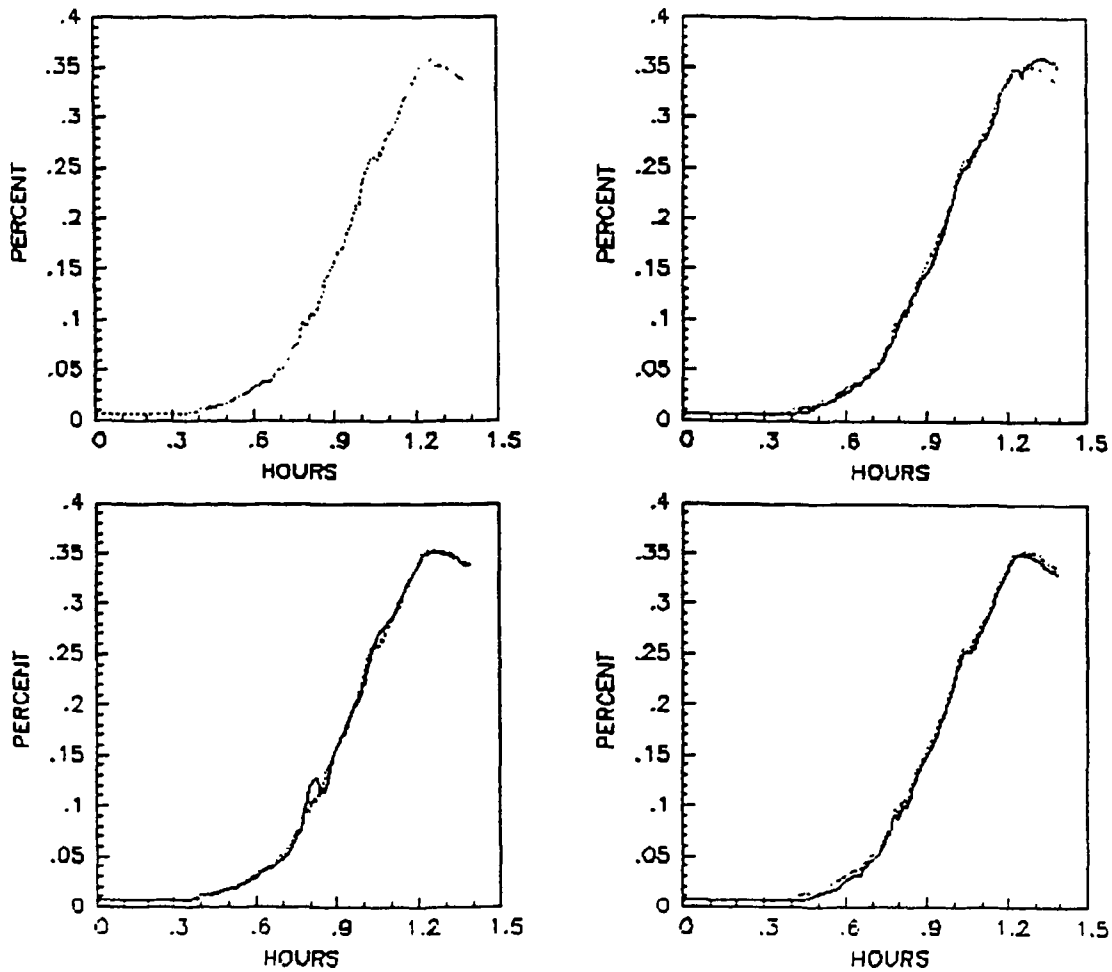

Fig. 5.1b. Core exit temperature change during startup at Experimental Breeder Reactor-II.
(1) Operator-driven actual data. Comparison of actual data with the simulation results of (2) fuzzy controller, (3) neural network controller, and (4) reconstructive inverse dynamics controller.

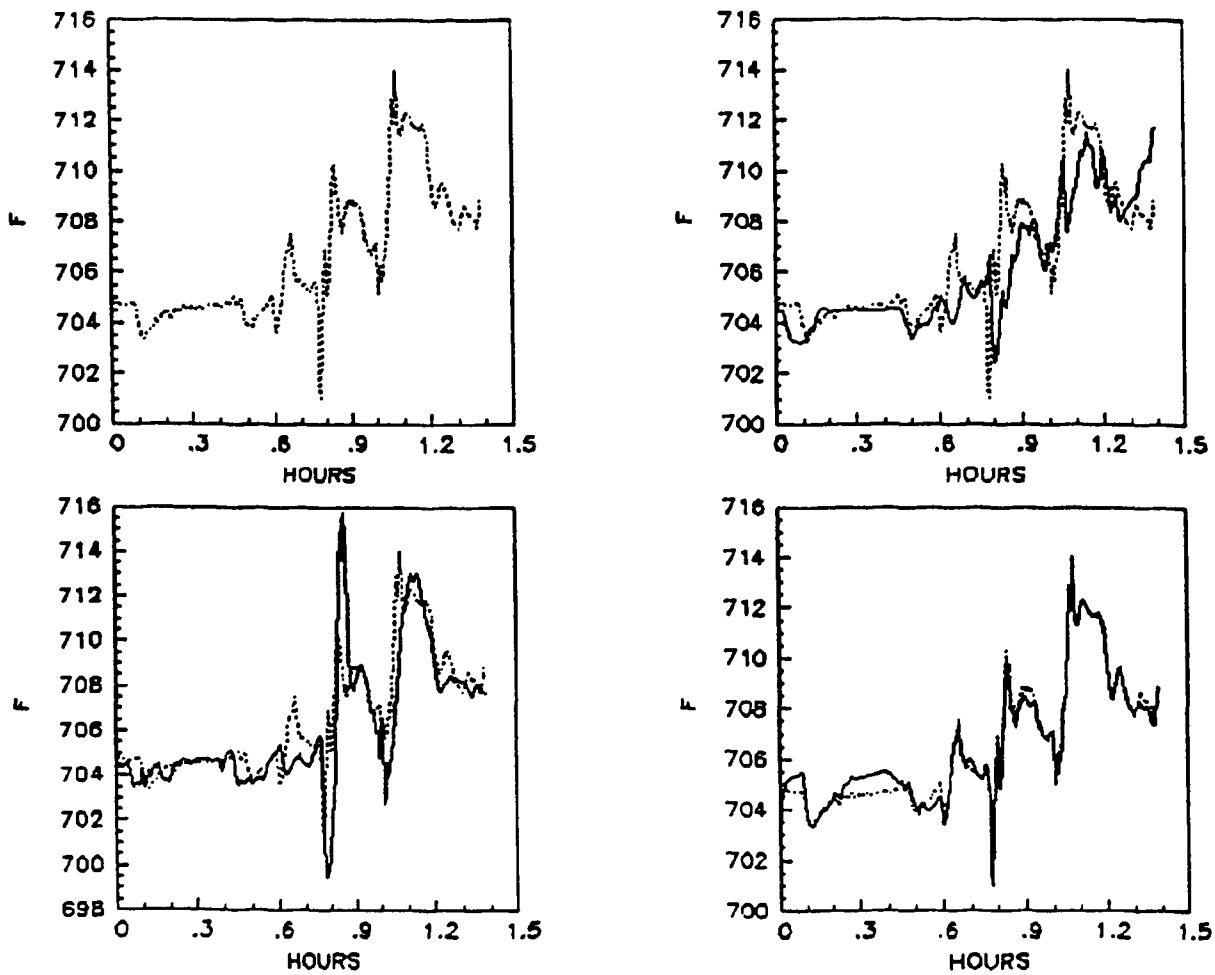

Fig. 5.1c. Sodium tank temperature change during startup at Experimental Breeder Reactor-II.
(1) Operator driven actual data. Comparison of actual data with the simulation results of (2) fuzzy controller, (3) neural network controller, and (4) reconstructive inverse dynamics controller.

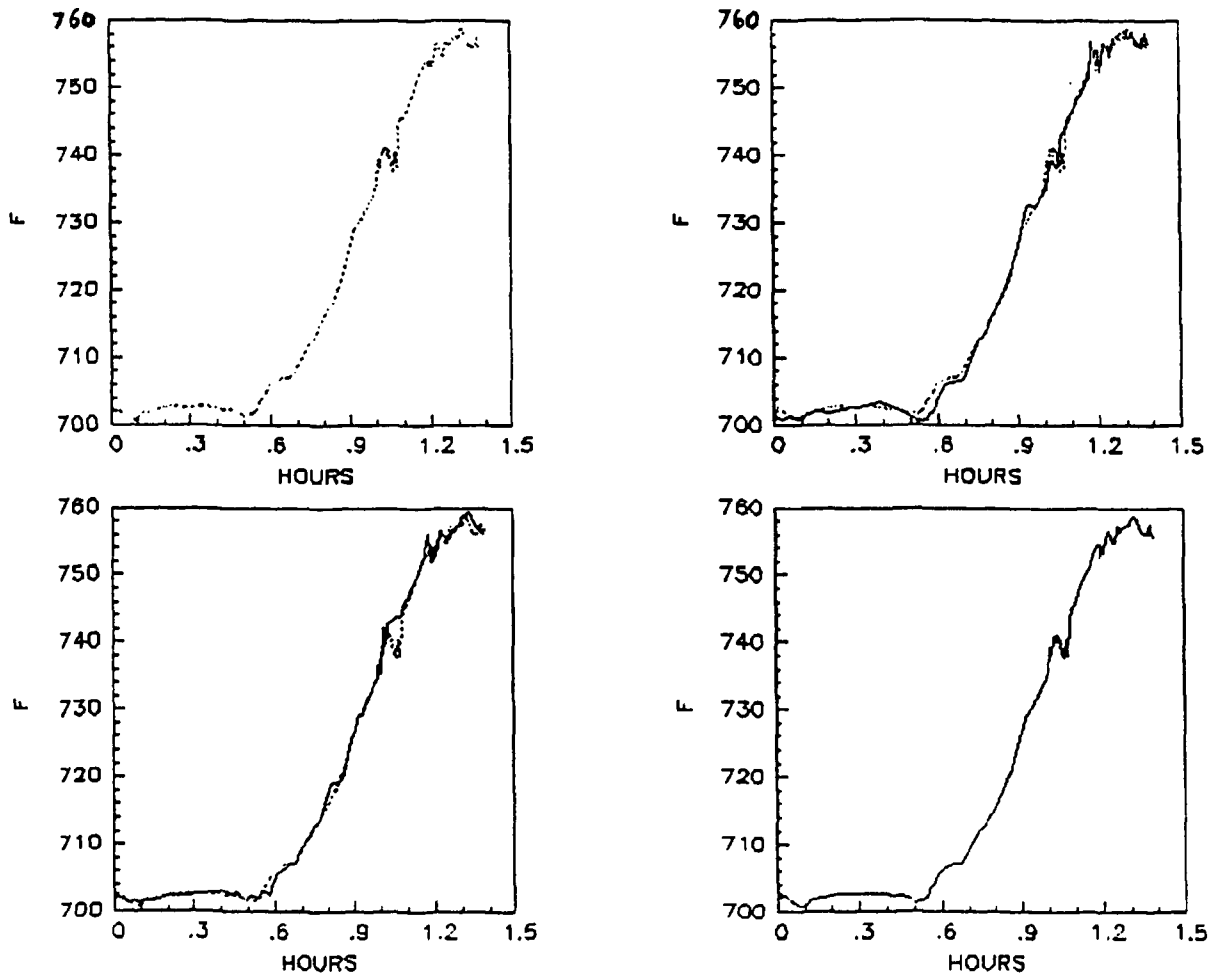

Fig. 5.1d. Intermediate heat exchanger–secondary outlet temperature change during startup at Experimental Breeder Reactor-II. (1) Operator-driven actual data. Comparison of actual data with the simulation results of (2) fuzzy controller, (3) neural network controller, and (4) reconstructive inverse dynamics controller.

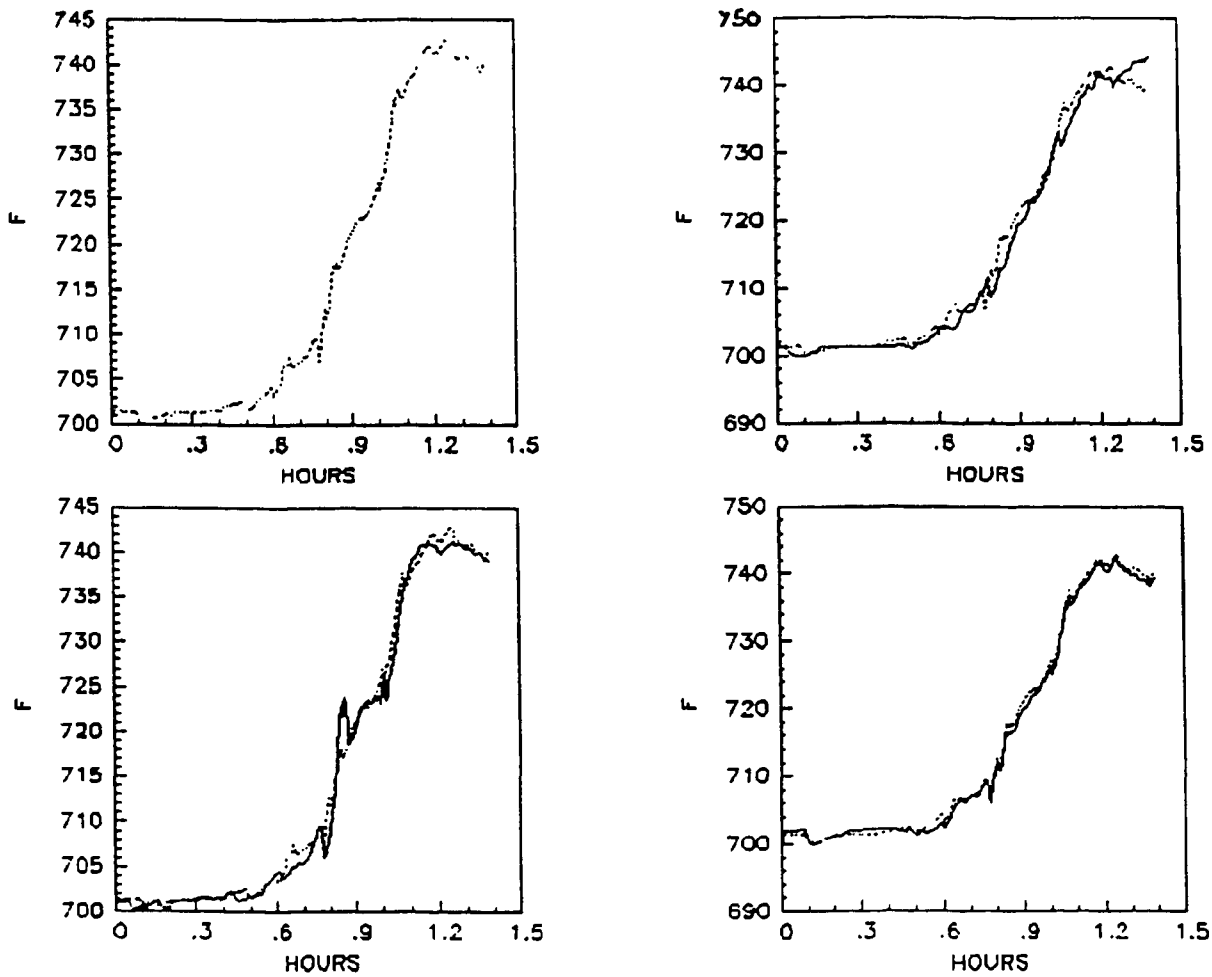

Fig. 5.1c. In-core sodium temperature during startup at Experimental Breeder Reactor-II.
(1) Operator-driven model response. Comparison of operator-driven model with the simulation results of (2) fuzzy controller, (3) neural network controller, and (4) reconstructive inverse dynamics controller.

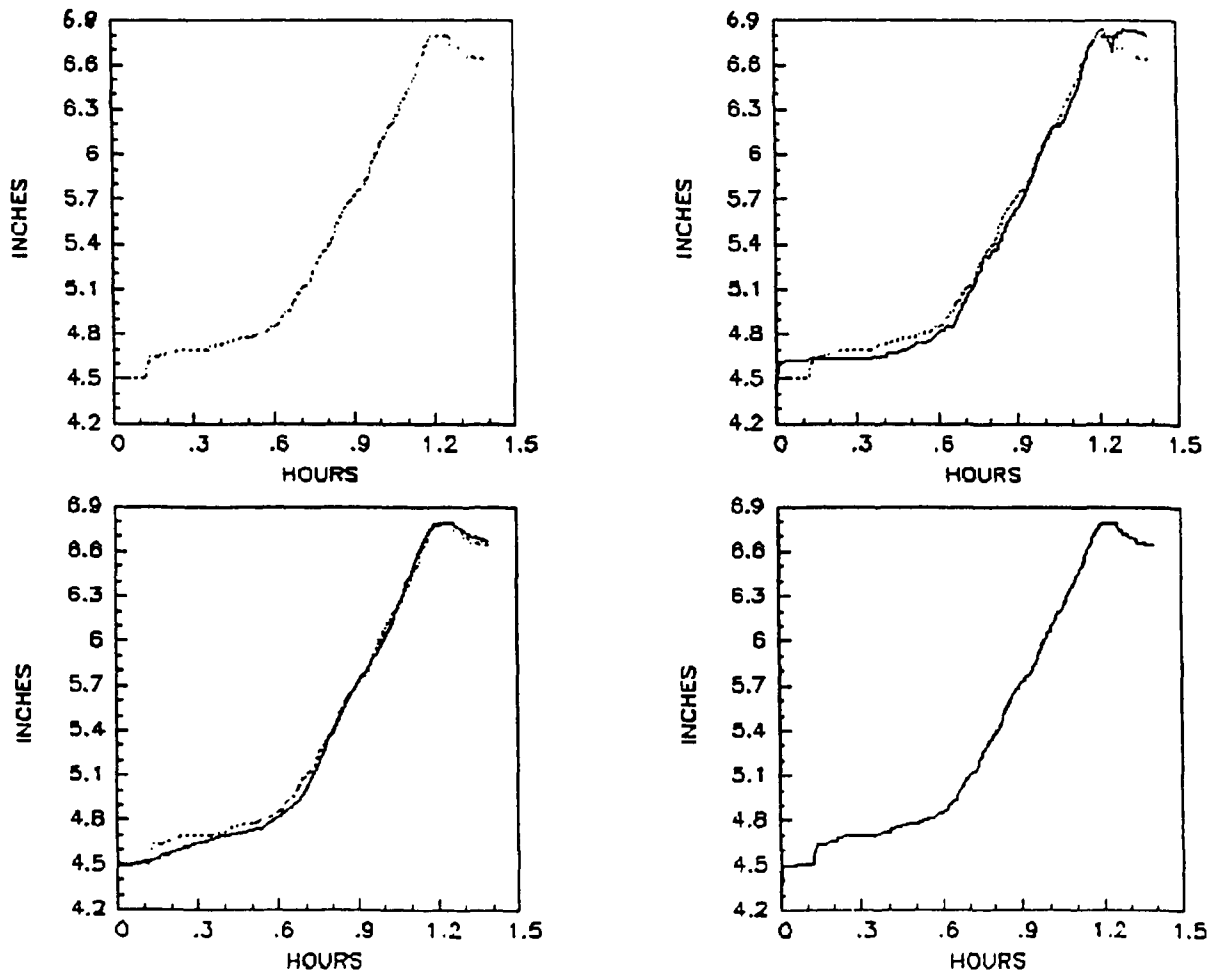

Fig. 5.1f. Rod motion during startup at Experimental Breeder Reactor-II. (1) Operator-driven actual data. Comparison of actual data with the simulation results of (2) fuzzy controller, (3) neural network controller, and (4) reconstructive inverse dynamics controller.

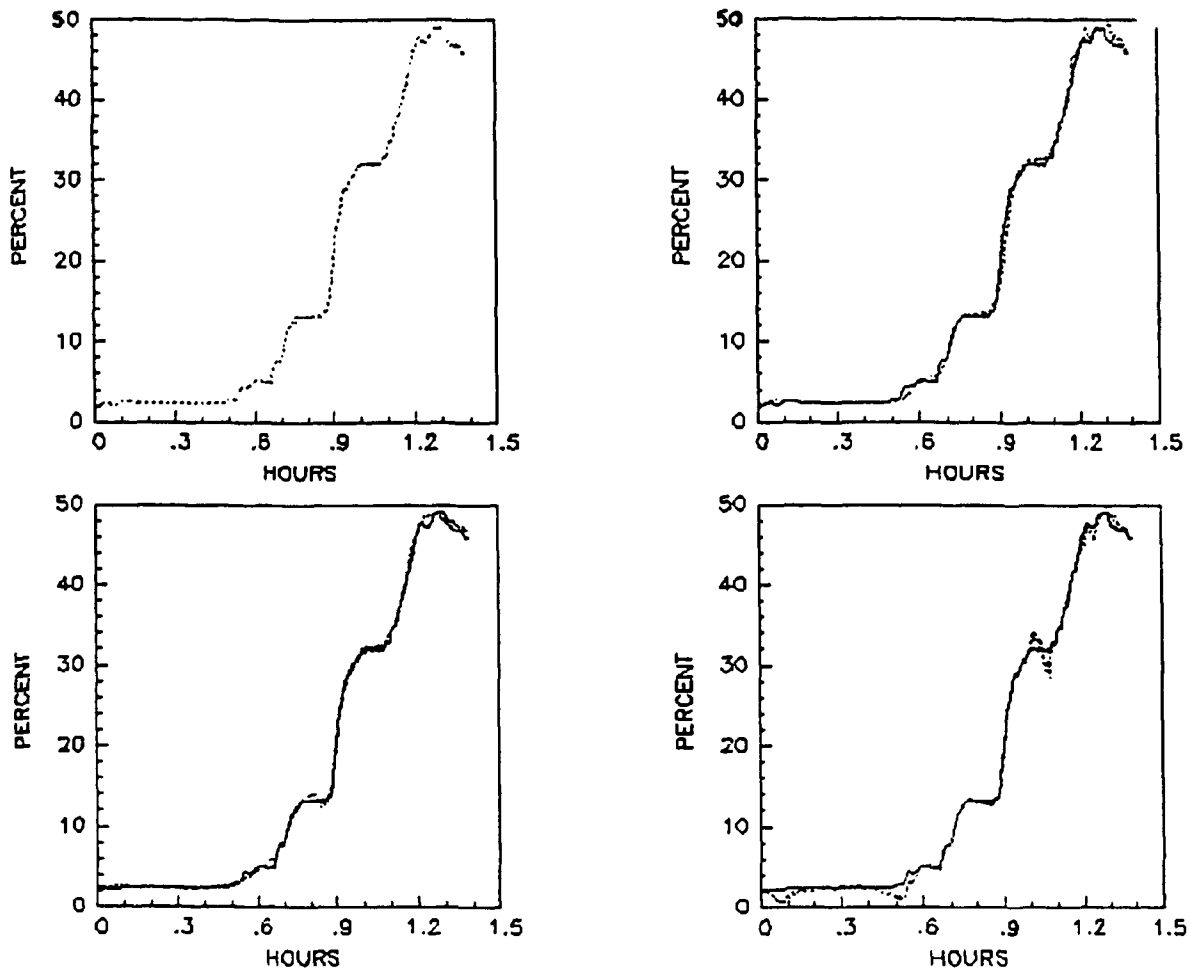

Fig. 5.1g. Secondary sodium flow control during startup at Experimental Breeder Reactor-II.
(1) Operator-driven actual data. Comparison of actual data with the simulation results of (2) fuzzy controller, (3) neural network controller, and (4) reconstructive inverse dynamics controller.

network design was restricted to a simple structure because of the difficulty in implementing control design in this particular simulation environment. Although the performance is the poorest among the others, the commands generated by this controller lie in the valid region, and the overall performance is reasonable. Note that the network for the rod reactivity control includes only three hidden-layer neurons. Similarly, the network for the secondary sodium flow control includes five hidden-layer neurons. Increasing the number of neurons in these networks will most likely improve the performance. Fuzzy controller is relatively easier to update compared with the neural networks approach. Depending on the changes in operational conditions or system configuration, new fuzzy rules can be added or old ones can be removed. With neural networks, updating may require challenging off-line training.

6. DESIGN TOOLS

6.1 PROCESS EMPIRICAL MODELING

One of the common techniques for signal estimation is based on empirical modeling of the process provided all the important measurements are available. The signal validation capability embodied within the ICS is taken from a previous work (Upadhyaya et al. 1987) that provides an algorithmic method for nonlinear, empirical modeling. The empirical model represents a critical signal as a function of a set of other measurements that influence the behavior of the variable under consideration. The functional form of the fit is, in general, nonlinear and has the form

$$y_i = f_i(x_1, x_2, \cdots, x_n) \tag{1}$$

where y_i is the state variable to be monitored, and $x = (x_1, x_2, \cdots, x_n)$ is the vector of subsystem variables that influence y_i. A previously developed software system (Upadhyaya et al. 1987) uses a modified version of the nonlinear curve-fitting technique first proposed by Desrochers and Mohseni 1984.

The general nonlinear steady-state system predictor has the form

$$y = C_O + \sum_{i=1}^{N} C_i \phi_i(x) \quad . \tag{2}$$

After choosing the functionals $\phi_i(x)$, the coefficients $(C_O, C_1, \cdots, C_N)$ are calculated by the least-squares procedure. Each ϕ_i is a nonlinear term or cross product of the components of x. The number of possible cross-product terms is a function of the polynomial order and the number of components in x. To handle the nonlinear models and reduce the number of terms or even the order of the model, several theories exist. Desrochers and Mohseni's method (1984) is used for these purposes. Detailed information about the analytical development and the algorithm is given in Upadhyaya et al. (1987).

6.2 NEURAL NETWORKS: BACKPROPAGATION PARADIGM

The use of neural networks for signal validation or control has several advantages. Defining a functional form relating a set of process variables is not required. The functional form employed in neural network paradigms is nonlinear. Once the network is completely trained, the estimation of the desired variable is efficiently interpolated during implementation. Both steady-state and transient system behavior can be predicted. The state estimation is less sensitive to measurement noise compared with model-based techniques.

One of the analog neural networks, the backpropagation network (BPN), is obtained from a previous work (Upadhyaya, Eryurek, and Mathai (1989). BPN is a multilayer, fully connected heteroassociative network. A typical network configuration for signal validation is shown in Fig. 6.1. The number of processing elements (PEs) in the input layer corresponds to the number of input signals. In this case, the output layer has only one element, the signal to be predicted. The number of PEs in the intermediate

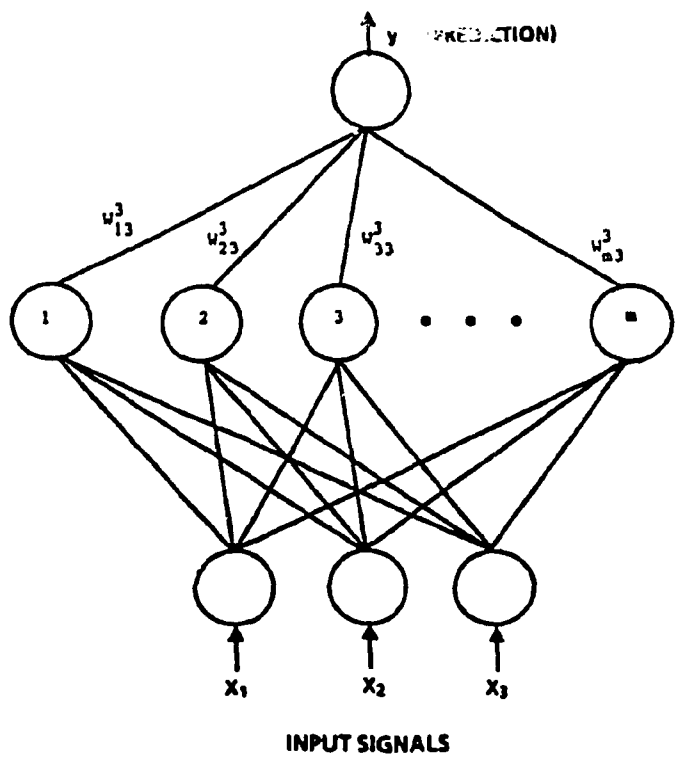

Fig. 6.1. Topology of a three-layer backpropagation network.

layer depends on the problem. The BPN algorithm computes the weights between pairs of processing elements such that the difference between the actual output and the network output is minimized in a least-squares sense.

The algorithm used to train the network uses the generalized delta rule (Upadhyaya, Eryurek, and Mathai 1989). The algorithm is outlined below.

1. Assign a random value r in the range $[+1, -1]$ to all the connection weights ω^p_{ij}, and bias θ^p_j to all processing elements.

2. Present the normalized input vector x to the first layer of the network and propagate it to the output layer as

$$x^p_j = \frac{1}{1+e^{-\beta(\Sigma_i \omega^{p-1}_{ij} x^{p-1}_i + \theta^p_j)}} \quad , \tag{3}$$

after which, each PE in the network will have an associated value.

3. For each PE at the output layer, the local error between the desired value and the actual value is computed by

$$\delta^p_j = x^p_j(1 - x^p_j)(t_j - x^p_j) \quad , \tag{4}$$

where p denotes the output layer.

4. For each PE in the hidden layers, starting at the layer below the output layer and ending at the layer above the input layer, the local error is found by

$$\delta^p_j = x^p_j(1 - x^p_j)\ \Sigma_i \delta^{p+1}_i \omega^{p+1}_{ji} \quad . \tag{5}$$

5. Compute all the connection weight correction as

$$\Delta\omega^p_{ij} = \alpha\ \delta^p_j\ x^{p-1}_i \tag{6}$$

and the bias correction as

$$\Delta\theta^p_j = \alpha\delta^p_j \quad . \tag{7}$$

6. Update all the weights by adding the weight corrections to the old weights.

7. Update all the PE bias values by adding the bias corrections to the previous bias values.

8. Repeat step 2 until the error between the desired and actual value of the output is sufficiently small.

6.3 FUZZY LOGIC

In actual practice, system operations often deviate from prescribed definitions and set points. Many control problems arise from this mismatch between design and practice. Actual solutions require an appropriate interpretation of the inexactness and the uncertainty that abounds the real systems. Fuzzy logic is descriptive, relies on emulating the operator of a process, and provides a framework for integrating artificial intelligence with control. Most important, it uses uncertainty as a tool to handle uncertainty.

The central notion in fuzzy logic (Zadeh 1983) is that of a linguistic (fuzzy) variable whose values are words or sentences in a synthetic language, appropriately represented by membership functions. A linguistic variable includes an adjective-like term (and its antonym), a modifier and a connective. The fuzzy control policy is represented as a finite collection of rules, called fuzzy productions (FP). FPs describe the dependence of one fuzzy variable on another. Their canonical form of the ith rule R^i is

$$\text{if} \Rightarrow (X_1 \ is \ A_1^i), \cdots, (X_n \ is \ A_n^i) \quad , \tag{8}$$

$$\text{then} \Rightarrow Y^i = a_o + a_1^i X_1 + \cdots + a_n^i X_n \quad , \tag{9}$$

where R^i is the ith rule; A_j^i is a linguistic value of X_j in R^i; Y^i is the control variable, and a_n^i are adjustable parameters. The truth value of the antecedent of R^i is given as

$$W_i = A_1^i(X_1) \wedge \cdots \wedge A_n^i(X_n) \quad , \tag{10}$$

where $A_j^i(X_j)$ is the grade of membership of X_j in A_j^i. The aggregated value of control Y is a normalized linear combination given by

$$Y = \frac{W_1 Y^1 + \cdots + W_n Y^n}{W_1 + \cdots + W_n} \quad . \tag{11}$$

The equation above suggests a weighted vote in the control logic. Generally, in a fuzzy production system, all rules are considered to be "fired" with different strengths. Rules that fire strongly contribute significantly to the final conclusion.

6.4 INVERSE DYNAMICS AND CONTROL

Consider a plant dynamics described by

$$\dot{x} = F(x, u) \quad , \tag{12}$$

where x and u are state and control variables respectively. The control is solved from Eq. (12) to yield

$$u = F'(x, \dot{x}) \quad , \tag{13}$$

where I indicates the inverse dynamics with respect to the solution of control u. The dynamic equilibrium of control is defined as

$$u_{eq} = F'(x, \dot{x} = 0) \quad . \tag{14}$$

The definition of the reconstructive control is given by

$$u_{rc} = \dot{x} = -k(x - x_d) \quad , \tag{15}$$

where k is a tunable gain and x_d is the demand. The dynamic equilibrium of control given by Eq. (14), when appended to the open-loop system of Eq. (12), cancels the forward dynamics denoted by F. The second segment of the total control given by Eq. (15) reconstructs the forward dynamics in the desired form. Following the definitions in Eqs. (14) and (15), the total control given in Eq. (13) can be rewritten as

$$u = G(u_{eq}, u_{rc}) \quad . \tag{16}$$

An alternative way of constructing the RID law includes the definition of a performance error $E(t)$ given by

$$E(t) = k_u[u(t) - u_{eq}(t)] + k_x[x(t) - x_d(t)] \quad , \tag{17}$$

where k_u and k_x are weights for the error terms. The control u is then solved from the above to satisfy the dynamic condition of $E(t) = 0$ at all times. Note that the dynamic equilibrium $u_{eq}(t)$ always works in the opposite direction with respect to the state variable $x(t)$; thus, the condition $E(t) = 0$ can be satisfied only if $x(t) - x_d(t) = 0$. By letting $E(t) = 0$ in Eq. (17)

$$u(t) = u_{eq}(t) - k[x(t) - x_d(t)] = u_{eq}(t) + u_{rc}(t) \quad . \tag{18}$$

The parameter k is an adjustable quantity. The RID control is specifically designed for trajectory-following control applications. Thus, it is assumed that the open-loop system operating at steady state is in stable condition, that is, $u(0) = u_{eq}(0)$ and $x(0) = x_d(0)$ at the beginning of the transient.

The RID design is performed in the subsystem level. A given system is decoupled according to the distribution of demands and control variables. Each control variable is designed to follow one demand. Thus, for every control-demand pair, a corresponding subsystem is defined. In case of MIMO systems, the control-demand pairs (and their corresponding subsystems) are selected according to the best strategy determined by the nature of the physical system. Among the many possibilities, the control-demand couplings fit one of the following most frequently encountered subsystem definitions.

A. Control law of direct path

Consider the following coupled nonlinear systems.

$$\dot{x}_1 = f(x_1, \bar{X}, u_1) \tag{19}$$

where

x_1 = state variable of subsystem 1,

$$\dot{\bar{X}} = F(\bar{X}, x_1, \bar{U}) \quad , \tag{20}$$

u_1 = control variable of subsystem 1,

$\bar{X}$ = state vector of the coupled subsystem,

$\bar{U}$ = control vector of the coupled subsystem.

Note that the control vector $\bar{U}$ does not include u_1.

The control law of the direct path defined for a given demand d_1 on the state variable x_1 is given by

$$u_1 = f^{-1}(x_1, \dot{x}_1, \bar{X}) \quad , \tag{21}$$

where

$$\dot{x}_1 = -k(x_1 - d_1) \tag{22}$$

and f^{-1} denotes the inverse dynamics.

B. Control law of indirect path

Consider the following coupled nonlinear subsystems.

$$\dot{x}_1 = f_1(x_1, x_2, \bar{X}) \quad , \tag{23}$$

$$\dot{x}_2 = f_2(x_1, x_2, u_2, \bar{X}, \bar{U}) \quad , \tag{24}$$

$$\dot{\bar{X}} = F(x_1, x_2, \bar{X}, \bar{U}) \quad . \tag{25}$$

As it can be seen from Eq. (23), a demand on x_1 can be satisfied only through the control of a coupled subsystem provided the combined subsystem is controllable. Suppose that the controllability condition exists for the combined subsystem given by Eqs. (23) and (24), then the control law of the indirect path for the control-demand pair of (u_2, d_1) is given as follows.

$$x_2^* = f_1^{-1}(x_1, \dot{x}_1, \bar{X}) \quad , \tag{26}$$

$$\dot{x}_1 = -k_1(x_1 - d_1) \quad , \tag{27}$$

$$u_2 = f_2^{-1}(x_1,\ x_2,\ \dot{x}_2,\ \bar{X},\ \bar{U}) \quad , \tag{28}$$

$$\dot{x}_2 = -k_2(x_2 - x_2^*) \quad . \tag{29}$$

As seen from Eqs. (26–29), the control u_2 forces the solution of state x_2 to match the dummy state x_2^*. The dummy state x_2^* is defined as the inverse dynamics of the state equation (23) where x_1 follows the demand d_1.

The term "indirect path" indicates that the control and demand are distributed over more than one state equation. Several different ways of defining the dummy state(s) can be used. The demand may also be assigned to an output equation where the control appears in the state equations. Thus, the generalization of the indirect path control law can not be carried out any farther than the above unless the system equations are explicitly defined and the strategic choices of demand-control pairs have already been made.

C. Adaptive phase, on-line model usage

The above derivation is based on the assumption that the open-loop dynamics is well defined through the system equations used to derive the RID control law. Once the control law is derived, the controller uses the plant state (measurements from the plant) in a feedback arrangement.

In general, not all the plant states used in the controller are measurable. The missing state variables are estimated by using an on-line model. However, the state estimation using models often includes errors that may significantly degrade the controller performance. Besides the estimation errors, the system equations used to design the control law, may not be adequate either. Thus, the RID design includes an adaptive design phase where a correction term is added in the control to compensate for the mismatches between the plant and model. In case of uncertain dynamics, tuning the adaptive controller before the on-line implementation requires testing where the available plant measurements are used. If none of the plant states used in the RID control law are available as measurements, the adaptation cannot be accomplished (the system is not observable). The adaptive control can be designed in numerous ways depending on the properties of the system under consideration. The following section describes the treatment of mismatches between the plant and model dynamics.

D. Unknown dynamics

Assume that the given system dynamics is known to be partially unknown and the modeling effort does not yield accurate results. Consider a subsystem given by

$$\dot{x}_1 = f_1(x_1, \bar{X}, u_1, g_x) \quad , \tag{30}$$

where $\bar{X}$ is the coupling state vector and g_x is the unknown dynamics. A model describing the same subsystem is given by

$$\dot{m}_1 = s_1(m_1, \bar{M}, u_1, g_m) \quad , \tag{31}$$

where g_m is the correction to the unknown dynamics g_x. The RID design for the control u_1 is

$$u_1 = s_1^{-1}(m_1, \dot{m}_1, \bar{M}, g_m) \quad , \tag{32}$$

where s_1^{-1} indicates the inverse dynamics of the model. Assume that the plant states are measured. Then the control given above will be implemented in the following form.

$$u_1 = h_1^{-1}(x_1, \dot{x}_1, \bar{X}, g_m) \quad . \tag{33}$$

Note that the inverse dynamics is denoted by h_1^{-1} because an estimate g_m is used. The design also includes

$$\dot{x}_1 = -k_x(x_1 - d_1) \quad , \tag{34}$$

where d_1 is the demand. The design is completed by the prediction of g_m. The unknown dynamics can also be treated as another control variable. The inverse dynamics solved from Eq. (31) is

$$g_m = p_1^{-1}(m_1, \dot{m}_1, \bar{M}, u_1) \quad , \tag{35}$$

where $\dot{m}_1$ is replaced by proportional and integral error

$$\dot{m}_1 = -k_m(m_1 - x_1) - k_i \int (m_1 - x_1)dt \quad . \tag{36}$$

The integral error takes care of the accumulative error and can be omitted, according to the problem.

The adaptive design can also be derived for the indirect path designs. It is important to note that the sensitivity of gains k_x, k_m, and k_i, with respect to the unknown dynamics, strictly depends on the nature of the uncertainty. The above derivation may also be used for parameter tracking. Figure 6.2 shows a block diagram of the RID control.

6.5 NONLINEAR MODELING OF EXPERIMENTAL BREEDER REACTOR-II

A previously developed linear model of EBR-II (Upadhyaya et al. 1989) is modified to take into account the nonlinearities. The modified model includes only the primary system. The primary system model consists of the reactor core, sodium tank, and intermediate heat exchanger. The model employs the state-space technique using 18 state variables.

Figure 6.3a shows the implementation using SYSTEM-BUILD blocks. The three superblocks (core2, ihx2, and tank) are connected to another superblock called "adapt." This block includes five adaptive routines to match the model dynamics with the plant response. The five outputs from the adaptive block provide corrections to the reactivity and heat transfer coefficients of the model. The adaptive model uses on-line measurements from the plant. A second, entirely isolated, version of this model is also developed to provide the same corrections. The second model does not use any on-line measurement; instead, it uses a set of look-up tables. These tables include phase-plane relationships between the corrections and state variables. The tables are developed from data from the previous EBR-II startup. The validation of the model can be seen in Figs. 5.1a–5.1g.

Figures 6.3b and 6.3c show the core and IHX models respectively. The interior of the adaptive block is shown in Fig. 6.3d. The adaptive routines are developed by using the RID method for unknown dynamics. The isolated adaptive model is generated after an operator-driven simulation, where the corrections are obtained and tabulated.

6.6 EXPERT SYSTEMS

The ICS design introduced in this work uses several logical prepositions to yield fault-tolerant operation. In its present form, the ICS also makes use of heuristic knowledge at the preliminary level. Although an expert system development is not in the scope of this work, the following discussion clarifies the areas where an expert system would be useful.

The implementation of the fault-tolerant logic can be enhanced by a supervisory routine that monitors the plant status in a wider range than the current ICS design. This enhancement requires an expert system environment in which the heuristic knowledge can be processed appropriately. As a supervisory routine, the expert system can also provide a link between the continuous control and startup procedure (or to the procedure prompting system). Note that several verifications in the standard procedure must be performed during startup.

The capacity of such a supervisory system can be extended to include more detailed tasks. For example, the signal and command validation blocks include routines developed off-line. These routines may have to be modified because of new plant conditions. The supervisory routine can be designed to conduct on-line training of the BPN and PEM modules and to modify the membership functions of the fuzzy controller. One of the most important capabilities an expert system can provide is the anticipatory control (Tsoukalas, Lee, and Ragheb 1989) that further enhances the fault-tolerance capability of the control system.

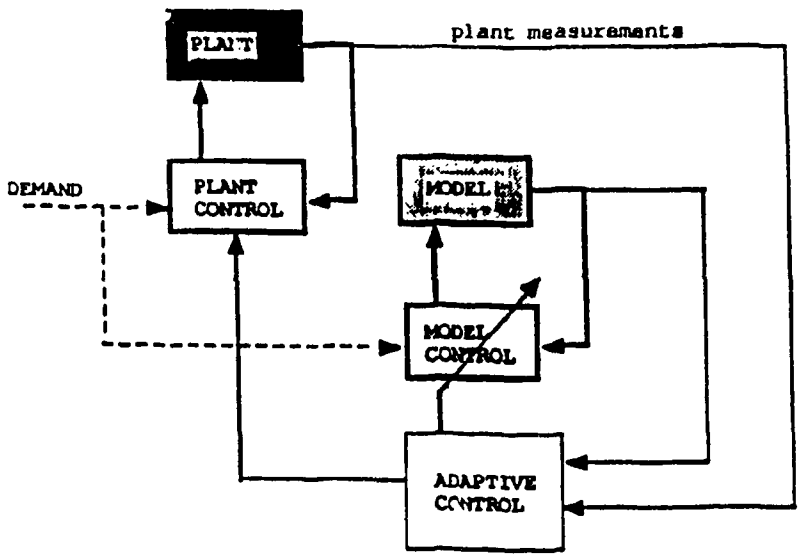

Fig. 6.2. Adaptive reconstructive inverse dynamics control system.

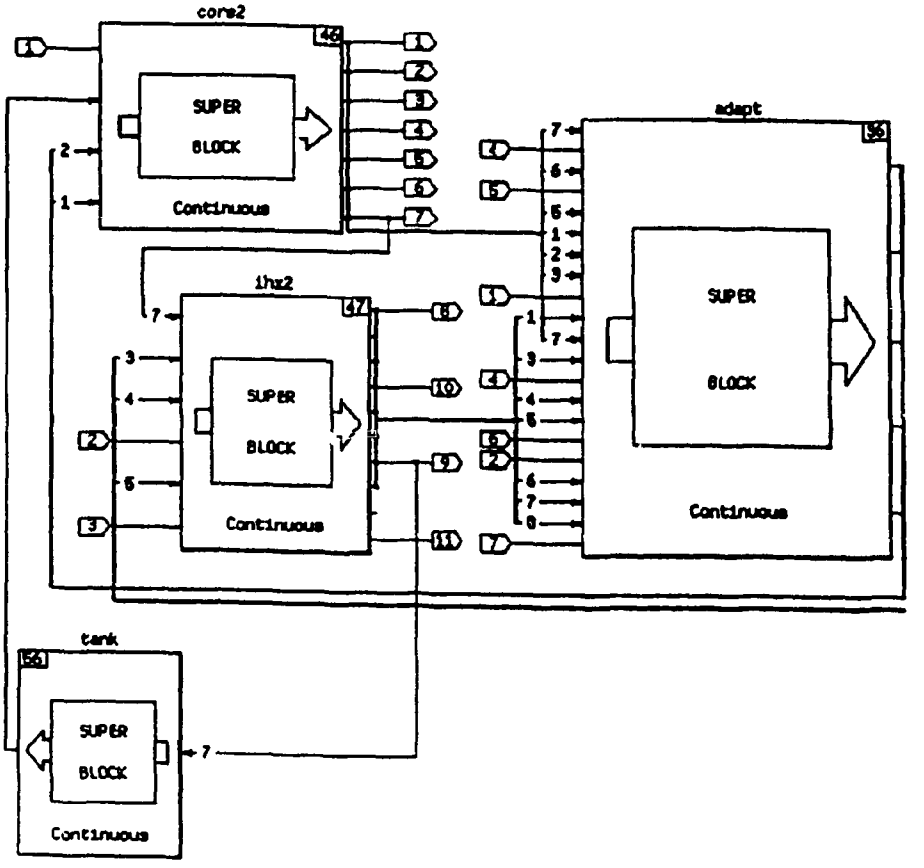

Fig. 6.3a. MATRIXx super blocks representing the adaptive, nonlinear Experimental Breeder Reactor-II model.

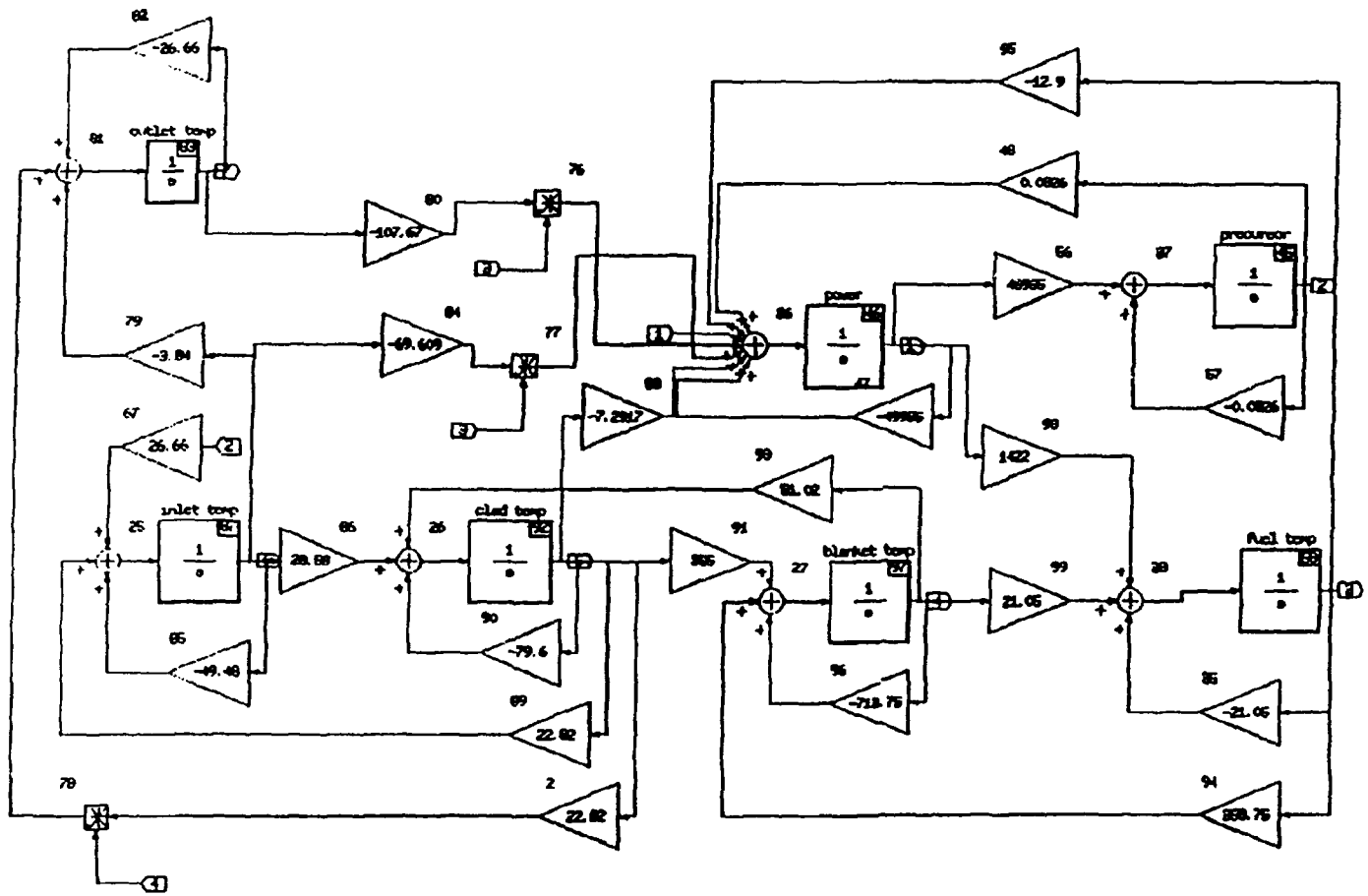

Fig. 6.3b. Nonlinear core model of the Experimental Breeder Reactor-II plant in MATRIXx.

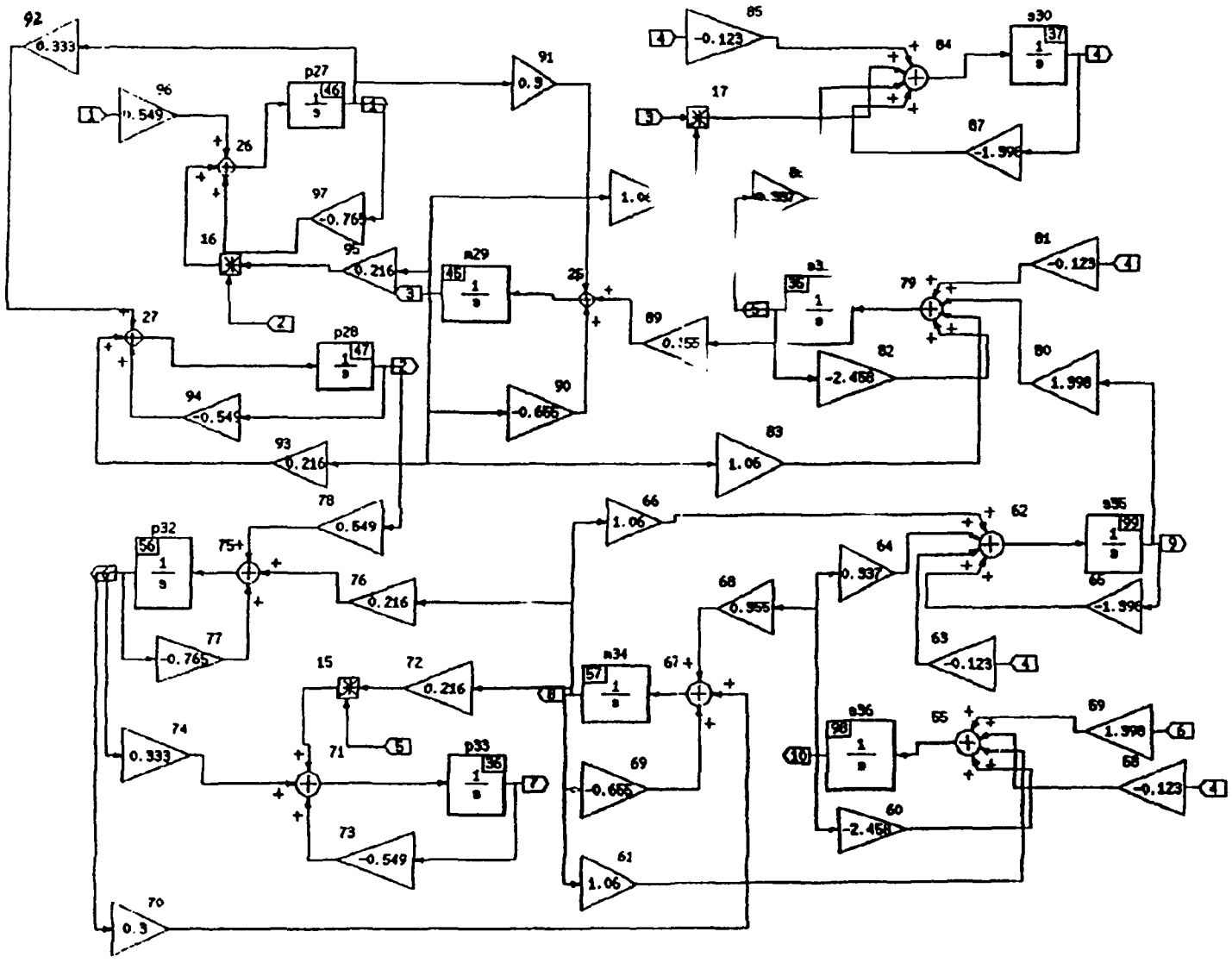

Fig. 6.3c. Nonlinear intermediate heat exchanger model of the Experimental Breeder Reactor-II plant in MATRIXx.

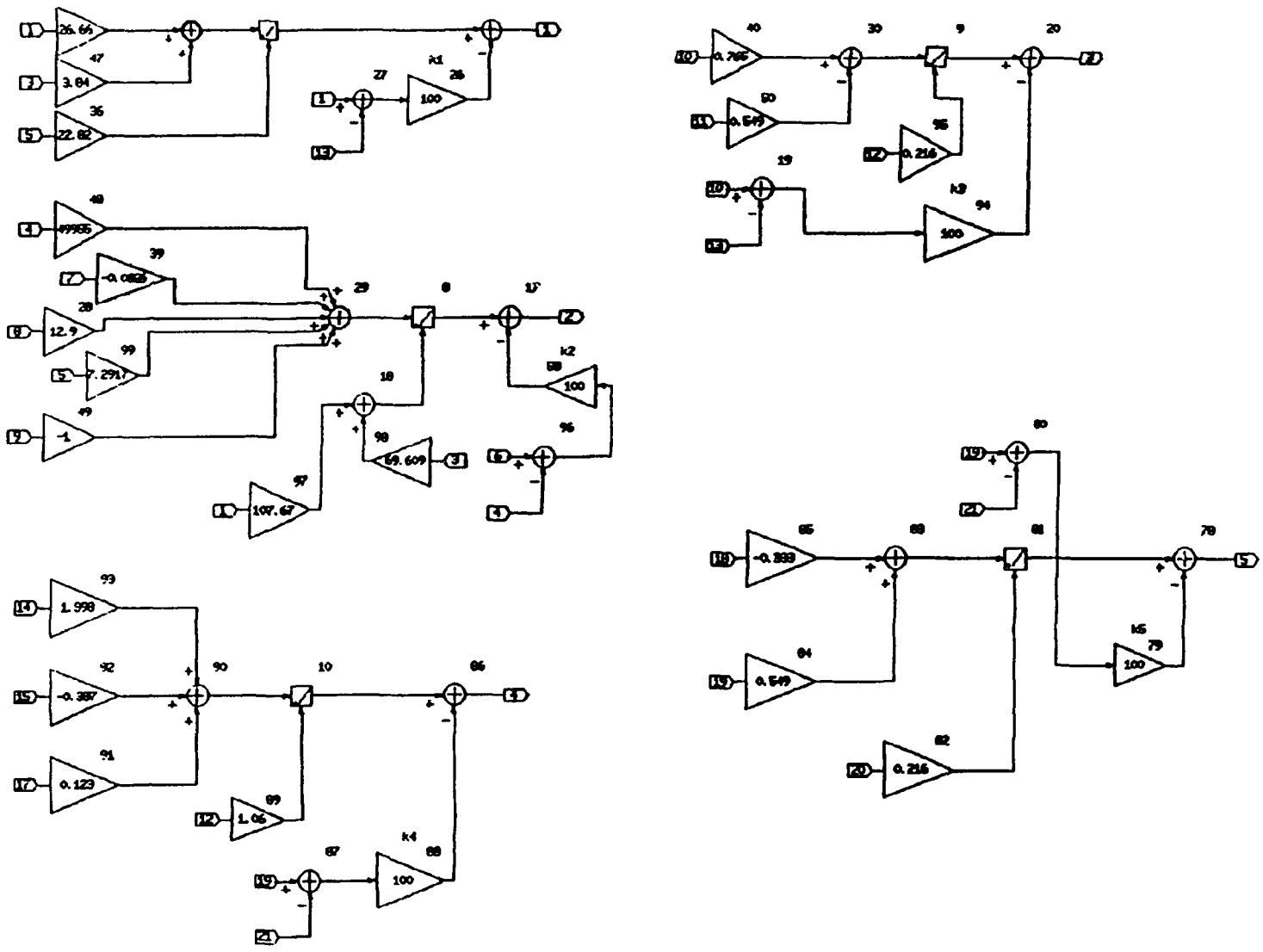

Fig. 6.3d. Adaptive block to track uncertain parameters of the model.

7. SUMMARY AND CONCLUDING REMARKS

In response to the increasing interest in automated nuclear reactor operations, a collection of advanced methods in diagnostics and controls as well as development of an integrated environment for automation is presented in this report. The integrated control system (ICS) architecture is a new concept within this context. It offers validation of plant information before and after it is processed for control purposes. The ICS concept also includes new control techniques that are easier to implement on-line compared with conventional techniques.

A particular application of the ICS is considered for automation of the EBR-II startup operation. The ICS design includes signal and command validation tasks that use artificial neural networks and process empirical modeling techniques. The control module of the ICS houses three different controllers running in parallel. These controller designs use reconstructive inverse dynamics, fuzzy logic, and neural network paradigms in a MIMO regime. Another diagnostic module provides a measure of the performance (performance analyzer). A mode selector unit facilitates the choice of appropriate techniques from the control, signal validation, and command validation modules. The mode selector evaluates the outputs produced by four other modules to determine the best strategy for startup control. Its primary function is to maximize the performance by safely maneuvering around the problems. The primary function of the mode selector is often referred to as fault tolerance. A subset of the inputs received by the mode selector contains information about the anticipated events of the plant. Thus, the anomalies are not allowed to propagate in time without detection, and the preventive actions are taken well before the plant enters an undesired regime.

The simulations presented here use a valid nonlinear model of EBR-II. The range of the startup transients is chosen long enough to show the nonlinear effects. The results indicate that each controller of the ICS is capable of performing automated startup at EBR-II. This conclusion can be verified by comparing the (operator-driven) actual plant data with the simulation results (Figs. 5.1a–5.1g). The simulations included all logical interactions of the command validator and performance analyzer. None of the commands are rejected by the command validator during simulations. The simulations do not include hypothetical sensory failures because of an infinite number of hypothetical cases. The prediction capability of the signal validator is found to be very effective, as illustrated by separate runs (Figs. 4.2a–4.2f). The implementation using the MATRIXx/SYSTEM-BUILD software package imposes no real-time problems. This application is observed to be faster than the actual startup at the EBR-II by a factor of 24.

This study should be considered as a feasibility analysis rather than as a final control design for the EBR-II automated startup. The proposed concept is potentially open for further enhancements. Improvement in monitoring and diagnostics will extend the scope of useful tasks. The use of expert systems is very important when much heuristic information processing is required.

REFERENCES

ANL (Argonne National Laboratory) 1985. *EBR-II System Description Manual*, Vol. 1-5, Argonne, Ill.

Berkan, R. C. 1988. "Dynamic Modeling of EBR-II for Simulation and Control," M.S. thesis, The University of Tennessee, Knoxville.

Berkan, R. C., et al. 1989. "A New Nonlinear Reconstructive Control Approach Applied to the Axial Xenon Oscillation Problem in PWRs," Proceedings of the Seventh Power Plant Dynamics, Control and Testing Symposium, Knoxville, Tennessee, Vol. 2, pp. 77.01–77.18.

Carter, R. J., and R. E. Uhrig 1990. *Human Factors Issues Associated with Advanced Instrumentation and Controls Technologies in Nuclear Plants*, NUREG/CR-5439, ORNL/TM-11319, Oak Ridge National Laboratory, Oak Ridge, Tenn.

Corcuera, R. P., et al. 1990. "Designing an AI-Environment Prototype for the Automatic Startup of EBR-II," ORNL/TM-11296, Oak Ridge National Laboratory, Oak Ridge, Tenn.

Desrochers, A., and S. Mohseni 1984. "On Determining the Structure of a Nonlinear System," *Int. J. Control*, **40**, 923–38.

Husseiny, A., et al. 1990. "Automation of Nuclear Power Plants," *Nucl. Technol.* **90**, 34–48 (April).

ISI (Integrated Systems, Inc.) 1989. *MATRIXx User's Guide*, Vax Work-Station Version 3.1, San Jose, Calif.

Lin, C., et al. 1989. "Optimal Control of a Boiling Water Reactor Load-Following Operation," *Nucl. Sci. Eng.* **102**, 134–39.

Nakakura, H., and A. Ishiguro 1988. "Automatic Load Follow Control System for PWR Plants," *Nucl. Saf.* **29**(4) 451–62.

Tsoukalas, L. H., G. W. Lee, and M. Ragheb 1989. "Anticipatory Monitoring and Control in a Process Environment," Proceedings of the Second International Conference on Industrial and Engineering Applications of Artificial Intelligence and Expert Systems, IEA/AIE-89, ACM/SIGART, Tullahoma, Tenn., June 6–9, 1989.

Upadhyaya, B. R., et al. 1989. "Development of an Integrated Signal Validation System in Nuclear Power Plants," Final Report, Vols. 1, 2, 3, DOE/NE/37959-34,35,36, Nuclear Engineering Department, The University of Tennessee, Knoxville.

Upadhyaya, B. R., E. Eryurek, and G. Mathai 1989. "Application of Neural Computing Paradigms for Signal Validation," Proceedings of the Seventh Power Plant Dynamics, Control and Testing Symposium, Knoxville, Tennessee, Vol. 1, pp. 27.01–27.18.

Zadeh, L. A. 1983. "The Role of Fuzzy Logic in the Management of Uncertainty in Expert Systems," *Fuzzy Sets Syst.* 11, 199–227.

ORNL/TM-11716
Dist. Category UC-530
Liquid Metal Fast Breeder Reactors

INTERNAL DISTRIBUTION

1. S. J. Ball
2. R. E. Battle
3-5. R. C. Berkan
6. C. R. Brittain
7. N. E. Clapp, Jr.
8. B. G. Eads
9. C. E. Ford
10. D. N. Fry
11. F. J. Homan
12-13. R. A. Kisner
14. K. Korsah
15. H. E. Knee
16. C. March-Leuba
17. J. K. Munro
18. P. J. Otaduy
19. J. C. Schryver
20. R. L. Shepard
21. L. H. Tsoukalas
22. R. E. Uhrig
23. B. R. Upadhyaya
24. J. D. White
25. T. L. Wilson
26. R. T. Wood
27. A. Zucker
28. J. B. Ball, Advisor
29. B. Chexal, Advisor
30. T. B. Sheridan, Advisor
31. R. M. Taylor, Advisor
32-33. Central Research Library
34. Y-12 Technical Reference Section
35-36. Laboratory Records Department
37. Laboratory Records ORNL-RC
38. ORNL Patent Section
39. I&C Division Publications Office

EXTERNAL DISTRIBUTION

40. Assistant Manager for Energy Research and Development, U.S. Department of Energy, Oak Ridge Operations Office, Oak Ridge, Tennessee 37831.
41-42. Office of Scientific and Technical Information, P.O. Box 62, Oak Ridge, Tennessee 37831.
43. Harry A. Alter, Manager, Division of Advanced Technology Development, U.S. Department of Energy, NE-462, Washington, DC 20545
44. Sid C. Bhatt, EPRI, Project Manager, 3412 Hillview Avenue, P.O. Box 10412, Palo Alto, California 94303
45. Doug G. Carroll, Program Manager, G.E. Nuclear Energy, 6835 Via Del Oro, Box 530954, San Jose, California 95153-5354
46. Mr. Robert L. Carroll, Department of Electrical Engineering and Computer Sciences, George Washington University, Washington, DC 20052
47. Dr. Yogi Dayal, G.E. Nuclear Energy, Advanced Nuclear Technology, Box 530954, San Jose, California 95153-5354
48. Mohammed Jamshidi, CAD Lab Systems/Robotics, Department of Electrical and Computer Engineering, Room 113A, EECE Building, University of New Mexico, Albuquerque, New Mexico 87131
49. Reed Monson, P.O. Box 2528, Idaho Falls, Idaho 83403-2528

50. Mr. H. P. Planchon, Argonne National Laboratory, 9700 S. Cass Avenue, Argonne, Illinois 60439
51. Dr. G.V.S. Raju, Professor and Director, The University of Texas at San Antonio, San Antonio, Texas 78285-0665
52. John I. Sackett, Argonne National Laboratory-West, P.O. Box 2528, Idaho Falls, Idaho 83402

53-108. Given distribution for Category UC-530, Liquid Metal Fast Breeder Reactors.